Molecular mechanism underlying disease resistance in Brassica rapa

Akter, Mst Arjina

(Degree)
博士（農学）

(Date of Degree)
2023-09-25

(Date of Publication)
2024-09-01

(Resource Type)
doctoral thesis

(Report Number)
甲第8746号

(URL)
https://hdl.handle.net/20.500.14094/0100485930

Doctoral Dissertation

Molecular mechanism underlying disease resistance in *Brassica rapa*

(*Brassica rapa* における病害抵抗性の分子機構**)**

AKTER MST ARJINA

August 2023

Graduate School of Agricultural Science

Kobe University

Contents

Chapter I

General introduction

Plants constantly face a plethora of biotic and abiotic stresses, and biotic constraints to agricultural production are broadly identified as plant diseases. In general, plant disease is considered a risk factor that affects healthy plants, modifies the normal structure, creates abnormal conditions, and disrupts or changes its vital role and other activities, in all species of plants including wild and cultivated. The prevalence and occurrence of plant diseases vary depending on different conditions although almost every species of plant have particular diseases (Agrios 2005, Savary et al. 2019). Normally, some plant varieties are subject to susceptible to some diseases while others are resistant to them. Many pathogenic organisms such as fungi, bacteria, viruses, nematodes, and mycoplasma cause infectious diseases in plants (Agrios 2005). Due to plant disease, huge loss occurs in crop production. Only plant diseases cause considerably reduce crop yield by 10–40% of crop loss (Yadav and Srivastava 2017, Savary et al. 2019). These crop losses result in drastic economic disadvantages, decrease the income of crop producers, increase the price of foods for consumers, and people to suffer from starvation, hunger, and malnutrition. In a nutshell, a significant number of the world's population is prone to food insecurity. Thus, with an ever-increasing world population, food security and crop protection are concerns of utmost significance (Shurtleff et al. 2021).

Brassica, a genus of plants in the Brassicaceae family; informally known as cruciferous vegetables, cabbages, and mustard plants but popularly called Cole crops have scientific interest due to their agricultural and horticultural importance. It is one of the most economically important genera having 39 species under the Brassicaceae family, and this family contains more than 338 genera and 3,700 species (Cheng et al. 2014). The genus *Brassica* is a good source of genetic resources necessary for plant breeding and it occupies the top place among vegetables and it provides the 10 most agronomically and economically important plant groups in the world.

About 135 million tons of *Brassica* crops are produced globally and nowadays, more than 150 countries cultivate *Brassica* plants, as vegetables and oilseed (Poveda et al. 2020, FAO 2018). *Brassica* plants are mainly grown for their leaves, stems, inflorescence, lateral and axillary buds, edible roots, flowers, and seeds. *Brassica* vegetables provide potential antioxidant, antimicrobial, and anticancer activities (Ramirez et al. 2020, Salehi et al. 2021). Six *Brassica* species, their evolution, and genomic relationship have been described by the “Triangle of U” and these six species have paramount importance in scientific interest as follows: three diploid

species, namely *Brassica rapa* (AA genome: 2n=2×=20), *Brassica nigra* (BB: 2n=2×=16), and *Brassica oleracea* (CC: 2n = 2× = 18), and three allotetraploid species, namely *Brassica juncea* (AABB: 2×= 4× = 36), *Brassica napus* (AACC: 2n = 4× = 38), and *Brassica carinata* (BBCC: 2n = 4× = 34) (U 1935, Dixon 2007, Kim et al. 2018).

It is noteworthy that *B. rapa* provides fresh leafy vegetables such as Chinese cabbage (var. *pekinensis*), pak choi (var. *chinensis*), and komatsuna (var. *perviridis*), and root vegetables such as turnip. These are rich in several beneficial molecules such as nutrition, vitamins, minerals, and other health-promoting substances (Lv et al. 2020a). Based on morphological characteristics, *B. rapa* has three well-defined groups: (1) the oleiferous or oil-type rape, (2) the leafy-type *B. rapa*, and (3) the uraniferous- *B. rapa* (Prakash and Hinata 1980, Lee et al. 2013).

Phytopathogens such as plant fungal, bacterial, viral, and nematode diseases have recently been reported on *B. rapa* vegetables. The most common diseases include Fusarium wilt, white rust, clubroot, black rot, sclerotinia stem rot, blackleg, downy mildew, etc. (Lv et al. 2020b). Among various diseases, Fusarium wilt (FW disease, also called Fusarium yellows), a soil-borne disease of many crucifer crops including *B. rapa* vegetables (Chinese cabbage, pak choi, komatsuna, and turnip) and *B. oleracea* vegetables (cabbage, cauliflower, broccoli, brussels sprout) is caused by two formae speciales of *F. oxysporum* f. sp. *conglutinans* (*Foc*) and f. sp. *rapae* (*For*) (Daly and Tomkins 1995, Enya et al. 2008). Soil temperature and soil nutrition especially potassium deficiency have a huge effect on this disease while soil moisture and soil reaction (pH) affect minimal causing this disease (Annonymous 1988). It occurs mainly in warm humid and semi-humid areas and infection by this fungus starts in roots, colonizes, and occludes the xylem vessels. The disease symptoms start as the yellowing of leaves and gradually it causes wilting, defoliation, stunted growth, and death of the host plant, resulting in detrimental effects on the quality and quantity of production (Walker 1930, Daly and Tomkins 1995, Enya et al. 2008). This pathogen is ubiquitous in nature and is able to survive in the soil for a long even in the absence of hosts, measures such as crop rotation, improved sanitation, and fungicides are ineffective for its control. Once the disease is present, the most successful strategy is to use disease resistant/tolerant cultivars. Indeed, disease resistance is the most feasible technique for developing a resistant cultivar, as conventional methods are ineffective to control this soil-borne disease (Pu et al. 2012, Xing et al. 2016, Nalini and Parthasarathi 2018, Yang et al. 2019).

White rust caused by oomycete pathogen *Albugo candida* is a devastating fungal disease of agro-economically important *Brassica* species with 30-60% yield loss; during stag head formation in susceptible cultivars, the loss is more severe to 89.8%. *B. rapa* is this pathogen's

primary host of race (Tanhuanp 2004, Varshney et al. 2004, Arora et al. 2019). Although yield loss depends on the disease severity according to different regions and countries, more than 63 genera and 241 species of the Brassicaceae family are infected by *A. candida*, globally (Choi et al. 2007, Singh et al. 2021). The most important favorable factors for occurring this disease are rain (Arora et al. 2019). The first and most apparent symptoms are white to cream-colored zoosporangial pustules that appear on all the aerial parts of the plants such as cotyledons, leaves, stems, and inflorescences and gradually the disease is characterized by white pustules containing zoospores on the abaxial leaf surface of susceptible plants; these pustules become more prominent as the disease progresses (Meena et al. 2014, Saharan et al. 2014). Consequently, due to this disease, sugars, phenol content, and chlorophyll concentration reduced and increased the number of proteins, amino acids, and auxins [indole-3-acetonitrile (IAN), indole-3- acetic acid (IAA)] leading to hyperplasia and hypertrophy in the plant parts and cause more yield loss (Verma and Petrie 1980, Kaur et al. 2011, Singh et al. 2021). As *A. candida* is an obligate biotrophic pathogen, a sufficient amount of inoculum for the inoculation of large segregating populations over generations is not satisfactory. Moreover, this pathogen cannot be cultured *in vitro* that's why it always needs an inoculation test for its study, which is also lengthy and laborious. Some other traditional techniques need more time, money, and labor and often cause health hazards to other plants and animals. A disease-resistant cultivar can be considered the most convenient method for the management of white rust disease in *Brassica*. For the development and improvement of white rust-resistant cultivars, the identification of *R* genes is crucial. Different methods in molecular biology can help to identify *R* genes in *Brassica* for white rust as well as effectively control the disease by genetic resistance approach (Varshney et al. 2004). Recently, many *R* genes have been identified in different species of *Brassica* including *B. rapa, B. oleracea*, *B. napus, B. juncea,* and also in the model plant *Arabidopsis thaliana*. These *R* genes play an important role in disease resistance in *Brassica* crops. It also enables the establishment of host-pathogen interactions as well as ensures production and yield in *Brassica* crops (Kole et al. 1996, Lv et al. 2020b, Singh et al. 2021).

Non-coding RNAs (ncRNAs) are RNAs that have no protein-coding ability and those non-coding RNAs that have more than 200 nucleotides (nt) are called long non-coding RNAs (lncRNAs). It is an important biological regulator in plants and animals for many developmental processes and nowadays, lncRNAs are considered "Star" rather than "Dark Matter" due to insight into regulation mechanisms (Ayub et al. 2019, Karlik et al. 2019, Chen et al. 2021a). There are two types of ncRNAs such as housekeeping ncRNAs and regulatory ncRNAs. Ribosomal RNAs (rRNAs), transfer RNAs (tRNAs), small nuclear RNAs (snRNAs), and small nucleolar RNAs (snoRNAs) are under the housekeeping ncRNAs. On the other hand, the

regulatory ncRNAs consist of two sub-groups: (a) small RNAs (sRNAs), including miRNAs and siRNAs, and (b) lncRNAs (Karlik et al. 2019). Basically, the size of lncRNAs is shorter than mRNA and lncRNAs have a lower number of exons of mRNAs (Shea et al. 2019, Chen et al. 2020, Lin et al. 2020). Many lncRNAs have been identified in a group of plant species and they are associated mainly with chromatin of the nucleus; also, in the cytoplasm (Karlik et al. 2019). It has low sequence conservation between species and the expression level of lncRNAs is lower than that of mRNAs and more tissue-specific expression. (Chen et al. 2020, Chen et al. 2021a). Based on genomic location, three types of lncRNAs are found as follows: i) long intergenic noncoding RNAs (lincRNAs), ii) natural antisense RNAs (NATs), and iii) intronic noncoding RNAs (incRNAs). Generally, incRNAs are obtained from introns whereas NATs are derived from complementary DNA strands (Chekanova et al. 2015, Liu et al. 2015, Karlik et al. 2019, Rai et al. 2019, Shea et al. 2019). LncRNAs play a vital role in plants through diversified activities including gene expression, transcriptional and post-transcriptional gene regulation, genome stability, and plant immunity (Liu et al. 2015, Seo et al. 2017, Karlik et al. 2019); tissue development, fertility, sexual reproduction, protein re-localization, flowering (Karlik et al. 2019); biochemical improvement of crops (Liu et al. 2015); vernalization (Swiezewski et al. 2009, Heo and Sung 2011, Kim and Sung 2017); photoperiod-sensitive male sterility (Ding et al. 2012), seed dormancy (Fedak et al. 2016), red-light-mediated seedling photomorphogenesis (Wang et al. 2014), nuclear domains organization (Chekanova 2015) and in response to abiotic and biotic stresses such as drought, salinity, heat stress, and disease infections (Xin et al. 2011, Kim et al. 2012, Liu et al. 2015, Uszczynska-Ratajczak et al. 2018, Karlik et al. 2019).

In *B. rapa*, 2088 lncRNAs including 1,444 lincRNAs, 551 NATs, and 93 incRNAs were identified (Shea et al. 2019). Unlike other epigenetic marks of the genome, the expression of lncRNAs can explosively change depending on the stage of tissue development, environment, and biotic and abiotic stress conditions (Chen et al. 2020). LncRNAs accelerate gene transcription by interacting with DNA, other RNA, protein, and epigenetic regulators (Ayub et al. 2019). Sometimes mRNA and NATs express coordinately and co-upregulation of mRNAs and their paired NATs that may play a vital role in the transcriptional response to abiotic stress including vernalization or cold treatment was found in *B. rapa* (Shea et al. 2019). Other studies showed the co-expression of mRNAs and their paired NATs in *A. thaliana* and tomato in response to biotic stresses such as *F. oxysporum* and *Phytophthora infestans* infection, respectively (Zhu et al. 2014, Cui et al. 2017).

Salicylic acid (SA), a plant hormone plays an important signaling role in the activation of various plant defense responses following pathogen attack through morphological,

physiological, and biochemical mechanisms. Plant innate immunity, including resistance in both local and systemic tissue upon biotic attacks, hypersensitive responses (HR), and cell death, all are required as key functions of SA at the whole plant level for disease resistance (Klessig et al. 2018, Huang et al. 2018a, Khan et al. 2022). SA plays a significant role in disease resistance involving pathogen-associated molecular pattern-triggered immunity (PTI), effector-triggered immunity (ETI), and systemic acquired resistance (SAR) (Pieterse et al. 2009, Dodds and Rathjen 2010, Spoel and Dong 2012, Tena 2021). SAR plays a role in resistance against hemibiotrophic pathogen *Foc* (Miyaji et al. 2017, Miyaji et al. 2021a) and biotrophic pathogen *A. candida* (Glazebrook 2005, Bari and Jones 2009, Pieterse et al. 2012, Klessig et al. 2018). Following a biotrophic pathogens attack, plants can initiate HR, a localized programmed cell death (PCD) response and SA contribute to the expression and regulation of HR (Heath 2000, Van Doorn 2011). SA-induced genes were identified at the whole genome level by RNA-sequencing (RNA-seq), and *Pathogenesis-related* (*PR*) genes were induced by SA treatments in *B. rapa* (Miyaji et al. 2021a). The signal molecule SA acts as a central regulator for SAR, and it is a mechanism of induced defense that confers long-lasting protection against a broad spectrum of microorganisms following initial localized infection (Kim and Lim 2023). SAR requires and is associated with the accumulation of PR proteins, which are thought to contribute to resistance. It occurs when a localized injury is created on the plant, resulting in a necrotic lesion (Pieterse et al. 2009, Vlot et al. 2009, Spoel and Dong 2012, Zhang et al. 2019).

To successfully defend against biotic stress-like diseases, plants' immune systems have the ability to recognize enemy molecules, and carry out signal transduction for surveillance, perception, and the activation of defense. Due to plant-pathogen interactions, a series of signal transmissions induce that accelerates the plant's host defense system against pathogens and as a result, leads to disease-resistance responses in turn. PTI and ETI are two plant innate immunity types that cooperate synergistically to provide robust immunity against pathogens. These are detected by cell surface-localized pattern-recognition receptors (PRRs) and intracellular nucleotide-binding domain leucine-rich repeat-containing receptors (NLRs). PTI is induced when membrane receptors perceive generic molecules from microorganisms; it provides basal immunity against entire classes of pathogens while ETI is activated by the recognition of secreted microbial effectors by intracellular receptors and induces strong, specific, and localized immune reactions (Chen et al. 2021b, Martel et al. 2021, Tena 2021, Ding et al. 2022).

Understanding the molecular mechanism(s) responsible for resistance in the control of disease is important for the breeding of disease resistance in *B. rapa* vegetables. We argued that *For* causes Fusarium yellows disease in *B. rapa* but no one identify the *R* gene. Generally,

mRNA regulates expression level and plays a role in defense mechanism but we wanted to know whether ncRNA including NATs regulates mRNAs following *Foc* inoculation and plays a role in defense response. We also wanted to know the role of SA treatment in transcriptional coordination between mRNAs and paired NATs. Another aim of this study was to gain insights into the immune responses of host plants against *A. candida* infection in *B. rapa* vegetables and to identify pathways or genes associated with the defense response to *A. candida* and contribute to understanding the disease resistance mechanism.

Chapter II

Development of a new DNA marker for Fusarium yellows resistance in *Brassica rapa* vegetables.

Abstract

In vegetables of *Brassica rapa* L., *Fusarium oxysporum* f. sp. *rapae* (*For*) or *F. oxysporum* f. sp. *conglutinans* (*Foc*) cause Fusarium yellows. A resistance gene against *Foc* (*FocBr1*) has been identified, and deletion of this gene results in susceptibility (*focbr1-1*). In contrast, a resistance gene against *For* has not been identified. Inoculation tests showed that lines resistant to *Foc* were also resistant to *For*, and lines susceptible to *Foc* were susceptible to *For*. However, prediction of disease resistance by a dominant DNA marker on *FocBr1* (Bra012688m) was not associated with disease resistance of *For* in some komatsuna lines using an inoculation test. QTL-seq using four F_2 populations derived from *For* susceptible and resistant lines showed one causative locus on chromosome A03, which covers *FocBr1*. Comparison of the amino acid sequence of *FocBr1* between susceptible and resistant alleles (*FocBr1* and *FocBo1*) showed that six amino acid differences were specific to susceptible lines. The presence and absence of *FocBr1* is consistent with *For* resistance in F_2 populations. These results indicate that *FocBr1* is essential for *For* resistance, and changed amino acid sequences result in susceptibility to *For*. This susceptible allele is termed *focbr1-2*, and a new DNA marker (focbr1-2m) for detection of the *focbr1-2* allele was developed.

Keywords: Fusarium yellows; *Fusarium oxysporum* f. sp. *rapae*; DNA marker; *R* gene; marker-assisted selection; QTL-seq; *Brassica rapa*

Introduction

Brassica rapa L. comprises a variety of vegetables that are rich sources of nutrients including vitamins, minerals, dietary fiber, and phytochemicals (Cheng et al. 2016, Lv et al. 2020a). In leafy vegetables of *B. rapa*, there are two morphotypes, heading types such as Chinese cabbage (var. *pekinensis*) and non-heading types such as pak choi (var. *chinensis*), komatsuna (var. *perviridis*) or chijimina (var. *narinosa*). Root vegetables such as turnip (var. *rapa*) also belong to *B. rapa* (Cheng et al. 2016, Lv et al. 2020a). Most commercial cultivars of these vegetables are F_1 hybrids, and hybrid vigor, disease resistance, and late bolting are important breeding traits (Fujimoto et al. 2018, Mehraj et al. 2020, Akter et al. 2021a). In particular, disease resistance is demanded by farmers, especially for soil-borne diseases that are difficult to control with chemicals (Lv et al. 2020b, Mehraj et al. 2020).

Plants have evolved their immunity to pathogens via two mechanisms (Jones and Dangl 2006, Dodds and Rathjen 2010). Pattern recognition receptors (PRRs) located in the plant cell membrane recognize pathogen-associated molecular patterns (PAMPs), which activate PAMP-triggered immunity (PTI) and restrict pathogen development. Most pathogens secrete effectors [(avirulence (AVR) proteins)] into plant cells to suppress PTI, while plants have various *resistance* (*R*) genes, which mainly encode Toll/Interleukin-1 receptor (TIR) or coiled-coil (CC), nucleotide- binding site (NBS), and leucine-rich repeat (LRR) domains, to detect effectors. Recognition of effectors by R proteins induces effector-triggered immunity (ETI), and recognition of specific effectors by R proteins is termed “gene-for-gene resistance” (Jones and Dangl 2006).

Fusarium oxysporum is a soil-borne fungus and comprises 150 host-specific formae speciales. *F. oxysporum* causes yellows in a wide range of host plants (Lv et al. 2020a, Mehraj et al. 2020). In *B. rapa* vegetables, two formae speciales of *F. oxysporum* f. sp. *conglutinans* (*Foc*) and f. sp. *rapae* (*For*) have been identified as causing Fusarium yellows (Enya et al. 2008). *Foc* was first reported as a causal agent of yellowing in cabbage (*Brassica oleracea* L. var. *capitata*) in 1913 (Lv et al. 2020a, Mehraj et al. 2020) and causes Fusarium yellows not only in *B. oleracea* vegetables including cabbage or broccoli but also in *B. rapa* vegetables including turnip, komatsuna, and pak choi (Enya et al. 2008, Pu et al. 2012, Lv et al. 2014, Shimizu et al. 2014, Shimizu et al. 2015). In contrast, *For* causes yellowing in *B. rapa* vegetables, but not in *B. oleracea* vegetables (Enya et al. 2008).

The Fusarium yellows *R* gene against *Foc* has been identified in *B. rapa* (*FocBr1*) and *B. oleracea* (*FocBo1*) (Lv et al. 2014, Shimizu et al. 2014, Shimizu et al. 2015, Akter et al.

2021b). *FocBr1* and *FocBo1* are orthologs and encode a TIR-NBS-LRR protein. In *B. rapa*, an approximately 35-kb deletion including *FocBr1* results in susceptibility (*focbr1-1*) and there are no reports of other causative mutations for susceptibility (Shimizu et al. 2014, Kawamura et al. 2016). In contrast, there are three different susceptible alleles of *FocBo1* in *B. oleracea* (*focbo1-1*, *focbo1-2,* and *focbo1-3*), but a 35-kb deletion similar to that in Fusarium yellows susceptible lines of *B. rapa* has not been identified (Lv et al. 2014, Shimizu et al. 2015, Kawamura et al. 2017, Sato et al. 2019).

The Fusarium yellows *R* gene against *For* (*ForBr1*) has not been identified. In this study, we performed QTL-seq to isolate *ForBr1*. We developed a DNA marker that can identify the susceptible alleles of Fusarium yellows and tested this marker in cultivars of *B. rapa* vegetables.

Materials and Methods

Plant materials and DNA and RNA extraction

The breeding lines and commercial F_1 hybrid cultivars of *B. rapa* vegetables were used as plant materials (Table II-1). F_2 populations were produced by bud pollination of F_1 hybrid crossing YBCG-11 x YBCG-12, YBCG-11 x YBCG-13, YBCG-11 x YBCG-14, YBCG-08 x YBCG-09, YBCG-TC01 x YBCG-10, and YBCG-11 x YBCG-10. Genomic DNA was isolated from leaves by the CTAB (cetyl trimethyl ammonium bromide) method (Murray and Thompson 1980). Total RNA was isolated from noninoculated leaves of ten-day-old seedlings by the SV Total RNA Isolation System (Promega Co., Madison, WI, USA).

Inoculation test

A strain of *F. oxysporum* f. sp. *rapae* (isolated from komatsuna) (provided by NARO, MAFF 240322) or *F. oxysporum* f. sp. *conglutinans* (isolated from cabbage) was used to prepare inocula. Liquid inocula were obtained by inoculating potato sucrose broth medium (200 g/L potato extract and 20 g/L sucrose in distilled water) with the isolate and shaking at 130 rpm on a rotary shaker for 1 week. Roots of ten-day-old seedlings were dipped in fungal spore suspension (fungal titer of ~5×10^6) for 5 h and then transplanted into a cell tray filled with soil. Plants were grown in the greenhouse, and two or three weeks after inoculation, individual plants were scored for interaction phenotype (IP) based on six categories that are 0 (no symptoms in tops and roots), 3 (darkening of roots, slight top stunting and no chlorosis), 5 (dark stunted roots, tops stunted and slight chlorosis of cotyledons), 7 (severe stunting of roots and tops and strong chlorosis) and 9 (severe stunting, necrosis, and death). To show the phenotype of breeding lines and cultivars, the average IP among 25 seedlings were categorized into resistant (IP = 0) or susceptible (IP = 3-9). Average IP of most resistant lines/cultivars was around 0 and average IP of most susceptible lines/cultivars was 9. However, some of the 25 seedlings of the line showed IP = 0 while others showed IP ≥ 3, and these exceptions are represented by R*. In the linkage analysis, F_2 seedlings were used for inoculation test, and phenotypes of individual seedlings were resistant (IP = 0) or susceptible (IP = 3-9). Chinese cabbage inbred lines RJKB-T23 and RJKB-T24 were used as a resistant and susceptible control (Shimizu et al. 2014).

QTL-seq

QTL-seq was performed following the method described in (Takagi et al. 2013). From F_2 populations derived from YBCG-11 x YBCG-12, YBCG-11 x YBCG-13, YBCG-11 x YBCG-14 and YBCG-08 x YBCG-09, about 20 plants were selected from resistant (IP = 0) and

susceptible (IP = 9) plants based on their perfect resistance or susceptible phenotype. The equal amount of DNA from each sample was bulked by resistant and susceptible phenotypes, and named R-bulk and S-bulk, respectively. Eight sequence libraries were prepared for DNA sequencing using TruSeq DNA PCR-Free kit (Illumina, Inc., San Diego, CA, USA), and sequenced by Illumina Hiseq 4000 (paired end, 150 bp). For detecting the parental SNPs, DNA from parental line (YBCG-08) was also sequenced.

Sequence reads were quality trimmed by FaQCs. Trimmed reads of R-bulk and S-bulk were aligned to the *B. rapa* reference genome version 3.0 (https://brassicadb.cn, accessed on 1 April 2021), and SNP index was calculated at all SNPs in R-bulk and S-bulk compared with resistant parental sequences, then the subtracted value of SNP-index of R-bulk from the SNP-index of S-bulk was calculated as ΔSNP-index using QTL-seq pipeline.

Prediction of Fusarium yellows resistance by DNA markers

To predict the Fusarium yellows resistance, the dominant marker Bra012688m (Kawamura et al. 2016) and codominant CAPS marker, focbr1-2m, were used. PCR was performed using QuickTaq®HS DyeMix (TOYOBO Co., Ltd., Osaka, Japan). The reaction mixture was incubated in the thermal cycler (TaKaRa PCR Thermal Cycler Dice® Gradient, Takara Bio Inc., Kusatsu, Japan) at 94 °C for 2 min followed by 35 cycles of 94 °C for 30 s, 55 °C for 30 s and 68 °C for 1 min. PCR products were detected by electrophoresis (i-MyRunII, COSMO BIO CO., LTD., Tokyo, Japan) using 1.0% agarose gel (Bra012688m). To distinguish the *FocBr1* and *focbr1-2* alleles, amplified DNA digested by *Hin*d III restriction enzyme were electrophoresed on 1.5% agarose gel. Two or more independent individual plants in each cultivar were tested for genotyping. The primer sets of the DNA markers are listed in Table II-2.

Gene expression analysis

cDNA was synthesized from 500 ng total RNA using ReverTra Ace qPCR RT Master Mix with gDNA Remover (TOYOBO Co., Ltd.). The specificity of the primer set of *FocBr1* was first tested by electrophoresis of RT-PCR amplified products using QuickTaq®HS DyeMix on 1.5% agarose gel in which a single product was observed. RT-PCR conditions were 94 °C for 2 min followed by 35 cycles of 94 °C for 30 s, 55 °C for 30 s, and 68 °C for 30 s. The absence of genomic DNA contamination was confirmed by the PCR of the no RT control. To distinguish the *FocBr1* and *focbr1-2* alleles, amplified DNA by RT-PCR digested by *Hin*d III restriction enzyme were electrophoresed on 1.5% agarose gel. The primer sets for RT-PCR are listed in Table II-2.

Results

Screening of lines for resistance to *F. oxysporum* f. sp. *rapae*

We have shown that *FocBr1* (Bra012688) is a resistance gene to *F. oxysporum* f. sp. *conglutinans* (*Foc*), and deletion of this gene results in susceptibility to *Foc* (Shimizu et al. 2014); this susceptible allele is termed *focbr1-1* (Akter et al. 2021b). We made a DNA marker (Bra012688m) to detect the deletion of *FocBr1* that is homozygous for the *focbr1-1* allele (Shimizu et al. 2014, Kawamura et al. 2016). In this study, we performed inoculation tests using *F. oxysporum* f. sp. *rapae* (*For*) for screening for resistant lines. Three Chinese cabbage (var. *pekinensis*), three turnip (var. *rapa*) and 22 komatsuna (var. *perviridis*) lines were tested of which 18 lines were resistant and 10 lines were susceptible (Table II-3). We also inoculated these 28 lines with *Foc*, and resistance to *For* and *Foc* was identical (Table II-3). We examined whether the results of the inoculation test were consistent with the prediction by *FocBr1* DNA marker (Bra012688m). In all lines of Chinese cabbage and turnip, the prediction by the DNA marker was identical to the resistance determined by the inoculation test, while in seven of 22 komatsuna lines (“Zaoh”, YBCG-12, YBCG-13, YBCG-14, YBCG-15, YBCG-TC02, and YBCG-TC05) the DNA marker prediction was not consistent with the results of the inoculation test (Table II-3). We tested an additional 15 lines of *B. rapa*; three lines (“Chijimikomatsuna”, “Tsunashima”, and “Hirose”) were not consistent between the DNA marker prediction and the results of the inoculation test using *For* (Table II-4).

Identification of the causative region of resistance for *F. oxysporum* f. sp. *rapae*

We performed linkage analysis using three individual F_2 populations derived from hybrids between *For* susceptible lines not containing the *FocBr1* deletion and resistant lines. In the 200 plants of the F_2 population derived from YBCG-11 (resistant) ×YBCG-12 (susceptible) hybrid, 169 plants were resistant and 31 plants were susceptible to *For*. The number of susceptible plants was too small to be explained by a single gene dominance (chi-squared test, $p < 0.05$) (Table II-5). This was also the case for the other two populations derived from YBCG-11 × YBCG-13 (susceptible) and YBCG-11 ×YBCG-14 (susceptible) hybrids (Table II-5). To identify the region covering the *R* gene for *For* (*ForBr1*), we performed QTL-seq analysis using bulked DNAs derived from about 20 resistant and susceptible individual plants derived from YBCG-11 ×YBCG-12, YBCG-11 × YBCG-13, or YBCG-11 × YBCG-14 hybrids and found one similar locus on chromosome A03 in all three populations (Figure II-1, II-2, II-3 and II-4). 22.0–33.5 Mb, 22.9–35.5 Mb, and 22.5–33.6 Mb region was detected as the QTL by 95% significance in the F_2 population derived from YBCG-11 × YBCG-12, YBCG-11 × YBCG-13, and YBCG-11

× YBCG-14 hybrid, respectively (Figure II-1). 1824, 1778, and 1734 genes were located in three QTLs, and 1655 genes overlapped (Figure II-5). A domain search using HMMSCAN with Pfam database and NCBI conserved domain search found nine genes encoding NBS-LRR proteins, including *FocBr1* (BraA03g047240.3C or Bra012688) (Table II-6).

A new susceptible allele of *FocBr1* was identified

Because *FocBr1* was included in three QTLs, we focused on *FocBr1* for further analysis. The expression level of *FocBr1* in three susceptible lines ("Zaoh", YBCG-12, and YBCG- 15) was similar to that of resistant lines (YBCG-11 and YBCG-16) (Figure II-6), indicating that expression levels are not related to susceptibility. Next, we compared the amino acid sequences of FocBr1 in resistant and susceptible lines. The amino acid sequence of FocBr1 in the resistant line, YBCG-11, was 100% identical to *FocBr1* in the resistant line, RJKB-T23 (Shimizu et al. 2014). Amino acid sequences of *FocBr1* were 100% identical among bulked DNAs of susceptible plants derived from F_2 populations of YBCG-11 × YBCG-12, YBCG-11 × YBCG-13, and YBCG-11 × YBCG-14 hybrids, but there were some substitutions of amino acid sequences compared with *FocBr1* in YBCG-11 (Figure II-7). There were eleven amino acid sequence differences in FocBr1 between resistant and susceptible lines; five (A546T, N721D, T803K, V805E, and K862N) of which were identical between FocBr1 in the susceptible lines and the resistant allele of FocBo1 (*B. oleracea*) (Figure II-7). Both FocBr1 and FocBo1 are resistance genes to *Foc*, indicating that the difference of amino acid sequences between FocBr1 and FocBo1 might not relate to the Fusarium yellows resistance, and the identical amino acid sequences between susceptible lines and *FocBo1* might not lead to its susceptibility. The remaining six amino acid changes (Q859W, M869K, L1060F, V1148L, K1212T, and Q1395L) differed between susceptible lines (YBCG-12, YBCG-13, and YBCG-14) and resistance lines of *B. rapa* and *B. oleracea* (Figure II-7), which are susceptible line specific, suggesting that some of these amino acid sequences specific to susceptible lines result in susceptibility to *For*; some mutations may result in loss of function.

We examined whether *FocBr1* deletion (*focbr1-1*) causes susceptibility to *For*. Linkage analysis using three individual F_2 populations derived from hybrids between *For* susceptible lines (*focbr1-1*) and resistant lines [(YBCG-08 (resistant) × YBCG-09 (susceptible), YBCG-TC01 (resistant) × YBCG-10 (susceptible), and YBCG-11 × YBCG-10)] showed that the number of resistant and susceptible plants segregated as 3:1 ratio (chi-squared test, $p > 0.05$) (Table II-5). QTL-seq analysis using bulked DNAs derived from about 20 resistant and susceptible plants of the F_2 population derived from YBCG-08 × YBCG-09 hybrid found one

causative locus (19.0–36.6 Mb) on chromosome A03, which covers the *FocBr1* locus (Figure II-1 and Figure II-8). We tested a DNA marker (Bra012688m) in 12 resistant and susceptible plants from these three F_2 populations, and the presence and absence of *FocBr1* was consistent with the inoculation test (Figure II-9). These results indicate that *FocBr1* is essential for resistance to not only *Foc* but also *For*, supporting the suggestion that mutations cause susceptibility to *Foc* and *For*. This susceptible allele was termed *focbr1-2*.

Development of a new DNA marker for Fusarium yellows resistance

Using sequence polymorphism between *FocBr1* and *focbr1-2*, a new cleaved amplified polymorphic sequence (CAPS) DNA marker (focbr1-2m) was developed. Using this DNA marker, genotypes of 12 resistant and susceptible plants in three F_2 populations derived from YBCG-11 × YBCG-12, YBCG-11 × YBCG-13, and YBCG-11 × YBCG-14 hybrids were confirmed, and genotypes were identical to the resistance determined by the inoculation test (Table II-7). All ten lines that were not consistent between *For* inoculation test and the DNA marker (Bra012688m) prediction had homozygous *focbr1-2* or heterozygous *focbr1-2* and *focbr1-1* alleles (Tables II-3, Table II-4 and II-8). Another 33 *B. rapa* lines were consistent between the inoculation test using *For* and prediction by DNA marker (focbr1-2m) (Table II-8). These results indicate that this new DNA marker can detect not only the *focbr1-1* susceptible allele but also the *focbr1-2* allele.

Prediction of Fusarium yellows resistance in commercial *B. rapa* by DNA marker

Using the focbr1-2m marker, we predicted the resistance to *For* in 157 cultivars of Chinese cabbage, 35 cultivars of turnip, 40 cultivars of pak choi, and 73 cultivars of komatsuna. Of 157 cultivars of Chinese cabbage, six cultivars (3.8%) were heterozygous for *FocBr1*/*focbr1-2*, and there were no cultivars homozygous for *focbr1-2*/*focbr1-2* or heterozygous for *focbr1-2*/*focbr1-1* (Table II-9). There were six Chinese cabbage cultivars (3.8%) homozygous for *focbr1-1*/*focbr1-1* (Table II-9), which could be susceptible to either *For* or *Foc*. Of 35 cultivars of turnip, five cultivars (14.3 %) were heterozygous for *FocBr1*/*focbr1-2*, and there were no cultivars homozygous for *focbr1-2*/*focbr1-2*, *focbr1-1*/*focbr1-1*, or heterozygous for *focbr1-2*/*focbr1-1* (Table II- 9). Of 40 cultivars of pak choi, 16 cultivars (40.0%) were heterozygous for *FocBr1*/*focbr1-2*, and there were no cultivars homozygous for *focbr1-2*/*focbr1-2*, *focbr1-1*/*focbr1-1*, or heterozygous for *focbr1-2*/*focbr1-1* (Table II-9). Of 73 cultivars of komatsuna, 21 cultivars (28.8%) were heterozygous for *FocBr1*/*focbr1-2*, and five cultivars (6.8%) were homozygous for *focbr1-2*/*focbr1-2* or heterozygous for *focbr1-2*/*focbr1-1*. There were three

cultivars (4.1%) homozygous for *focbr1-1*/*focbr1-1* (Table II-9). Cultivars with *focbr1-2*/*focbr1-2* or *focbr1-2*/*focbr1-1* were found only in komatsuna.

Discussion

Previously, we identified a resistance gene to *Foc* (*FocBr1*), which is a single dominant gene. In susceptible lines, a 35 kb deletion, which includes *FocBr1,* was found (Shimizu et al. 2014), and the susceptible allele was termed *focbr1-1* (Akter et al. 2021b). A dominant DNA marker (Bra012688m) has been made and the prediction of *Foc* resistance using Bra012688m was consistent with phenotypes of *Foc* resistance confirmed by an inoculation test in inbred lines of Chinese cabbage (Shimizu et al. 2014, Kawamura et al. 2016). In this study, we inoculated *Foc* and other formae speciales, *For*, to Chinese cabbage, turnip, pak choi, komatsuna, and chijimina lines, and we found the prediction using Bra012688m was not consistent with phenotype using inoculation test in some lines, especially in komatsuna. To clarify the inheritance pattern of the *R* gene to *For*, we performed linkage analysis. Three F_2 populations derived from crosses between *For* resistant and susceptible lines (*focbr1-1*) showed a 3:1 ratio of resistant to susceptible plants. In contrast, the other three F_2 populations derived from crosses between *For* resistant and susceptible lines (*focbr1-2*) did not show a 3:1 ratio of resistant to susceptible plants; the number of susceptible plants of the F_2 population is smaller than the expected number. However, QTL-seq using these populations identified one causative locus. This could be a difference in the detail of the loss of function; *FocBr1* of *focbr1-2* allele might have a weak function against *For* or be susceptible to environmental effects, although the *focbr1-1* allele has completely lost its function. However, as both alleles showed a strong susceptible phenotype and we could not identify any significant difference between these two alleles in *B. rapa* lines, further analysis will be needed to identify this minor difference between *focbr1-1* and *focbr1-2* alleles.

QTL-seq analysis using F_2 populations derived from crosses between *For* resistant and susceptible lines with the *FocBr1* deletion (*focbr1-1*) or without the *FocBr1* deletion (*focbr1-2*) identified the same single causative locus for *For* resistance, which covered *FocBr1*. There was no difference in expression levels of *FocBr1* between resistant and susceptible lines, but there were some amino acid sequence differences between For susceptible allele *(focbr1-2*) and resistant alleles (FocBr1 and FocBo1), suggesting that changes of amino acid sequence result in loss of function. Some substitutions were in the LRR region, and these susceptible line-specific amino acid changes may lead to loss of recognition of AVR. This new allele might be useful for identifying the sequence that is important for the interaction between R and AVR proteins. To prove this amino acid sequences change results in loss of function, which might be due to loss of recognition to AVR, further experiments such as making transgenic plants for complementation or loss of function by CRISPR-Cas9 system will be required.

Alternatively, other gene(s) linked to the *FocBr1* locus may work together with *FocBr1* for *For* resistance, because the peak detected by QTL-seq is upstream from the *FocBr1* position in three F_2 populations derived from crosses between *For* resistant and susceptible lines (*focbr1-2*). In *Arabidopsis thaliana*, TIR-NBS-LRR type *Resistance to Ralstonia solanacearum 1* (*RRS1*) and *Resistance to Pseudomonas syringae 4* (*RPS4*) are neighboring genes and both are required for resistance to *Colletotrichum higginsianum*, *Ralstonia solanacearum,* and *Pseudomonas syringae* pv. *tomato* strain DC3000 expressing *avrRps4* (Narusaka et al. 2009). *RRS1* encodes a WRKY domain protein as well as a TIR-NBS-LRR protein and works as a "sensor" to detect the effector, and RPS4 works as a "helper" to activate cell death (Huh et al. 2017, Ma et al. 2018) If a similar function is applied to Fusarium yellows resistance, *FocBr1* will work as a "sensor" NBS- LRR with other "helper" gene(s), which may be located on a region upstream from *FocBr1*. Resistant and susceptible alleles of "sensor", *FocBr1* and *focbr1-2*, might be able to recognize AVR to greater or lesser degrees, respectively, and other "helper" gene(s) might have different functions between resistant and susceptible lines, resulting in a shift of QTL peak to upstream. Further analyses using plants recombined between QTL peak locus and *FocBr1* gene are required to clarify whether other factor(s) are important for *For* resistance and the *For* infection mechanisms. There is also another possibility that minor QTLs not linked to *FocBr1* locus are important for resistance to *For*.

Using a new DNA marker, focbr1-2m, we screened genotypes of *B. rapa* breeding lines and cultivars. There were six lines that showed weak resistance against *For* and *Foc*, and three of the six lines ("CR-Taiga", "Natsurakuten", and YBCG-TC04) showed heterozygosity of *FocBr1* and *focbr1-2*. However, in the remaining three lines ("CR-Yukiakari", NSI-01, and YBCG-18), we cannot distinguish between the homozygosity of *FocBr1* and the heterozygosity of *FocBr1* and *focbr1-1*, because *focbr1-1* results in deletion of *FocBr1* and focbr1-2m cannot amplify *focbr1-1* allele. In *B. rapa*, plants having a homozygous clubroot resistance gene show more stable clubroot resistance than plants having a heterozygous resistance gene (Suwabe et al. 2003, Nomura et al. 2005, Nagaoka et al. 2010). Three lines may be heterozygous for *FocBr1* and *focbr1-1*. In the case of *focbr1-1*, it is desirable to develop a DNA marker to distinguish between *FocBr1*/*focbr1-1* heterozygosity and *FocBr1*/*FocBr1* homozygosity, i.e., using a linked marker close to the 35-kb deletion (Akter et al. 2021b). In the case of *focbr1-2*, the codominant DNA marker, focbr1-2m, distinguish the heterozygosity of *FocBr1* and *focbr1-2* alleles, which will be useful for breeding stable Fusarium yellows resistant cultivars.

In Chinese cabbage cultivars, there were no cultivars homozygous for *focbr1-2*, and a few lines heterozygous for *FocBr1*/*focbr1-2*. In our previous study using the Bra012688m

marker, there was complete agreement between the DNA marker-based prediction and the inoculation test in Chinese cabbage lines (Kawamura et al. 2016). Thus, there is little risk that the presence of the *focbr1-2* allele leads to susceptibility during the breeding of Fusarium yellows resistant cultivars in Chinese cabbage. Like in Chinese cabbage, most turnip cultivars (about 85%) did not have *focbr1-2* alleles, so this allele will not be a problem for breeding. However, in pak choi, 40% of cultivars were heterozygous for *FocBr1* and *focbr1-2* alleles. In komatsuna, about 30% of cultivars were heterozygous for *FocBr1* and *focbr1-2* alleles and about 7% of cultivars were homozygous for *focbr1-2* allele or heterozygous for *focbr1-2* and *focbr1-1* alleles. For the breeding of Fusarium yellows resistant cultivars in pak choi or komatsuna, the presence of the *focbr1-2* allele should be mapped in breeding lines, and the DNA marker, focbr1-2m, developed in this study will be useful for DNA marker-assisted selection.

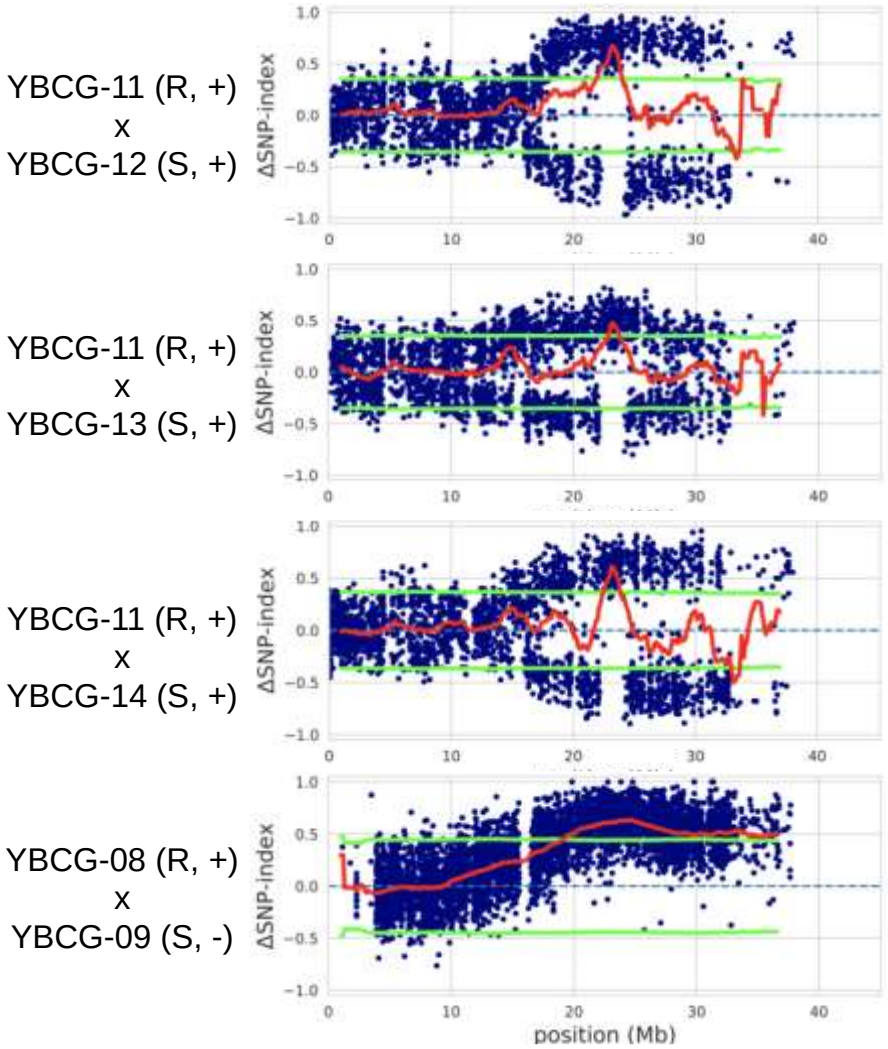

Figure II-1. QTL-seq results on chromosome A03. F_2 populations derived from YBCG-11 x YBCG-12, YBCG-11 x YBCG-13, YBCG-11 x YBCG-14, and YBCG-08 x YBCG-09 were used. Blue dots indicate ΔSNP-index, and the red line indicates the sliding window average of ΔSNP-index. Light green lines represent $p < 0.05$. R and S represent resistant and susceptible, respectively. + and − represent the presence and absence of PCR amplification of Bra012688m marker, respectively.

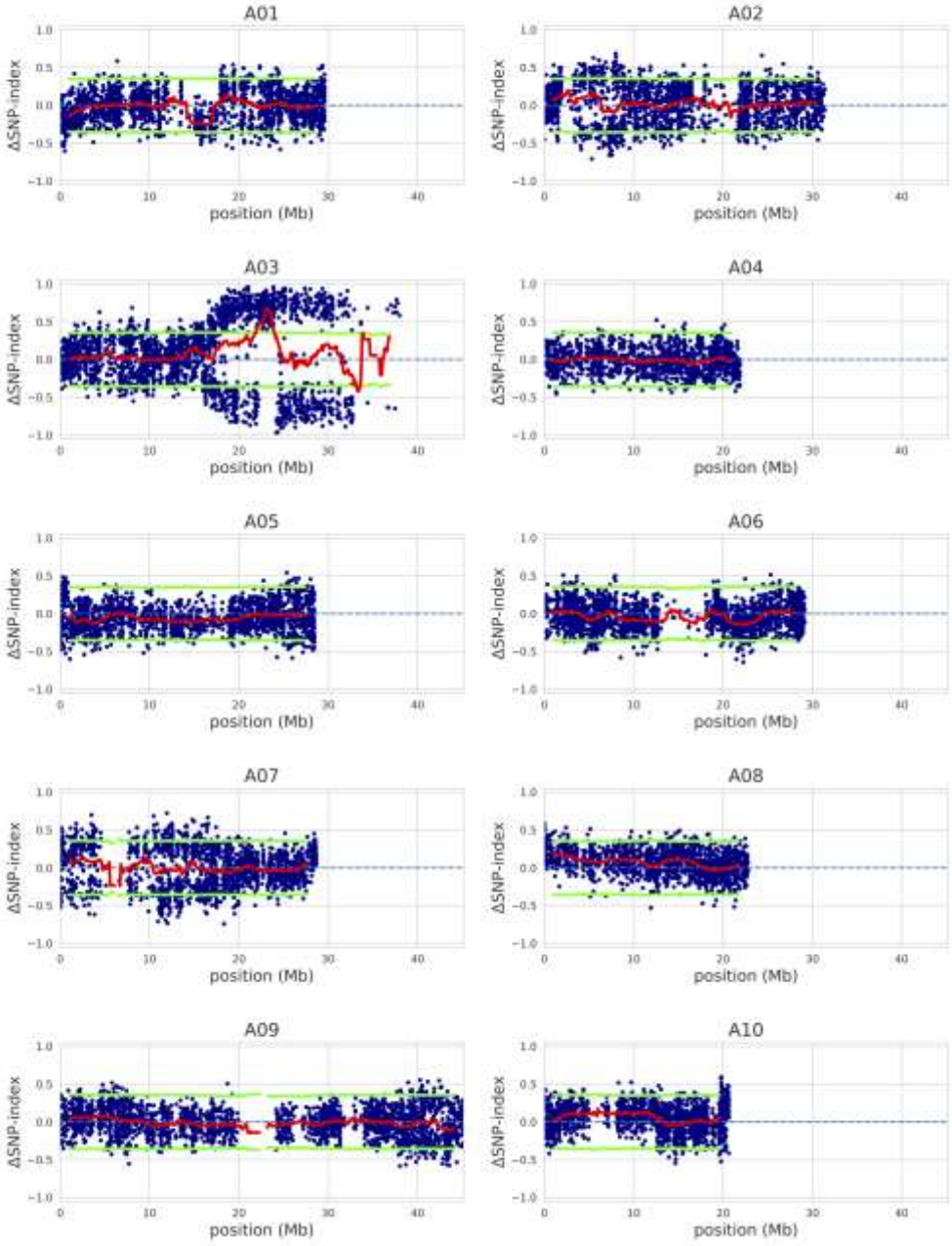

Figure II-2. QTL-seq results of all chromosomes of F_2 populations derived from YBCG-11 x YBCG-12 hybrid. Blue dots indicate ΔSNP-index, and red line indicates the sliding window average of ΔSNP-index. Light green lines represent $p < 0.05$.

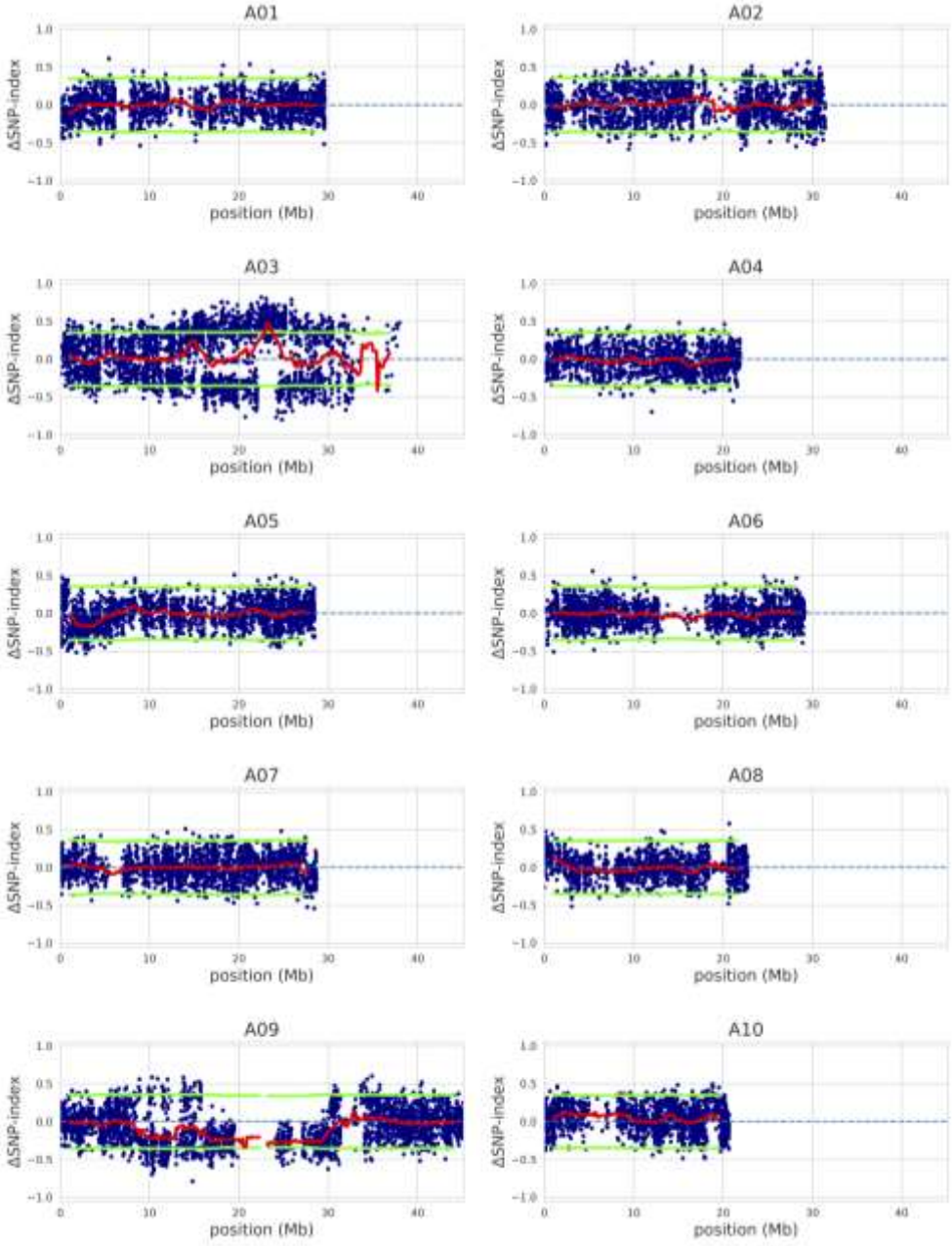

Figure II-3. QTL-seq results of all chromosomes of F_2 populations derived from YBCG-11 x YBCG-13 hybrid. Blue dots indicate ΔSNP-index, and red line indicates the sliding window average of ΔSNP-index. Light green lines represent $p < 0.05$.

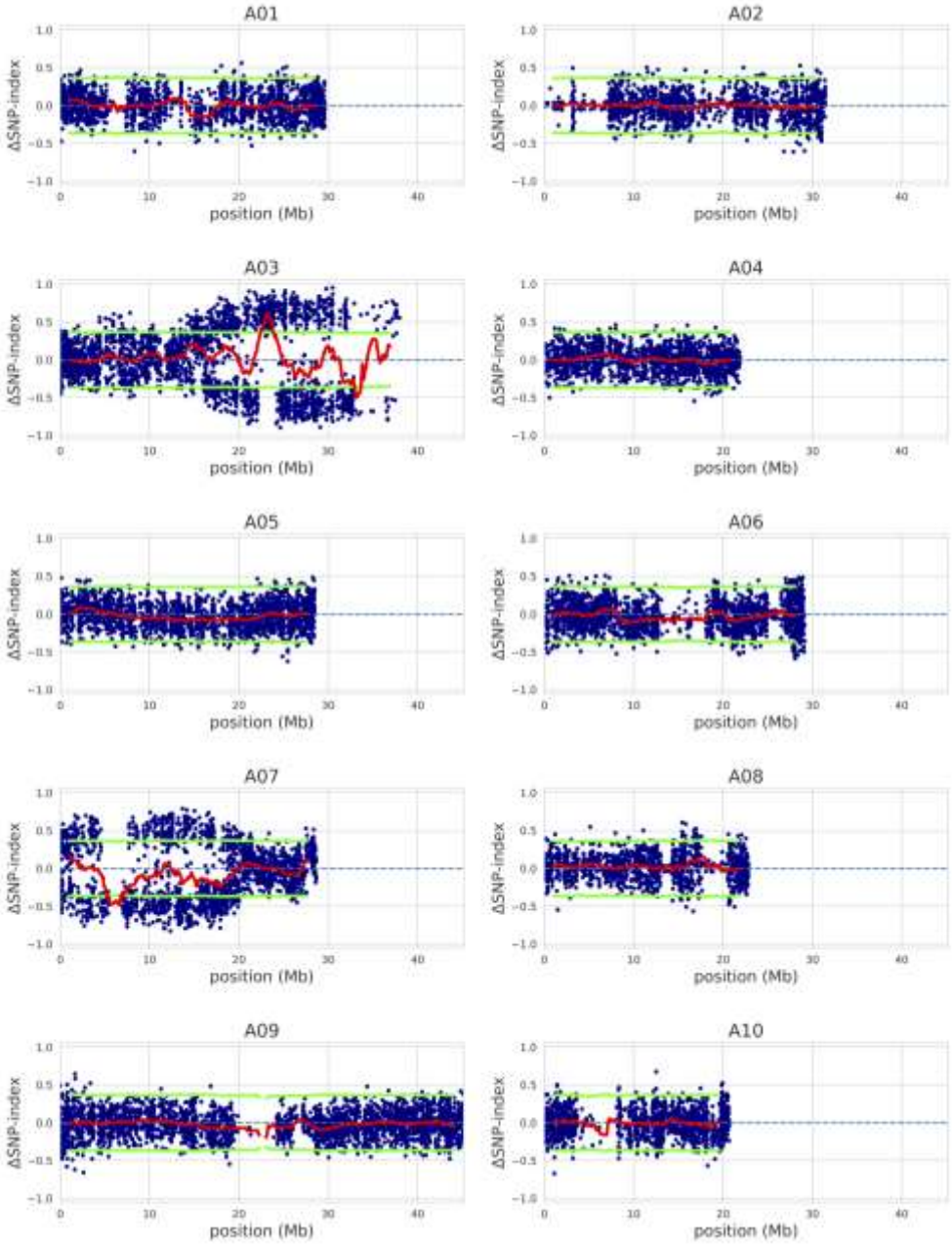

Figure II-4. QTL-seq results of all chromosomes of F_2 populations derived from YBCG-11 x YBCG-14 hybrid. Blue dots indicate ΔSNP-index, and red line indicates the sliding window average of ΔSNP-index. Light green lines represent $p < 0.05$.

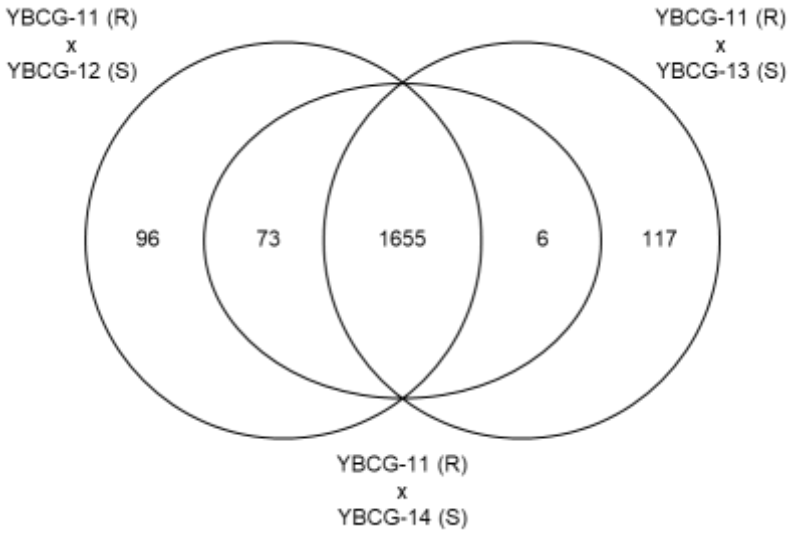

Figure II-5. Overlapped candidate genes in three F_2 populations. Coding genes on each candidate locus on chromosome A03 were compared between three F_2 populations derived from YBCG-11 x YBCG-12, YBCG-11 x YBCG-13, or YBCG-11 x YBCG-14.

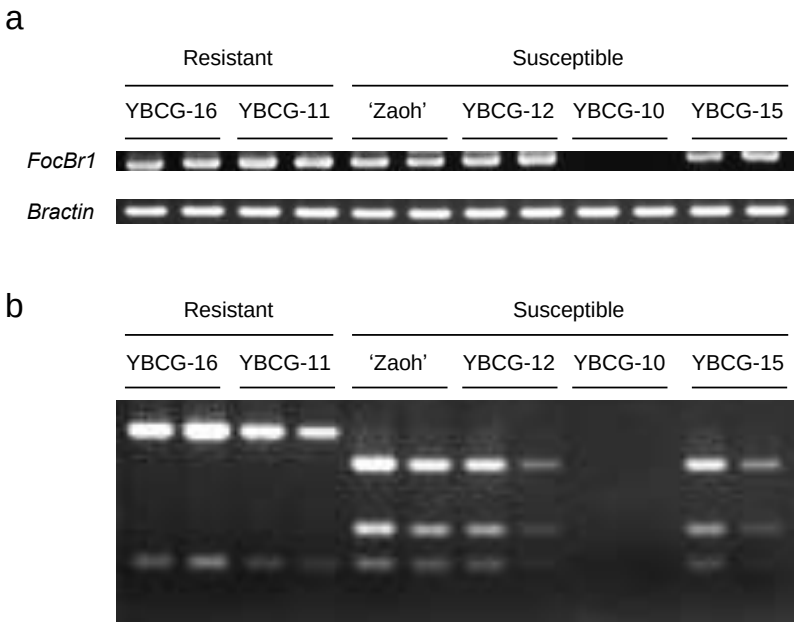

Figure II-6. Expression and genotype of *FocBr1* in *For* resistant and susceptible lines. (a) Expression of *FocBr1* and *Bractin* (control) was confirmed by RT-PCR. (b) DNA fragments of RT-PCR products digested by Hind III. YBCG-16 and YBCG-11 have *FocBr1*/*FocBr1* homozygous or *FocBr1*/*focbr1-1* heterozygous alleles. "Zaoh", YBCG-12 and YBCG-15 have *focbr1-2*/*focbr1-2* homozygous or *focbr1-2*/*focbr1-1* heterozygous alleles, and YBCG-10 has *focbr1-1*/*focbr1-1* homozygous allele.

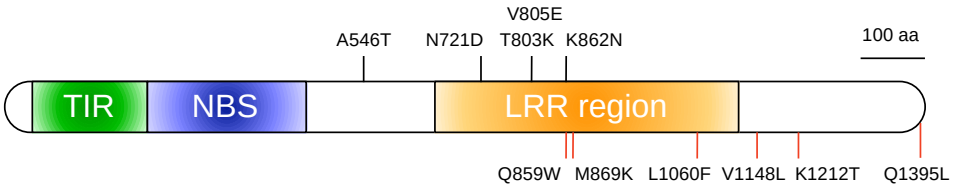

Figure II-7. Protein structure of *FocBr1* in the resistant line of *B. rapa*. TIR (green box), NBS (blue box), and LRR region (orange box) were identified. Black lines represent the position of difference of amino acid sequences between resistant and susceptible lines in *B. rapa*, while amino acid sequences of FocBr1 in the susceptible lines were identical to the FocBo1 (*Foc* resistance gene in *B. oleracea*). Red lines represent the position of susceptible line-specific amino acid substitutions. Domains were predicted using HMMSCAN with Pfam database. (https://www.ebi.ac.uk/Tools/hmmer/, accessed on 1 April 2021) and NCBI conserved domain search (https://www.ncbi.nlm.nih.gov/Structure/cdd/wrpsb.cgi, accessed on 1 April 2021).

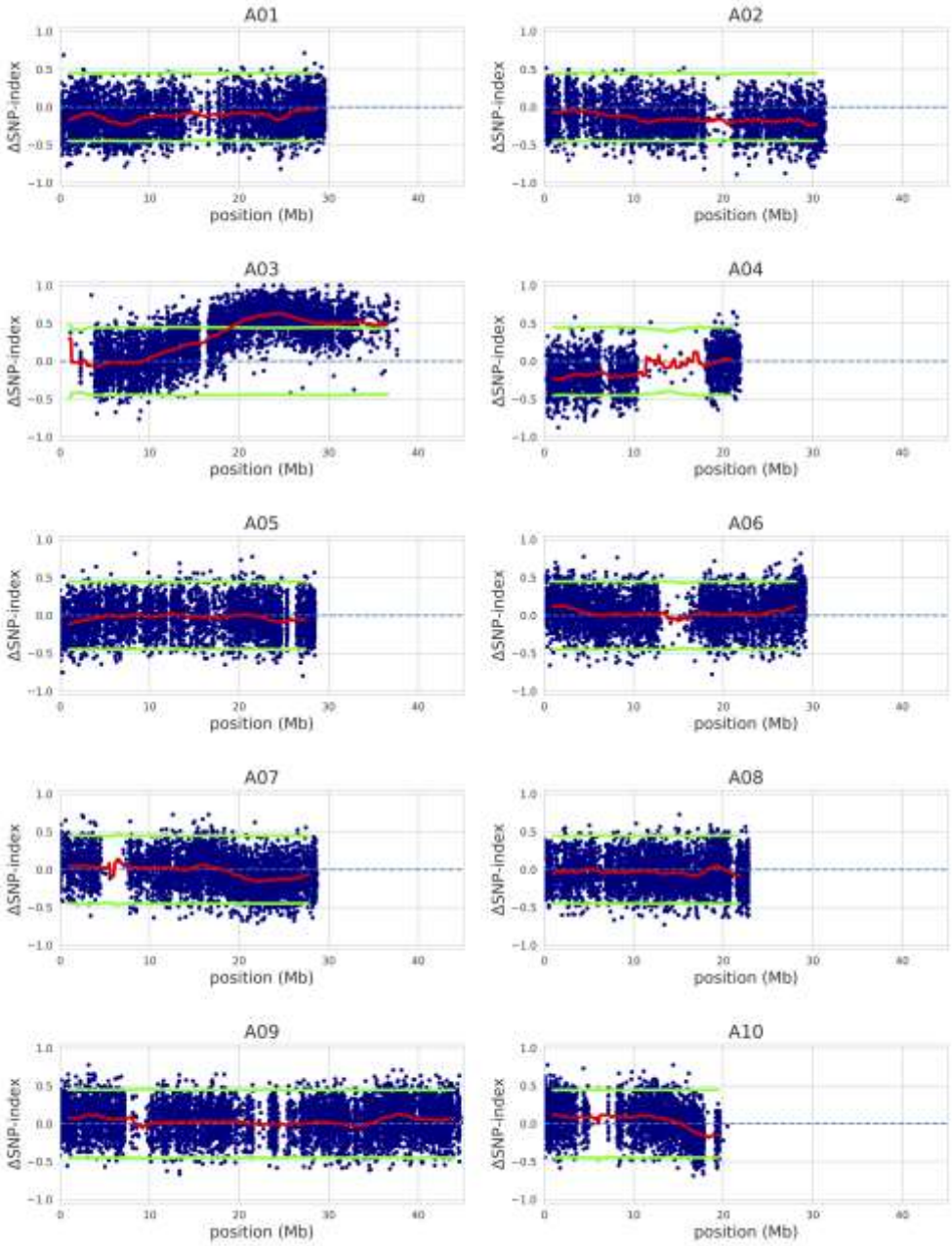

Figure II-8. QTL-seq results of all chromosomes of F_2 populations derived from YBCG-08 x YBCG-09 hybrid. Blue dots indicate ΔSNP-index, and red line indicates the sliding window average of ΔSNP-index. Light green lines represent $p < 0.05$.

Figure II-9. *FocBr1* genotype of resistant and susceptible plants in three F_2 populations (YBCG-08 x YBCG-09, YBCG-TC01 x YBCG-10, and YBCG-11 x YBCG-10). Twelve resistant and susceptible plants were confirmed using *FocBr1* DNA marker (Bra012688m).

Table II-1. List of cultivars used in this study

Chinese cabbage	Turnip	Komatsuna	Pak choi
Ishii Seed Growers CO., LTD.			
‘CR-Seiga-65’			
‘CR-Seiga-75’			
‘Fuyusae’			
‘Kinami 90’			
‘Ryokuun’			
‘Saegi-90’			
‘Senju’			
‘Tokimeki-85’			
KANEKO SEEDS CO., LTD.			
‘Bandou’	‘Yukiwarashi’	‘Inasena’	‘Natsugozen’
‘Eiki‘		‘Koishiina’	‘Fuyugozen’
‘Gokui‘		‘Sugoina’	
‘Kibouhou-90’		‘Sutekidana’	
‘Kibouhou-65’		‘Yokattana’	
‘Kibouhou-80’		‘Yokattana-G’	
‘Kisho’			
‘Kishou’			
‘Kizuki-90’			
‘Moegi’			
‘Shouki’			
Kobayashi-Seed CO., LTD.			
		‘Ajinami‘	
MARUTANE CO., LTD.			
‘Chikara’	‘CR-ajikurabe’		
‘CR-kyotakara-80’			
‘Kisaku-60’			
‘CR-kisaku-80’			
‘Kyouryoku-60-nichi’			
‘Mini-raiou-65’			
‘Ousan’			
‘Raiou-65’			
‘Raiou-90’			
‘Shin-hayabusa’			
Matsunaga Seed CO., LTD.			
‘Renpa’			
‘Soumei’			
MIKADO KYOWA SEED CO. LTD			

	‘Natsuhakurei’		
Musashino Seed CO., LTD.			
	‘Aishinku No.3’	‘Fuyusato’	‘Daigomi’
	‘CR-takamaru’	‘Ryokutomi’	‘Fuyusyomi’
	‘CR-shirayuki’	‘Satoakari’	‘Fuyutaisyo’
	‘CR-yukimine’	‘Satogokoro’	‘Harusyomi’
	‘Hakuba’	‘Satokirari’	‘Ikigomi’
	‘Hakuju’	‘Satoshizuku’	‘Koropokkuru’
	‘Hakutaka‘		‘Natsusyomi’
	‘Hekiju‘		‘Natsusyomi No.2’
	‘Manju’		‘Rakusyomi’
	‘Shirokamome’		‘Tsurin’
	‘Tamasato’		
	‘Yukibotan’		
Nakahara Seed Product CO., LTD.			
‘Chabo-hakusai’		‘Komatsuna’	
‘Kokuhou-65-nichi’		‘Natsuwakana’	
‘Kokuhou-85-nichi’		‘Yumewakana’	
‘Ouriki-75-nichi’			
Nanto Seed CO., LTD.			
‘CR-Ifu-gogo’		‘Yamato Mana’	
‘CR-Kinsyachi-75’			
‘CR-Kinsyachi-85’			
‘Kimusan-75’			
‘Medaka’			
‘Taibyou-Apolo-60’			
Nippon Norin Seed CO.			
‘Akifuku’	‘CR-Kirarinonatsu’	‘Edonokomachi’	‘Enron’
‘Akimeki’	‘Kirarinoyume’	‘Edonomai’	‘Furon’
‘Akirisou’		‘Edonomatsuri’	‘Hairon’
‘CR-Kanki No.100’		‘Kagurazaka’	‘Seiron’
‘EX-King-Santou’		‘Nogizaka’	‘Shenron’
‘Harurisou’			‘Taron’
‘Kanjiro’			
‘Kanmidori’			
‘Kien 75’			
‘Kien-80’			
‘Kifuku-65’			
‘Kikumusume 65’			
‘Kikumusume-80’			
‘Shin-Risou’			

‘Shin-Risou-Megumi’			
‘Super-CR-Akinishiki’			
‘Super-CR-Shinrisou’			
Noguchi seed			
		‘Shinbansei Komatsuna’	
NOHARA SEED CO., LTD.			
		‘Hiromi’	
		‘Nacchan’	
NOZAKI SAISHUJO LTD.			
‘Chi-chai-na’	‘Wase Imaichikabu’	‘Manaka’	
‘Eishun’			
‘Futamiki’			
‘Fuyu-no-megumi’			
‘Hanaki’			
‘Maiko’			
‘Megumi No.2’			
‘Mibae’			
‘No. 1’			
‘No. 2’			
‘No. 3’			
‘Nozaki-Harumaki No.1’			
‘Nozaki-hifumi’			
‘Nozakihakusai No.2’			
‘Retasai’			
‘Teruki’			
‘Wase-Eiho’			
SAKATA SEED CORPORATION			
‘Chiyobuki-85’	‘Mifune’	‘Hakkei’	‘Aosae’
‘Fuyutsuki-90’	‘Nitou’	‘Hamami No.2’	‘Entei’
‘Minebuki-505’		‘Hamatsuzuki’	‘Kunyan’
‘Satobuki-613’		‘Hazuki’	‘Butei’
‘Tainishushu’		‘Inamura’	‘Natsumikado’
‘Tomikaze’		‘Kiyosumi’	‘Raiko’
‘Toyokaze’		‘Misugi’	‘Ryobu’
‘Yukikaze’		‘Nakamachi’	‘Seitei’
‘Yumebuki 502’		‘Sakuragi’	‘Syanhai’
		‘Tsunashima’	

		‘Wakami’	
Syngenta			
‘Kirami’			
TAKAYAMA SEED CO., LTD.			
		‘Haruna’	
TAKII & CO., LTD.			
‘Banki’	‘CR Mochibana’	‘Gokurakuten’	
‘CR-Okiniiri’	‘CR-Shirowarabe’	‘Nanako’	
‘Fuyutouge’	‘CR-Yukibana’	‘Nanami’	
‘Haregi-60’	‘Fukukomachi’	‘Nanase’	
‘Haregi-65’	‘Koyukimaru’	‘Natsurakuten’	
‘Haregi-75’	‘Kyokomachi’		
‘Haregi-85’	‘Natsukomachi’		
‘Haregi-90’	‘Suwan’		
‘Homare-2-gou’			
‘Kigokoro-65’			
‘Kigokoro-75’			
‘Kigokoro-80’			
‘Kigokoro-85’			
‘Kigokoro-90’			
‘Kinshou-2-gou’			
‘Kinshu’			
‘Kiraboshi 80’			
‘Kiraboshi-65’			
‘Kiraboshi-77’			
‘Kiraboshi-85’			
‘Kiraboshi-90’			
‘Kyoto-3-gou’			
‘Meishun’			
‘Muso’			
‘Nozaki-2-gou’			
‘Oushou’			
‘Puchihiri’			
‘Shin-Azuma’			
‘Shoushun’			
‘Taibyou-60-nichi’			
TOHOKU SEED CO., LTD.			
‘Daifuku 206’	‘CR-Hakuryo’	‘Hitomi’	‘Kazue’
‘Daifuku-209’	‘CR-Shirane’	‘Masami’	‘Ryokuyou’
‘Daifuku-234’	‘Houmi’	‘Minami’	
‘Daifuku-75’	‘Nyushirane’	‘Natsuki’	
‘Harutourai’	‘Tokinashikokabu’	‘Shosai’	

‘Kikunishiki’	‘Yukinohana’		
‘Kiraku-60’			
‘Kiraku-70’			
‘Kiraku-80’			
‘Kiraku-90α’			
‘Yuifuku’			
‘Yuifuku-78’			
TOKITA SEED CO., LTD.			
‘Mainoumi’		‘Harunosenbatsu’	‘Kako’
‘Wawasai’		‘Kuniyoshi’	‘Tonko’
		‘Natsunokoshien’	
		‘Sharaku’	
		‘Shutonoesu’	
WATANABE SEED CO., LTD.			
‘Chushu’	‘CR-Yukiakari’	‘Chijimi Komatsuna’	‘Ryoutou’
‘CR Olympia’		‘Kahoku’	
‘Fuyunosaiten’		‘Zao’	
‘Harunosaiten’			
‘Harusakari’			
‘Kiai 90’			
‘Kiai-65’			
‘Kian 75’			
‘Kikou’			
‘Kikou-85’			
‘Kurimu No. 2’			
‘Matsushimajun-2-go’			
‘Megohime’			
‘Menkoi’			
‘Natsu-no-saiten’			
‘Olympia’			
‘Oushin-Sprinter’			
‘Shin No. 6’			
‘Shin-Ryutoku’			
‘Shoutoku’			
‘Strong CR75’			
‘Tsuyoki’			
‘W77’			
Watanabe Noji CO., LTD.			
‘Fuyutourai-75’		‘Enka’	‘Niihaosanka’
‘Fuytourai-90’		‘Misui’	‘Niihao-syan’
		‘Murasakimatsuri’	‘Niihao-shin No.1’
		‘Seiichiro’	‘Niihao-mei’

		‘Yousui’	‘Niihao 114’
		‘Yusui’	
SNOW BRAND SEED CO., LTD.			
		‘Acchan’	
		‘Hamachan’	
		‘Kenchan’	
		‘Macchan’	
		‘Norichan’	
		‘Suchan’	
YAMATO NOEN CO., LTD.			
‘Ama-Baby’			
‘Eigyoku’			
‘Ooyorokobi’			
‘Sankimakihaou’			
Breeding materials			
RJKB-T23	NSI-01	YBCG-08	YBCG-TC01
RJKB-T24		YBCG-09	YBCG-TC02
RJKB-T36		YBCG-10	YBCG-TC03
RJKB-T37		YBCG-11	YBCG-TC04
RJKB-T38		YBCG-12	YBCG-TC05
RJKB-T39		YBCG-13	YBCG-TC06
RJKB-T40		YBCG-14	
		YBCG-15	
		YBCG-17	
		YBCG-18	

Table II-2. List of primer sequences.

	Forward primer (5' to 3')	Reverse primer (5' to 3')
Genotyping		
Bra012688m	AGTCGCTTGGAAGTCTGAGG	GAGCTAACCAACTATACATTGAACC
focbr1-2m	AAATTCCTGATCTGTCAAATGCC	AGCCTCACCAGATTTCCAAGTGA
RT-PCR		
FocBr1	CGTCCTCAGACTTCCAAGCG	CGTCCTCAGACTTCCAAGCG
Bractin-RT	CGGTCCAGCTTCGTCATACTCAGCC	AAATGTGATGTGGATATCAGGAAGG

Table II-3. Assessment of Fusarium yellows resistance by inoculation test.

Name	Inoculation Test		Prediction by DNA Marker
	For	*Foc*	Bra012688m
"W77"	R	R	+
RJKB-T23	R	R	+
RJKB-T24	S	S	-
"CR-Yukiakari"	R*	R*	+
"Hekiju"	R	R	+
NSI-01	R*	R*	+
"CR-Taiga"	R*	R*	+
"Manaka"	R	R	+
"Nanami"	R	R	+
"Natsurakuten"	R*	R*	+
"Zaoh"	S	S	+
YBCG-08	R	R	+
YBCG-09	S	S	-
YBCG-10	S	S	-
YBCG-11	R	R	+
YBCG-12	S	S	+
YBCG-13	S	S	+
YBCG-14	S	S	+
YBCG-15	S	S	+
YBCG-16	R	R	+
YBCG-17	R	R	+
YBCG-18	R*	R*	+
YBCG-TC01	R	R	+
YBCG-TC02	S	S	+
YBCG-TC03	R	R	+
YBCG-TC04	R*	R*	+
YBCG-TC05	S	S	+
YBCG-TC06	R	R	+

R and S represent resistant and susceptible, respectively, to *Foc* or *For*. * represents weak resistance (some of the 25 seedlings showed IP = 0, while others showed IP ≥ 3). +, amplification by Bra012688m; -, no amplification by Bra012688m.

Table II-4. Assessment of Fusarium yellows resistance by inoculation test.

Name	Inoculation test	Prediction by DNA marker
	For	Bra012688m
Chinese cabbage (var. *pekinensis*)		
RJKB-T36	R	+
RJKB-T37	R	+
RJKB-T38	R	+
RJKB-T39	R	+
RJKB-T40	S	-
Turnip (var. *rapa*)		
'Yukibotan'	R	+
Pak choi (var. chinensis)		
'Entei'	R	+
'Ryoutou'	R	+
Komatsuna (var. *perviridis*)		
'Kahoku'	R	+
'Nakamachi'	R	+
'Nanane'	R	+
'Norichan'	R	+
'Chijimikomatsuna'	S	+
'Tsunashima'	S	+
Chijimina (var. *narinosa*)		
'Hirose'	S	+

Table II-5. Linkage analysis using six individual F_2 populations.

	F_2 Population		χ^2	Resistant	Bra012688m	Susceptible	Bra012688m
	Resistant	Susceptible	(R:S = 3:1)	Parent		Parent	
1	169	31	$p < 0.05$	YBCG-11	+	YBCG-12	+
2	171	29	$p < 0.001$	YBCG-11	+	YBCG-13	+
3	171	29	$p < 0.001$	YBCG-11	+	YBCG-14	+
4	160	40	$p > 0.05$	YBCG-08	+	YBCG-09	-
5	149	51	$p > 0.05$	YBCG-TC01	+	YBCG-10	-
6	156	44	$p > 0.05$	YBCG-11	+	YBCG-10	-

+; amplification by Bra012688m, -; no amplification by Bra012688m.

Table II-6. NBS-LRR encoded genes in significant QTL

Gene ID of v3.0	Gene ID of v1.5
BraA03g047230.3C	Bra012689
BraA03g047240.3C	Bra012688
BraA03g048820.3C	Bra012541
BraA03g048830.3C	Bra012540
BraA03g049860.3C	Bra019409-Bra019410
BraA03g051400.3C	Bra019273
BraA03g053580.3C	Bra019063
BraA03g057980.3C	Bra036995
BraA03g060530.3C	Bra017807

Table II-7 Genotype using focbr1-2m marker in resistant and susceptible plants derived from F_2 population.

Resistant lines	focbr1-2m	Susceptible lines	focbr1-2m
F_2 population derived from YBCG-11 x YBCG-12			
1	C	1	B
2	C	2	B
3	A	3	B
4	A	4	B
5	C	5	B
6	A	6	B
7	A	7	B
8	A	8	B
9	A	9	B
10	A	10	B
11	C	11	B
12	A	12	B
F_2 population derived from YBCG-11 x YBCG-13			
1	C	1	B
2	A	2	B
3	C	3	B
4	A	4	B
5	C	5	B
6	C	6	B
7	C	7	B
8	C	8	B
9	C	9	B
10	C	10	B
11	C	11	B
12	C	12	B
F_2 population derived from YBCG-11 x YBCG-14			
1	A	1	B
2	A	2	B
3	A	3	B
4	C	4	B
5	A	5	B
6	C	6	B
7	A	7	B
8	A	8	B
9	A	9	B
10	C	10	B
11	C	11	B
12	C	12	B

A; Resistant allele (*FocBr1/FocBr1*), B; Susceptible allele (*focbr1-2/focbr1-2*) C; Heterozygous allele (*FocBr1/focbr1-2*)

Table II-8. *F. oxysporum* f. sp. *rapae* resistance and *FocBr1* genotype determined by focbr1-2m marker.

Name	Inoculation Test	Prediction by DNA Markers	
	For	**Bra012688m**	**focbr1-2m**
Chinese cabbage (var. *pekinensis*)			
"W77"	R	+	A
RJKB-T23	R	+	A
RJKB-T24	S	-	D
RJKB-T36	R	+	A
RJKB-T37	R	+	A
RJKB-T38	R	+	A
RJKB-T39	R	+	A
RJKB-T40	S	-	D
Turnip (var. *rapa*)			
"CR-Yukiakari"	R*	+	A
"Hekiju"	R	+	A
"Yukibotan"	R	+	A
NSI-01	R*	+	A
Pak choi (var. *chinensis*)			
"Entei"	R	+	C
"Ryoutou"	R	+	A
Komatsuna (var. *perviridis*)			
"Chijimikomatsuna"	S	+	B
"CR-Taiga"	R*	+	C
"Kahoku"	R	+	C
"Manaka"	R	+	C
"Nakamachi"	R	+	A
"Nanami"	R	+	A
"Nanane"	R	+	A
"Natsurakuten"	R*	+	C
"Norichan"	R	+	A
"Tsunashima"	S	+	B
"Zaoh"	S	+	B
YBCG-08	R	+	A

YBCG-09	S	-	D
YBCG-10	S	-	D
YBCG-11	R	+	A
YBCG-12	S	+	B
YBCG-13	S	+	B
YBCG-14	S	+	B
YBCG-15	S	+	B
YBCG-16	R	+	A
YBCG-17	R	+	A
YBCG-18	R*	+	A
YBCG-TC01	R	+	A
YBCG-TC02	S	+	B
YBCG-TC03	R	+	A
YBCG-TC04	R*	+	C
YBCG-TC05	S	+	B
YBCG-TC06	R	+	A
Chijimina (var. *narinosa*)			
"Hirose"	S	+	B

R and S represent resistant and susceptible to *For*, respectively. * represents weak resistance (some of the 25 seedlings showed IP = 0, while others showed IP ≥ 3). +; amplification by Bra012688m, -; no amplification by Bra012688m. A, Resistant allele (*FocBr1*/*FocBr1* or *FocBr1*/*focbr1-1*). B, Susceptible allele (*focbr1-1*/*focbr1-2* or *focbr1-2*/*focbr1-2*). C, Heterozygous allele (*FocBr1*/*focbr1-2*). D, No PCR amplification (*focbr1-1*/*focbr1-1*).

Table II-9. Genotype distribution of *FocBr1* in *B. rapa* subspecies.

	Chinese Cabbage	**Turnip**	**Pak Choi**	**Komatsuna**
	(var. *pekinensis*)	**(var. *rapa*)**	**(var. *chinensis*)**	**(var. *perviridis*)**
FocBr1/*FocBr1* or *FocBr1*/*focbr1-1*	145	30	24	44
FocBr1/*focbr1-2*	6	5	16	21
focbr1-1/*focbr1-1*	6	0	0	3
focbr1-2/*focbr1-2* or *focbr1-2/focbr1-1*	0	0	0	5
Total	157	35	40	73

Chapter III

Transcriptional association between mRNAs and their paired natural antisense transcripts following *Fusarium oxysporum* inoculation in *Brassica rapa* L.

Abstract

Long noncoding RNAs (lncRNAs) play important roles in abiotic and biotic stress responses; however, studies on the mechanism of regulation of lncRNA expression are limited in plants. As coordinate expression of mRNAs and paired NATs under biotic stress treatment has been identified, the transcriptional relationship between mRNAs and their paired NATs following *Fusarium oxysporum* f. sp. *conglutinans* (*Foc*) inoculation was examined. A positive association of expression levels between mRNAs and their paired NATs following *Foc* inoculation was observed. This association held for several defense-response-related genes and their NAT pairs. These results suggest that coordinate expression of mRNAs and paired NATs plays a role in the defense response against *Foc*.

Keywords: *Brassica rapa*; fusarium yellows; *Fusarium oxysporum* f. sp. *conglutinans*; mRNA; long noncoding RNAs; natural antisense transcripts; transcription; inoculation; gene expression

Introduction

Brassica rapa L. includes leafy vegetables such as Chinese cabbage (var. *pekinensis*), pak choi (var. *chinensis*), and komatsuna (var. *perviridis*) and root vegetables such as turnip (var. *rapa*) (Lv et al. 2020b). These vegetables provide nutrition, vitamins, minerals, dietary fibre, and health-promoting substances. Most of the modern cultivars of these vegetables are F_1 hybrids (Fujimoto et al. 2018). Disease resistance is an important trait in a breeding program of F_1 hybrid cultivars (Mehraj et al. 2020), and a major disease problem is Fusarium yellows. Fusarium yellows is caused by infection with a soil-borne fungus, *Fusarium oxysporum* f. sp. *conglutinans* (*Foc*) or *F. oxysporum* f. sp. *rapae* (*For*), in *B. rapa* vegetables, and infection leads to the yellowing, wilting, defoliation, stunting, and plant death (Enya et al. 2008, Mehraj et al. 2020, Akter et al. 2021b, Miyaji 2021b). A Fusarium yellows resistance gene has been identified in *B. rapa* (Shimizu et al. 2014, Miyaji et al. 2021b), and a system for DNA marker selection of Fusarium yellows resistance developed (Kawamura et al. 2016, Akter et al. 2021b). The transcriptional response to *Foc* inoculation also has been examined (Miyaji et al. 2017), and SA-induced genes involved in systemic acquired resistance (SAR) are considered to play a role in resistance against *Foc* (Miyaji et al. 2021a).

Recent advances in sequencing technology enable us to detect various types of transcripts, not only mRNAs but also noncoding RNAs (ncRNAs), which are defined as RNAs devoid of protein-coding potential (Chen et al. 2021a). There are two types of ncRNAs, housekeeping ncRNAs and regulatory ncRNAs. Ribosomal RNAs (rRNAs), transfer RNAs (tRNAs), small nuclear RNAs (snRNAs), and small nucleolar RNAs (snoRNAs) are classified as housekeeping ncRNAs (Collins and Penny 2009, Cech and Steitz 2014, Ariel et al. 2015). Regulatory ncRNAs are classified into two groups based on their size, small RNAs (sRNAs) and long ncRNAs (lncRNAs). sRNAs are usually 18 to 30 nucleotides (nt) in length such as microRNAs (miRNAs) or small interfering RNAs (siRNAs). LncRNAs are longer than 200 nt in length. LncRNAs are classified into three major groups: long intergenic noncoding RNAs (lincRNAs), natural antisense RNAs (NATs) transcribed from the complementary DNA strand of their associated genes, and intronic noncoding RNAs (incRNAs) derived from introns (Ponting et al. 2009, Cech and Steitz 2014, Ariel et al. 2015, Chekanova 2015, Rai et al. 2019,). LncRNAs have been identified at the whole genome level in many plant species and are generally expressed at lower levels than mRNAs and have low sequence conservation between species (Chen et al. 2020, Zhang et al. 2020, Chen et al. 2021a). Only 10-15% of the lncRNAs in Chinese cabbage had relatively high sequence similarity with lncRNAs of other *Brassica* species, and less than 2% had similarity with *A. thaliana* sequences (Song et al. 2021).

Transcriptome analyses have shown high diversity of lncRNA expression in different tissues or under abiotic and biotic stresses, suggesting that lncRNAs might play important roles in plant development or abiotic and biotic stress responses. However, the functions of only limited numbers of lncRNAs have been elucidated (Wu et al. 2020).

RNA-sequencing (RNA-seq) has shown coordinate expression of mRNAs and paired NATs under stress treatment (Zhu et al. 2014, Shea et al. 2019, Song et al. 2021), which suggests a role for NATs in stress response. We have identified differentially expressed genes following *Foc* inoculation (Miyaji et al. 2017) and mRNA and NAT pairs (Shea et al. 2019). From these datasets, we searched for lncRNAs that are paired with genes whose expression is changed by *Foc*. We examined the transcriptional relationship of mRNAs and their paired NATs following *Foc* inoculation in *B. rapa*.

Materials and Methods

Plant materials and growth conditions

Fusarium yellows susceptible and resistant inbred lines of Chinese cabbage RJKB-T24 and RJKB-T23, respectively were used as plant materials (Shimizu et al. 2014). To examine the transcription of NATs, an additional four inbred lines of Chinese cabbage (RJKB-T39, RJKB-T41, RJKB- T42, and RJKB-T43), four komatsuna commercial cultivars [('Inasena' (KANEKO SEEDS Co., Ltd., Maebashi, Japan), 'Nacchan' (Nohara Seed Co., Ltd., Kuki, Japan), 'Nanane' (Takii & Co., Ltd., Kyoto, Japan), and 'Wakami' (Sakata Seed Corporation, Yokohama, Japan)], four commercial pak choi cultivars, [('Kunyan' (Sakata Seed Corporation), 'Natsu-Mikado' (Sakata Seed Corporation), 'Niihao-syan' (Watanabe Noji Co., Ltd., Noda, Japan), and 'Raiko' (Sakata Seed Corporation)], and four commercial turnip cultivars [('Mifune' (Sakata Seed Corporation), 'Nitou' (Sakata Seed Corporation), 'Shiro-Warabe' (Takii & Co., Ltd.), and 'Yukibotan' (Musashino Seed Co., Ltd., Tokyo, Japan)] were used. After surface sterilization, the seeds were placed on Murashige and Skoog (MS) agar supplemented with 1% (*w*/*v*) sucrose and grown under long day (LD) condition (16 h light/8 h dark) at 21 °C. First and second leaves were collected from 14-day-old plants.

RNA extraction and gene expression analysis

Total RNAs were isolated from whole plants that were mock and *F. oxysporum* f. sp. *conglutinans* (*Foc*) inoculated [(at 24 and 72 h after inoculation (HAI)] by using SV Total RNA Isolation System (Promega Co., Madison, WI, USA). Differentially expressed genes of mock- and *Foc*-inoculated samples were identified from RNA-seq analysis in RJKB-T24 and RJKB-T23 (Miyaji et al. 2017). For quantitative real-time RT-PCR (qPCR), 500 ng total RNA was used for cDNA synthesis using ReverTra Ace® qPCR RT Master Mix with gDNA Remover (TOYOBO Co., Ltd., Osaka, Japan). Prior to qPCR, single PCR amplification products and the absence of genomic contamination were confirmed by RT-PCR. Using a Light-Cycler 96 (Roche Molecular Systems, Inc., Pleasanton, CA, USA), qPCR was performed using FastStart Essential DNA Green Master (Roche). The qPCR conditions were 95 °C for 10 min followed by 45 cycles of 95 °C for 10 s, 60 °C for 10 s, and 72 °C for 10 s. Melt temperature analysis (65–97 °C at 0.1 °C /s) was performed for each reaction after amplification cycles to confirm the presence of single amplified product. The relative expression level of all mRNAs and NATs relative to *ACTIN* (*Bractin*) was automatically calculated using automatic CQ calling according to the manufacturer's instructions (Roche) (Fujimoto et al. 2006). Data presented are the average and standard error of three biological and experimental replicates and statistically analyzed using

Student's *t* test, *p* value < 0.05, 0.01, or 0.001. The primer sets used in this study are listed in Table III-1.

Total RNAs from first and second leaves were extracted by SV Total RNA Isolation System (Promega) in RJKB-T24 for RNA-sequencing (RNA-seq) for detection of lncRNAs. A more detailed description of lncRNA identification can be found in (Shea et al. 2019). To examine the transcriptional conservation among four different varieties of *B. rapa*, total RNAs from first and second leaves were extracted by SV Total RNA Isolation System (Promega) in sixteen *B. rapa* lines. cDNA was synthesized, and RT-PCR using QuickTaq®HS DyeMix was performed. RT-PCR amplified products were electrophoresed using 1.5% agarose gel. PCR conditions were 94 °C for 2 min followed by 30, 35, or 40 cycles of 94 °C for 30 s, 55 °C for 30 s, and 68 °C for 30 s. The primers used in this study are listed in Table III-1.

DNA extraction and PCR

The cetyl trimethyl ammonium bromide (CTAB) method was used to isolate genomic DNA (Murray and Thompson 1980). PCR amplification of genomic DNA as template was performed to test whether the coding genomic sequences of NATs were conserved in the sixteen *B. rapa* lines. PCR amplification of genomic regions corresponding to all six NATs was confirmed by electrophoresis of PCR amplified products using QuickTaq®HS DyeMix (TOYOBO) on 1.5% agarose gel in all sixteen *B. rapa* lines. PCR conditions were 94 °C for 2 min, 35 cycles of 94 °C for 30 s, 55 °C for 30 s, and 68 °C for 30 s, and final extension at 68 °C for 3 min. Primer sequences used in this study are shown in Table III-1.

Results

Relationship between mRNA and their paired NAT transcription following *F. oxysporum* f. sp. *conglutinans* (*Foc*) inoculation

Previously, we identified differentially expressed genes following 24- or 72-h *Fusarium oxysporum* f. sp. *conglutinans* (*Foc*) inoculation (HAI) in the resistant line RJKB-T23 and the susceptible line RJKB-T24 (Miyaji et al. 2017). In RJKB-T23, 260 and 88 genes showed differential expression at 24 and 72 HAI, respectively, and in RJKB-T24, 253 and 109 genes showed differential expression at 24 and 72 HAI, respectively (Miyaji et al. 2017). We identified overlapped genes between two data sets, DEGs following *Foc* inoculation (24 and 72 HAI in RJKB-T23 and RJKB-T24) and paired genes overlapping lncRNAs (in RJKB-T24); twelve mRNA and NAT pairs were identified (Figures III-1, III-2 and III-3).

We selected six of the twelve mRNA and NAT pairs (Bra025668/MSTRG.13790, Bra028523/MSTRG.16709, Bra033549/MSTRG.1355, Bra035320/MSTRG.26084, Bra029414/ MSTRG.4734, and Bra009234/MSTRG.25721) and performed qPCR following *Foc* inoculation at 24 and 72 HAI in RJKB-T23 and RJKB-T24 (Figure III-2, Table III-2). All six mRNAs showed upregulation following *Foc* inoculation at 24 and 72 HAI in both RJKB-T23 and RJKB-T24 (Figure III-2, Table III-2). In NATs, out of a total of 24 comparisons, 16 comparisons showed upregulation following *Foc* inoculation (Figure III-2, Table III-2). In MSTRG.1355, the expression levels increased following *Foc* inoculation at 24 and 72 HAI both in RJKB-T23 and RJKB-T24 (Figure III-2, Table III-2). Following *Foc* inoculation, expression was increased in three of the four comparisons in MSTRG.13790, MSTRG.16709, and MSTRG.25721 (Figure III-2, Table III-2). In MSTRG.4734, the expression levels following *Foc* inoculation at 24 and 72 HAI were increased in RJKB-T23, while the expression level at 72 HAI was decreased in RJKB- T24 (Figure III-2, Table III-2). In MSTRG.26084, the expression level increased following *Foc* inoculation only at 72 HAI in RJKB-T24 (Figure III-2, Table III-2).

The correlation coefficient between the ratios of the expression change of non-inoculated (NI) and inoculated samples (I) (I/NI ratio) in mRNA and NAT pairs was examined to observe whether the change of NAT expression is associated with the change of expression level of the mRNAs covering NATs. In total, there was a positive correlation in the I/NI ratio between mRNA and paired NAT ($r = 0.69$, $p < 0.001$) (Figures III-4, Table III-3). In each combination of mRNA and NAT pair, Bra033549/MSTRG.1355 ($r = 0.94$, $p > 0.05$) and Bra029414/MSTRG.4734 ($r = 0.73$, $p > 0.05$), there was a high positive correlation in the I/NI ratio, but not significant (Table III-3). When examined in each condition, 72 HAI in RJKB-T23

($r = 0.87$, $p < 0.05$) and RJKB-T24 ($r = 0.99$, $p < 0.001$) showed a positive correlation in the I/NI ratio (Table III-3).

Transcriptional conservation of NATs among *B. rapa* varieties

As there is low sequence conservation of lncRNAs between closely related species, SNP number per length in each lncRNA (mutation rate) was examined in RJKB-T23 and RJKB-T24 using previously generated SNP data (Shea et al. 2018). Contrary to our expectation, the average mutation rate of the lincRNA and incRNA encoding regions of RJKB-T23 was lower than that of the genic region, and the average mutation rate of the NAT encoding region was similar to that of the genic region in RJKB-T23 (Figure III-5). In RJKB-T24, there was no difference in the average of mutation rate of the region encoding lincRNA, incRNA, or NAT compared with that of the genic region (Figure III-5). Next, to examine the transcriptional conservation of NATs, we tested whether six NATs were expressed in 14-day leaves of sixteen *B. rapa* lines comprising four varieties. All six NATs were expressed in all sixteen lines of *B. rapa*, though there was a small variation of expression levels among lines (Figure III-6).

Discussion

LncRNAs are not just transcriptional noise, and thousands of lncRNAs have been identified in plants (Ariel et al. 2015, Chekanova 2015, Liu et al 2015, Wang and Chekanova 2017, Chen et al. 2020, Chen et al. 2021a). In general, expression levels of lncRNAs are lower than those of mRNAs and are more tissue-specific (Wang et al. 2014, Wang et al. 2015, Huang et al. 2018b, Deforges et al. 2019, Yu et al. 2019, Chen et al. 2020), suggesting a difference in transcription regulation between mRNAs and lncRNAs. However, our knowledge of the mechanisms of the regulation of lncRNA expression is limited.

Transcriptional coordination of mRNAs and their paired NATs has been identified in plants (Zhao et al. 2018, Deforges et al. 2019, Yu et al. 2019, Reis and Poirier 2021), and our previous study showed co-upregulation of some mRNAs and their paired NATs following four weeks of cold treatment (Shea et al. 2019). In particular, *BrHSFB2a* and its paired NAT showed similar expression patterns following two, four, and six weeks of cold treatment and six weeks of cold treatment followed by seven days under normal growth conditions (Shea et al. 2019). In *A. thaliana*, both *HSFB2a* and its paired NAT, asHSFB2a, were induced by heat stress (Wunderlich et al. 2014). These examples suggest that the co-expression of mRNA-NAT pairs plays a role in abiotic stress. Co-expression of mRNA-NAT pairs has also been identified in biotic stress (Zhu et al. 2014, Cui et al. 2017). In *A. thaliana*, 15 NATs were detected that were responsive to *F. oxysporum* infection, and one pair showed a co-regulation pattern following *F. oxysporum* infection (Zhu et al. 2014). In this study, we examined the association of transcriptional changes between six mRNAs and their paired NATs following *Foc* inoculation at 24 and 72 HAI in Fusarium yellows resistant and susceptible lines. A strong association between mRNAs and their paired NATs was found, especially in Bra033549-MSTRG.1355 and Bra029414-MSTRG.4734. Bra033549 encodes a putative beta-1,3-endoglucanase, which is known to be involved in defense by hydrolyzing the cell walls of fungal pathogens, and the Bra033549-MSTRG.1355 pair was upregulated following *Foc* inoculation in both resistant and susceptible lines, suggesting that upregulation of this gene may be a basic defense response and may not be specific to Fusarium yellows resistance. The Bra033549-MSTRG.1355 pair had the bivalent active and repressive (H3K4me3- and H3K27me3-marks) histone marks, suggesting a role in rapid response of transcription to pathogen infection. In contrast, the Bra029414-MSTRG.4734 pair was clearly upregulated following *Foc* inoculation in the resistant line. The *A. thaliana* ortholog of Bra029414 belongs to the superfamily of 2-oxoglutarate Fe (II)-dependent dioxygenases that is upregulated by pathogen infection or SA treatment (van Damme et al. 2008) and encodes a salicylic acid 5-hydroxylase that fine-tunes SA homeostasis (Zhang

et al. 2017). In *B. rapa*, Bra029414 was upregulated by salicylic acid treatment and was more induced in the Fusarium yellows resistant line than in the susceptible line (Miyaji et al. 2021a). As previous studies have suggested that systemic acquired resistance (SAR) may be important for Fusarium yellows resistance in *B. rapa* (Miyaji et al. 2017, 2021a), Bra029414 is an important gene for Fusarium yellows resistance and may be involved in SA homeostasis following *Foc* infection in resistant lines. In *A. thaliana*, knocking down expression of a NAT resulted in a decreased expression level of its paired mRNA (Zhao et al. 2018), suggesting that this NAT regulates the expression of its paired mRNA. In tomato, overexpression of a NAT induced its paired mRNA and enhanced resistance to *Phytophthora infestans* infection (Cui et al. 2017). The effect of knockdown or overexpression of MSTRG.4734 on the expression of Bra029414 should be examined, but MSTRG.4734 may be involved in Fusarium yellows resistance through co-expression with Bra029414.

We showed that the expression patterns of mRNAs and their paired NATs were similar following *Foc* inoculation, suggesting that the transcriptional responses are interdependent. Although sequences of lncRNAs are poorly conserved between species (Mehraj et al. 2021), the sequences of lncRNAs were conserved within *B. rapa*. Thus, transcriptional coordination of mRNAs and their paired NATs following *Foc* inoculation may be widely found in *B. rapa*. The role of transcriptional coordination of mRNAs and their paired NATs will be clarified by increasing the number of lines and by studying the expression of mRNA-NAT pairs under different stress conditions.

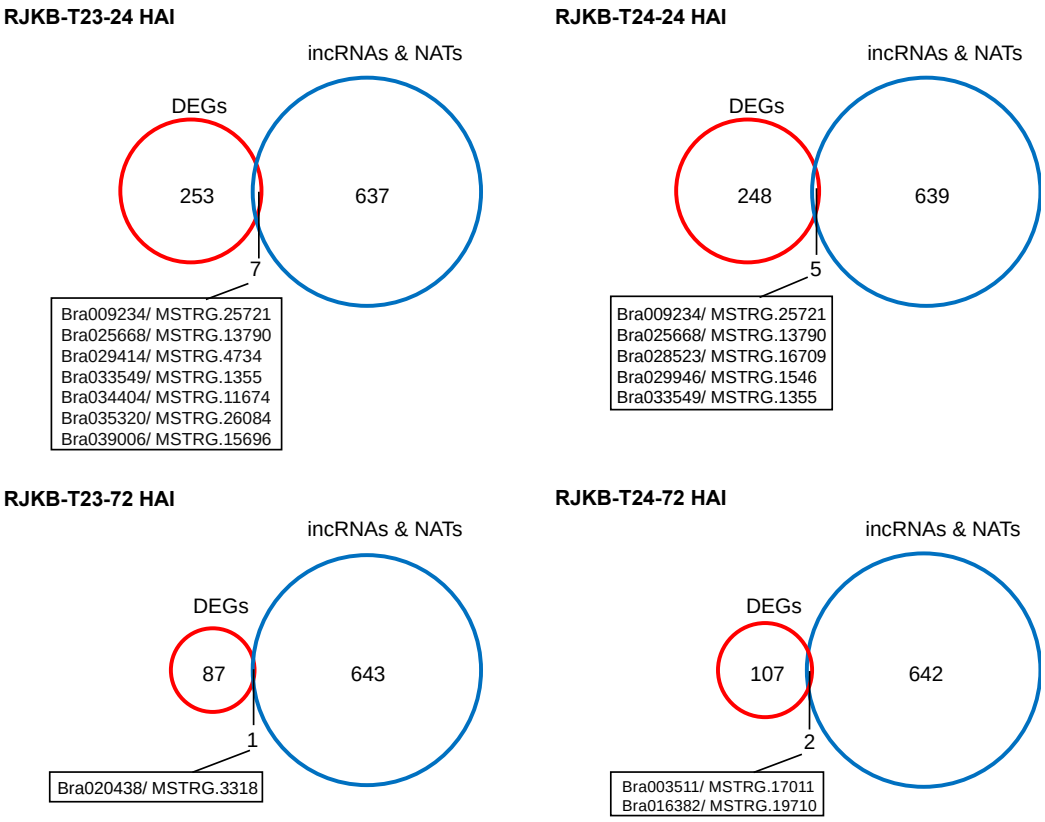

Figure III-1. Venn diagrams between differentially expressed genes (DEGs) following *F. oxysporum* f. sp. *conglutinans* (*Foc*) and paired genes overlapping incRNAs or NATs. HAI of 24 or 72 indicates 24 or 72 h after *Foc* inoculation, respectively.

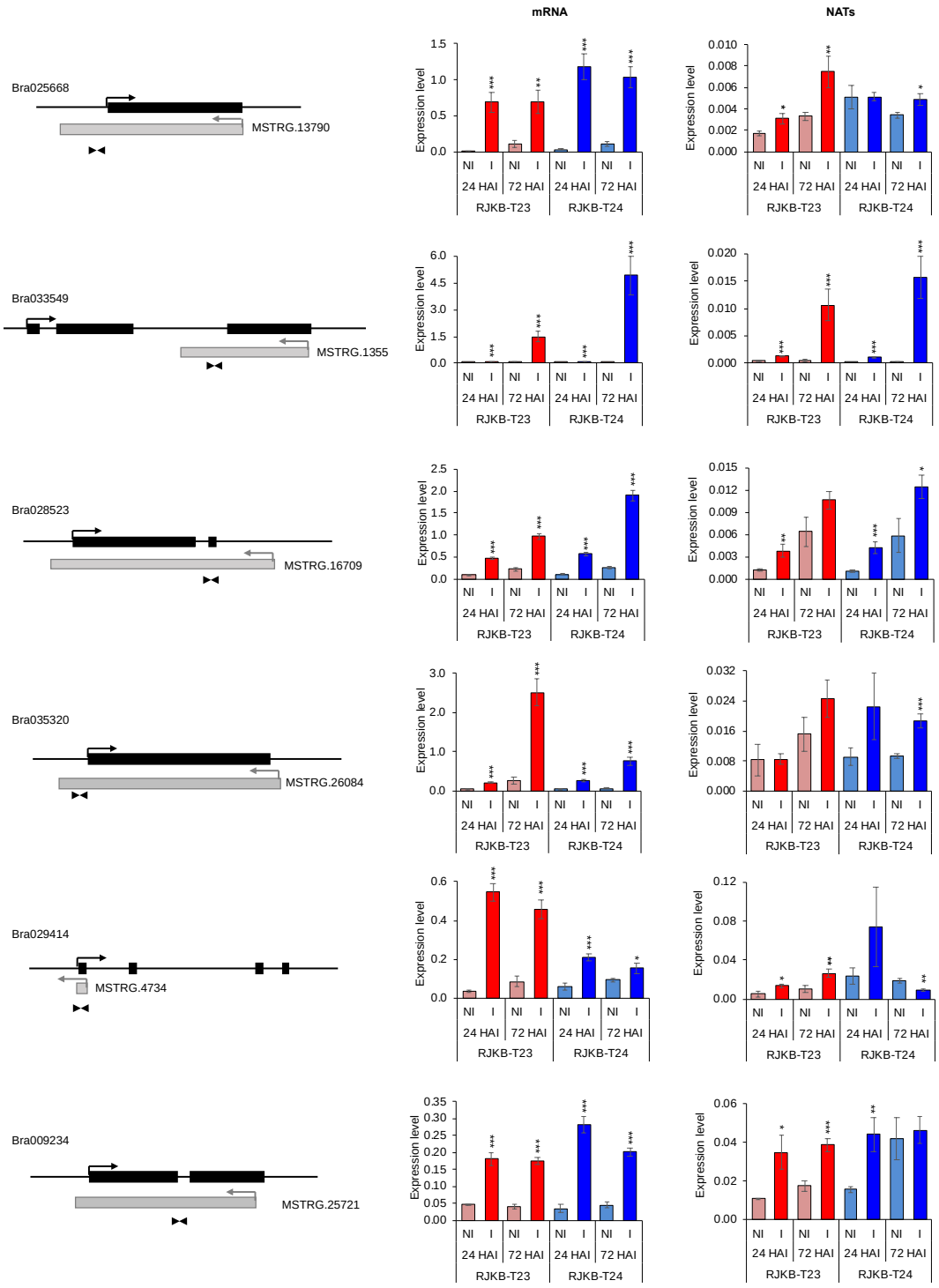

Figure III-2. Expression levels in mRNAs and their paired NATs following *F. oxysporum* f. sp. *conglutinans* (*Foc*) inoculation. Black and gray boxes represent the exon regions of gene or NATs, respectively. Arrows represent the direction of transcription. Arrowheads represent the position of primer sets for qPCR to detect the NAT transcripts. Bar graph represents values that are meant ± standard error (s.e.; three biological and technical replicates) of relative *Bractin* expression levels. *, $p < 0.05$; **, $p < 0.01$; ***, $p < 0.001$ (Student's *t*-test). NI, non-inoculated; I, inoculated.

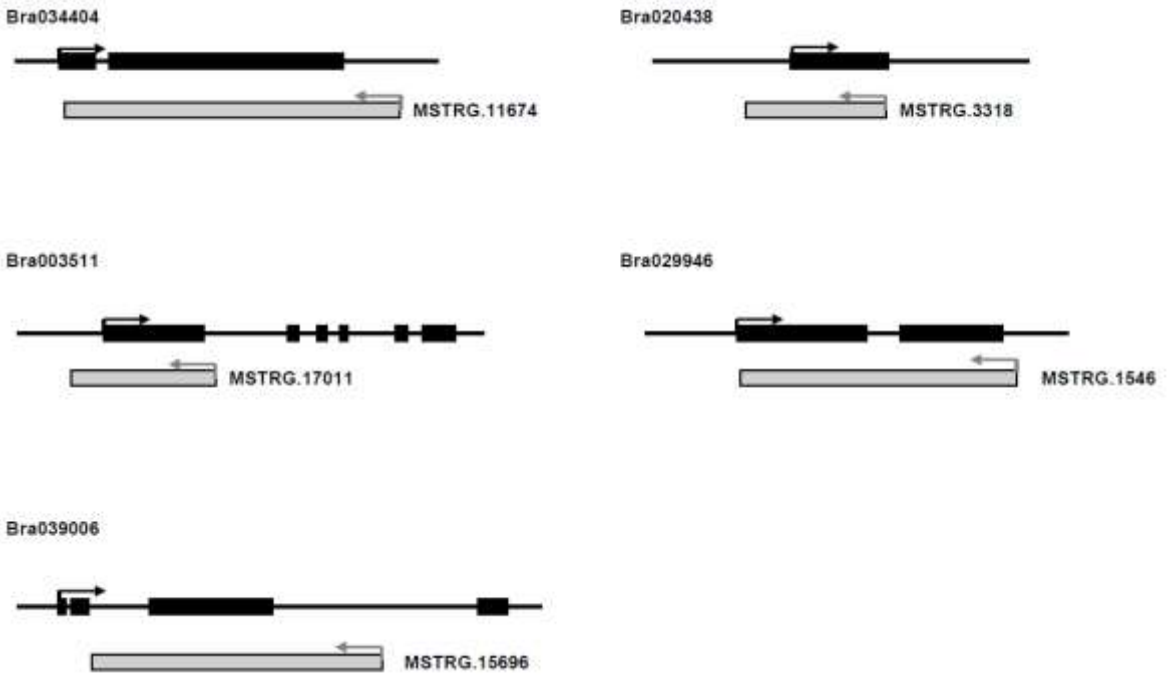

Figure III-3. Structure of genes and their paired NATs. Black and gray boxes represent the exon regions of the genes and NATs, respectively. Arrows represent the direction of transcription.

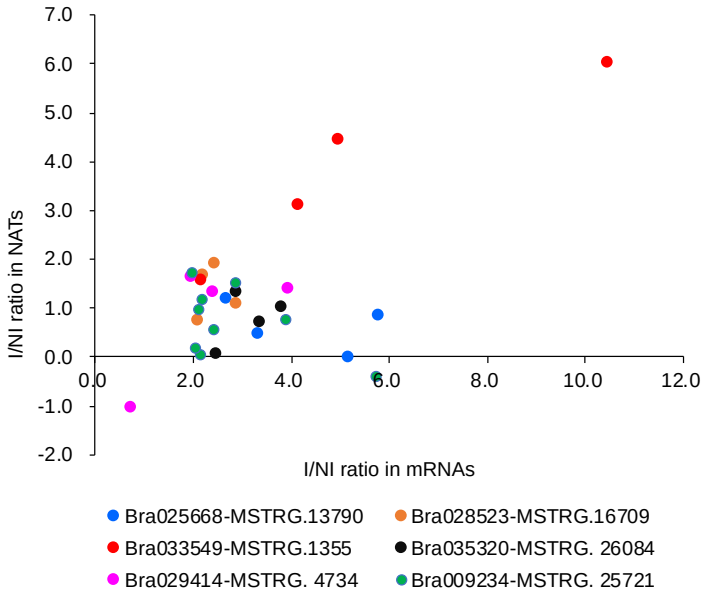

Figure III-4. Scatter plot representing the ratio of the expression levels of mRNAs and their paired NATs following *F. oxysporum* f. sp. *conglutinans* (*Foc*) inoculation (I) compared with non-inoculated (NI).

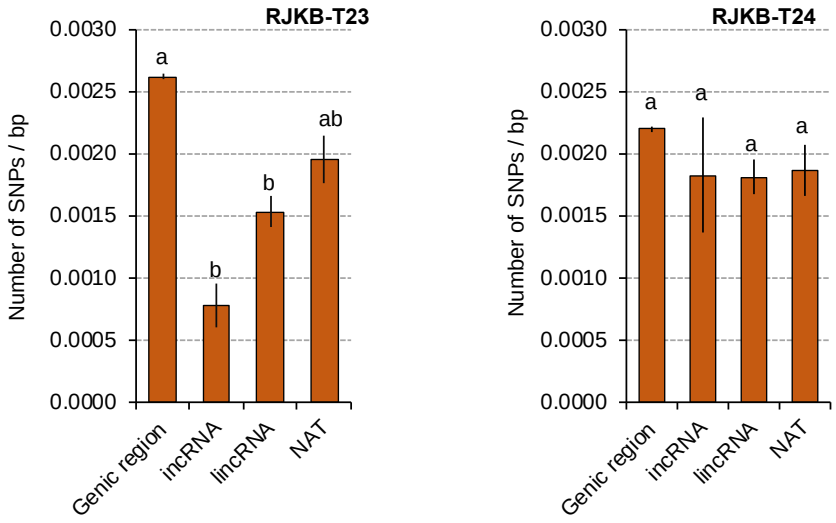

Figure III-5. The average number of SNPs per length (base pair) in region coding lncRNAs of RJKB-T23 and RJKB-T24. The values with the same letter are not significantly different with $p < 0.001$ by Tukey's HSD test. Values are means ± standard error (s.e.) of SNP number per base pair.

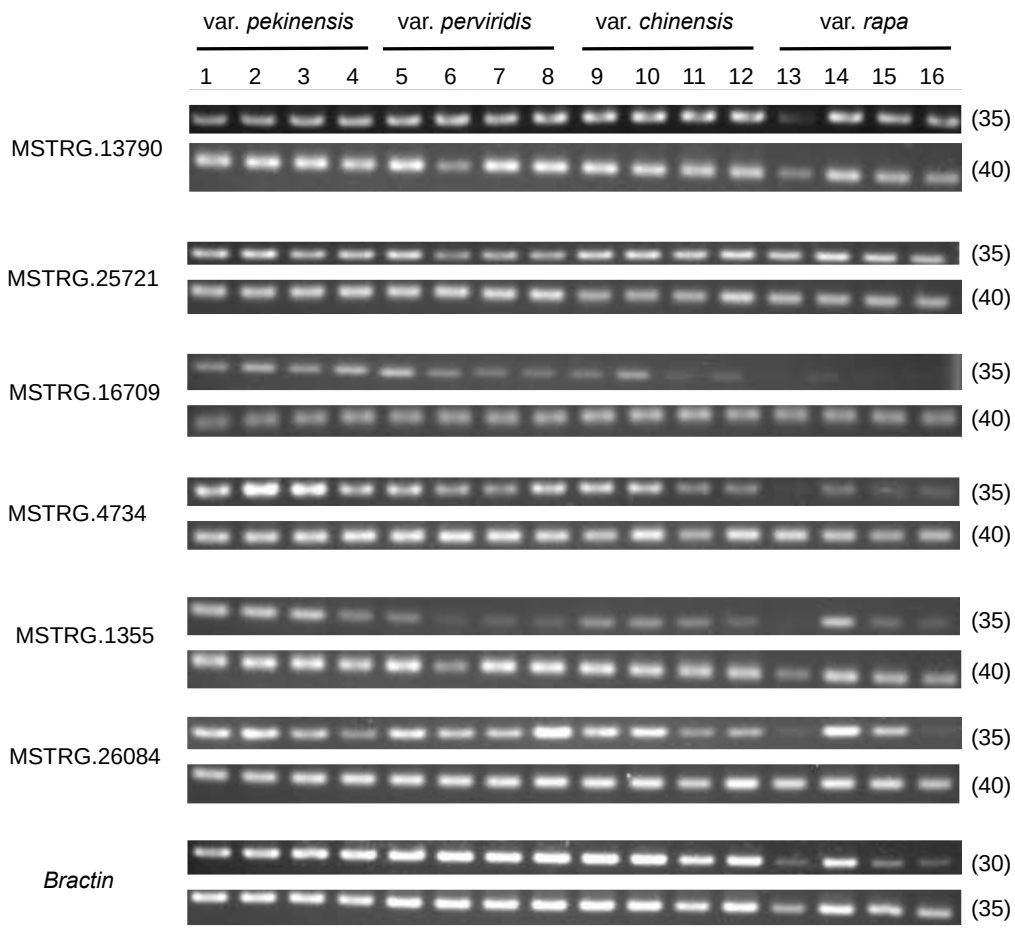

Figure III-6. RT-PCR of NATs in sixteen *B. rapa* lines. The number in parentheses (30, 35, or 40) represents the number of PCR cycles. The number represents each line as follows: For Chinese cabbage lines (var. *pekinensis*), 1 = RJKB-T39, 2 = RJKB-T41, 3 = RJKB-T42, 4 = RJKB-T43. For komatsuna lines (var. *perviridis*), 5 = 'Inasena', 6 = 'Nacchan', 7 = 'Nanane', 8 = 'Wakami'. For pak choi lines (var. *chinensis*), 9 = 'Kunyan', 10 = 'Natsu-Mikado', 11 = 'Niihao-syan', 12 = 'Raiko'. For turnip lines (var. *rapa*), 13 = 'Mifune', 14 = 'Nitou', 15 = 'Shiro-Warabe', 16 = 'Yukibotan'.

Table III-1. Sequence of primers used in this study

Name	Forward primer (5'-3')	Reverse primer (5'-3')
For qPCR		
Bra025668	ACACGCTCTTCTCCACTCAC	AAAGCCTCCTCGATGCTAAT
Bra033549	CGAGCGTATTACACGAACCT	GGGAAAAACAAACCGAAGTT
Bra028523	AACCCCTGGAAATTCAACTC	TGTTCTTTTTCCCTCCTCCT
Bra035320	GAGCTCACGAAATCAGTCGT	ACTCCTCCGCTCTTTCAAAT
Bra029414	GTCTCTCCGAAGTTTCTCAG	GCATGCCAAAGAACTCATGT
Bra009234	ACCGCCCTAACCATATTTTC	TCCGGAGATACTTGAGCTTG
MSTRG.13790	CACGTTGTTGGTAAACTAGTATAC	CAGAGATGATGGTTTGTGTTTCTC
MSTRG.1355	CTGGAAATAGATGGATTATCACTC	CGGTTTTGAGAATTTATAAACCC
MSTRG.16709	CTCTTTTTAAGTTTCTGGTTCTG	GGGAACTTTAGTCTGTCTTC
MSTRG.26084	GAATATACCAGCTCGGCCGG	GAATATACCAGCTCGGCCGG
MSTRG.4734	CACATACACGATGCACATAG	CTTCGGAGAGACGTGGACGGTC
MSTRG.25721	CCTGCTTGCATGAAAAGTTTC	CTCCAGTGGGTAGACCTTTCC
Reference for qPCR		
Bractin	CGGTCCAGCTTCGTCATACTCAGCC	AAATGTGATGTGGATATCAGGAAGG

Table III-2. Expression levels of six mRNAs and their paired NATs

mRNAs and their paired NATs	RJKB-T23 (I/NI)		RJKB-T24 (I/NI)	
	24 HAI	**72 HAI**	**24 HAI**	**72 HAI**
Bra025668	Up	Up	Up	Up
MSTRG.13709	Up	Up	No	Up
Bra033549	Up	Up	Up	Up
MSTRG.1355	Up	Up	Up	Up
Bra028523	Up	Up	Up	Up
MSTRG.16709	Up	No	Up	Up
Bra035320	Up	Up	Up	Up
MSTRG. 26084	No	No	No	Up
Bra029414	Up	Up	Up	Up
MSTRG. 4734	Up	Up	No	Down
Bra009234	Up	Up	UP	Up
MSTRG. 25721	Up	Up	Up	No

Up, Down, and No represent the upregulation, downregulation, and no difference of expression levels following Fusarium oxysporum inoculation, respectively.

Table III-3. Correlation coefficient of expression levels between mRNAs and their paired NATs

mRNAs and their paired NATs	Correlation coefficient	*p* value
Pair basis (four comparisons, 24 HAI and 72 HAI in two lines)		
Bra025668-MSTRG. 13790	-0.43	NS
Bra033549-MSTRG.1355	0.94	NS
Bra028523-MSTRG.16709	0.03	NS
Bra035320-MSTRG. 26084	0.53	NS
Bra029414-MSTRG. 4734	0.73	NS
Bra009234-MSTRG. 25721	0.31	NS
Condition basis (six comparisons, six mRNAs and NATs pairs)		
RJKB-T23-24HAI	-0.27	NS
RJKB-T23-72HAI	0.87	*
RJKB-T24-24HAI	-0.32	NS
RJKB-T24-72HAI	0.99	***
All		
Six pairs and four conditions	0.69	***

*, $p < 0.05$; ***, $p < 0.001$; NS, $p > 0.05$

Chapter IV

The role of salicylic acid responsive genes in disease resistance in *Brassica rapa* vegetables

Abstract

Salicylic acid (SA) is a plant hormone that regulates many stress responses and developmental processes including the plant immune response, thermogenesis, senescence, and abiotic stress responses. To identify SA-responsive genes at the whole genome level, we performed RNA-sequencing analysis with and without SA treatment in two komatsuna cultivars (*Brassica rapa* var. *perviridis*). We identified 1,061 up and 994 downregulated genes that overlapped between the two cultivars, and these genes were defined as *B. rapa* SA-induced genes (BrSAIGs) and *B. rapa* SA-suppressed genes (BrSASGs), respectively. In this study, we identified genes overlapping between BrSAIGs/BrSASGs and paired genes overlapping natural antisense transcripts (NATs) or intronic noncoding RNAs (incRNAs) in their encoding regions. 33 mRNA/NAT pairs and three mRNA/incRNA pairs were identified. The transcriptional relationship between mRNAs and their paired NATs following SA treatment was examined, and two of four pairs showed a positive association of expression levels between mRNAs and their paired NATs. These results suggest that the transcriptional association of mRNAs and their paired NATs plays a role in SA response. Previously SA treatment was performed by adding SA to the solid medium, but this method has limitations on the number of samples that can be assayed simultaneously. In this study, we sprayed SA on the samples, which is more high-throughput. The upregulation of all six genes that were shown to be upregulated following SA treatments on the medium was found following spraying. Transcriptional induction was faster with SA spraying than by adding SA into the medium. These results indicate that SA spraying is applicable for further experiments.

Keywords: transcriptome, long noncoding RNAs, natural antisense transcripts, intronic noncoding RNAs, komatsuna

Introduction

Brassica rapa L. shows extreme morphological divergence and includes important vegetables and oilseed. *B. rapa* fresh leafy vegetables such as Chinese cabbage (var. *pekinensis*), komatsuna (var. *perviridis*), and pak choi (var. *chinensis*) have a moisture content of over 90%, are low in calories, and contain high levels of vitamins, minerals, and fibre. Since *B. rapa* vegetables are important for human health, many types of cultivars have been developed. However, various diseases such as clubroot, Fusarium yellows, downy mildew, soft rot, white rust, etc. are becoming a problem for production (Lv et al. 2020b, Mehraj et al. 2020). Soil born-diseases such as clubroot or Fusarium yellows are difficult to be controlled by chemical treatments, and the use of disease-resistant cultivars is the most effective protection (Lv et al. 2020b, Mehraj et al. 2020). Thus, having disease resistance is essential in the development of new cultivars.

Most resistance breeding is based on the use of resistance (*R*) genes in *B. rapa* vegetables. Several *R* genes such as clubroot resistance genes or Fusarium yellows resistance gene have been identified in *B. rapa* (Ueno et al. 2012, Hatakeyama et al. 2013, Shimizu et al. 2014, Miyaji et al. 2021b). These isolated *R* genes encode a toll interleukin-1 receptor-nucleotide-binding site-leucine-rich repeat (TIR-NBS-LRR) protein. Most pathogens secrete effectors [(avirulence (Avr) proteins)] into plant cells to suppress pathogen-associated molecular patterns-triggered immunity (PTI), which is the first layer of plant immunity. To counteract this, plants express R proteins, which recognize specific AVRs and induce effector-triggered immunity (ETI). Following attempted local infection, a long-lasting, broad-spectrum immune response is induced throughout the entire plant, which is called systemic acquired resistance (SAR) (Spoel and Dong 2012).

The plant hormone, salicylic acid (SA), plays a role in PTI, ETI, and SAR. Infection of biotrophic pathogens induces the accumulation of SA, and biosynthesis of SA is mediated by two distinct pathways, the isochorismate (IC) pathway and the phenylalanine ammonia-lyase (PAL) pathway in plastids, of which the IC pathway is the main pathway for pathogen-induced SA synthesis in *A. thaliana* (Kumar 2014, Klessig et al. 2018, Rekhter et al. 2019). Pathogen-induced SA synthesis activates the defense signaling pathway. SA also plays a role in plant development and response to abiotic stresses (Miura and Tada 2014). In *B. rapa*, SA-induced genes were identified at the whole genome level by RNA-sequencing (RNA-seq). *Pathogenesis-related* (*PR*) genes and genes encoding transcription factors such as NAC and WRKY were induced by SA treatments (Miyaji et al. 2021a).

RNA-seq has identified long noncoding RNAs (lncRNAs) that are devoid of protein-coding potential and are longer than 200 nucleotides (nt). Based on their genomic location, lncRNAs are classified into three types, long intergenic noncoding RNAs (lincRNAs), natural antisense transcrips (NATs), and intronic noncoding RNAs (incRNAs). Alteration of lncRNA expression under biotic stress suggests that lncRNAs play a role in defense response. There was a positive relationship of expression levels between mRNAs and their paired NATs following inoculation of Fusarium yellows causative pathogen, *Fusarimu oxysporum* f. sp. *conglutinans* in *B. rapa* (Akter et al. 2022). This transcriptional coordination of mRNAs and their paired NATs has been identified in abiotic stress treatments (Shea et al. 2019).

In this study, we examined the transcriptional relationship between mRNAs and their paired NATs following SA treatment in *B. rapa*. Instead of adding SA to the solid medium, we established a method of spraying SA and examined the expression levels of SA response genes over time.

Materials and Methods

Plant materials, growth condition, and salicylic acid (SA) treatment

Two commercial komatsuna (*B. rapa* var. *perviridis*) cultivars 'Misugi' (Sakata Seed Corporation, Japan) and 'Nanane' (Takii & Co., Ltd., Japan) were used as plant material. Seeds were surface sterilized and sown in plastic pots containing Murashige and Skoog (MS) agar medium supplemented with 1.0 % sucrose (pH 5.7). Plants were grown in growth chambers under a 16-h/8-h light/dark cycle at 22 °C for seven days. Seedlings were transplanted into plastic pots containing MS agar medium with 1.0 mM salicylic acid (SA) at seven days after sowing. Before transplanting (0 h), and at 12, 24, 48, and 72 h after SA treatment (HAT), cotyledons were harvested and frozen with liquid nitrogen for RNA extraction. For spraying SA, seeds were sown on plastic dishes with wet paper, and seedlings were transplanted into cell trays containing soil at seven days after sowing. Seedlings sprayed with 1.0 mM SA at 7 days after sowing, and cotyledons before spaying and at 3, 6, 12, 24, and 48 h after SA treatments were harvested for RNA extraction.

RNA sequencing (RNA-seq)

Total RNA from cotyledons was extracted by SV Total RNA Isolation System (Promega Co., USA). Details of preparing sequence libraries for RNA sequencing were shown in Miyaji et al. (2021a). RNA-seq was performed at 0 and 72 HAT in 'Misugi' and 'Nanane' using BGISEQ-500 (pair-end, 100 bp). Sequenced reads were quality-checked and trimmed. Trimmed reads were mapped to the *B. rapa* reference genome version 1.5 by HISAT2 (Kim et al. 2019). 16.2 M to 16.9 M reads were mapped to the reference genome, and 13.2 M to 13.8 M reads (about 80 % of total reads) were uniquely mapped to the reference genome. The expression level of each gene was calculated by cuffdiff (Trapnell et al. 2013), and differentially expressed genes (DEGs) (two-fold difference ($|\log2 \text{ ratio}| \geq 1$) and q value < 0.01) were identified (Miyaji et al. 2021a).

Gene expression analysis

cDNA was synthesized from 500 ng total RNA using ReverTra Ace qPCR RT Master Mix with gDNA Remover (TOYOBO Co., Ltd.). Real-time RT-PCR (qPCR) was performed using a LightCycler 96 (Roche Molecular Systems, Inc., USA). cDNA was amplified using FastStart Essential DNA Green Master (Roche). qPCR conditions were 95 °C for 10 min followed by 40 cycles of 95 °C for 10 s, 60 °C for 10 s, and 72 °C for 10 s, and Melting program

(65-97 °C at 0.1 °C/s). After amplification cycles, each reaction was subjected to melt temperature analysis to confirm the presence of single amplified products. The relative expression level of each gene or NAT relative to *ACTIN* (*Bractin*) was calculated using automatic CQ calling according to the manufacturer's instructions (Roche) (Fujimoto et al. 2006). Data presented are the average and standard error of three biological and experimental replicates and statistically analyzed using Student's *t*-test, *p*-value < 0.05, 0.01, or 0.001. The primers used in this study are listed in Table IV-1.

Table IV-1. Sequence of primers used in this study

Name	Forward primer (5'-3')	Reverse primer (5'-3')
For qPCR		
Bra029414	GTCTCTCCGAAGTTTCTCAG	GCATGCCAAAGAACTCATGT
Bra026809	GCCAGCAGATTACTCTGCAG	GATTGTATCTTTCTTCTCTGCCC
Bra007907	GCGACCAATGCTACTAACTG	CAGGACTGAACTGTCTGCAG
Bra008627	CCCCAAGCCCTCTTTGTCAACC	CAAGCCAGCTTGGAGATGAG
MSTRG.4734	CACATACACGATGCACATAG	CTTCGGAGAGACGTGGACGGTC
MSTRG.23624	GAGAGAATCTTAATCCAGTCC	GCTTCGCCGGGAAGTCACCGCC
MSTRG.3751	CAGCAGAGATACAAAAAGGA	CGCAATGCGTGGACATCTGACA
MSTRG.25281	TCCGGACGAGCTAGTGGAGATCG	GAAAGTTAAGCCGGCCCTGCC
Reference for qPCR		
Bractin	CGGTCCAGCTTCGTCATACTCAGCC	AAATGTGATGTGGATATCAGGAAGG

Results and discussion

We performed RNA-seq using samples before and 72 hours after SA treatment in 'Misugi' and 'Nanane', and 3,423 and 3,780 DEGs were identified. 1,061 up and 994 downregulated genes were identified in both 'Misugi' and 'Nanane', and these genes were defined as *B. rapa* SA-induced genes (BrSAIGs) and *B. rapa* SA-suppressed genes (BrSASGs), respectively (Miyaji et al. 2021a). We also performed RNA-seq analysis on 14-day first and second leaves of the Chinese cabbage (*B. rapa* L. var. *pekinensis*) inbred line RJKB-T24 with and without four weeks of cold treatments, and encoding regions of 551 NATs and 93 incRNAs were identified (Shea et al. 2019). In this study, we identified overlapped genes between BrSAIGs/BrSASGs and paired genes overlapping NATs or incRNAs in their encoding regions, and 33 mRNA and NAT pairs and three mRNA and incRNA pairs were identified (Figure IV-1). Of 33 mRNA and NAT pairs, 14 and 19 genes were up and downregulated, respectively, at 72h after SA treatment. Of three mRNA and incRNA pairs, two and one genes were up and downregulated, respectively, at 72h after SA treatment (Figure IV-1)

We selected four of the 33 mRNA and NAT pairs (Bra029414/ MSTRG.4734, Bra026809/ MSTRG.23624, Bra007907/MSTRG.3751, and Bra008627/MSTRG.25281) and performed qPCR at 12, 24, 48, and 72 h after SA treatments (HAT). Two of the four mRNAs (Bra029414 and Bra026809) showed upregulation and two mRNAs (Bra008627 and Bra007907) showed downregulation after SA treatment in 'Misugi' and 'Nanane'. In NATs, the expression levels of MSTRG.4734 and MSTRG.23624 increased and expression levels of MSTRG.3751 decreased after SA treatments in 'Misugi' and 'Nanane' (Figure IV-2). In MSTRG.25281, the expression level following SA treatments increased in 'Nanane', while the expression level did not change in 'Misugi' (Figure IV-2). Three pairs showed similarities in expression pattern between mRNA and its paired NAT; Bra029414/MSTRG.4734 (r = 0.80, p < 0.01) and Bra026809/MSTRG.23624 (r = 0.74, p < 0.05) pairs showed a high positive correlation. We also identified the transcriptional coordination of mRNAs and their paired NATs following four weeks of cold treatment or following *F. oxysporum* f. sp. c*onglutinans* inoculation (Shea et al. 2019, Akter et al. 2022). Bra029414 encodes a salicylic acid 5-hydroxylase that fine-tunes SA homeostasis (Zhang et al. 2017) and transcriptional coordination of Bra029414/MSTRG.4734 was also observed following *Fusarium oxysporum* f. sp. *conglutinans* inoculation (Akter et al. 2022). There is some evidence that knockdown or overexpression of NATs results in decreased or increased levels of paired mRNAs, respectively (Cui et al. 2017, Zhao et al. 2018), suggesting that transcriptional coordination of Bra029414/MSTRG.4734 and Bra026809/MSTRG.23624 plays a role in SA response.

Adding SA into MS agar medium limits the plant size and the number of plants that can be assayed. Therefore, we performed SA treatment by spraying and examined the transcriptional response of six genes at 3, 6, 12, 24, and 48 HAT in 'Misugi'. The expression level of *ETHYLENE-RESPONSIVE ELEMENT BINDING FACTOR 15* (*BrERF15*) and *WRKY DNA-BINDING PROTEIN 70* (*BrWRKY70*) rapidly increased at 3HAT and then gradually decreased after 3HAT (Figure IV-3). The expression level of *GLUTATHIONE S-TRANSFERASE 25* (*BrGST25*) increased until 6HAT and then decreased (Figure IV-3). The expression level of *PATHOGENESIS-RELATED 1* (*BrPR1*), *BrPR2*, and *BrPR4* gradually increased until 12HAT and then rapidly decreased after 12HAT (Figure IV-3). The expression levels of *BrERF15* and *BrPR2* were saturated at 3 and 12 HAT, respectively, similar to the results of SA treatment on MS medium (Miyaji et al. 2021a). Of the other four genes, expression levels were saturated earlier during SA spraying than when SA was added into MS medium (Miyaji et al. 2021a). We found one clear peak of the expression levels by SA spraying, while there were several peaks using SA added into MS medium, suggesting that SA treatment by spraying is superior to adding SA into MS medium.

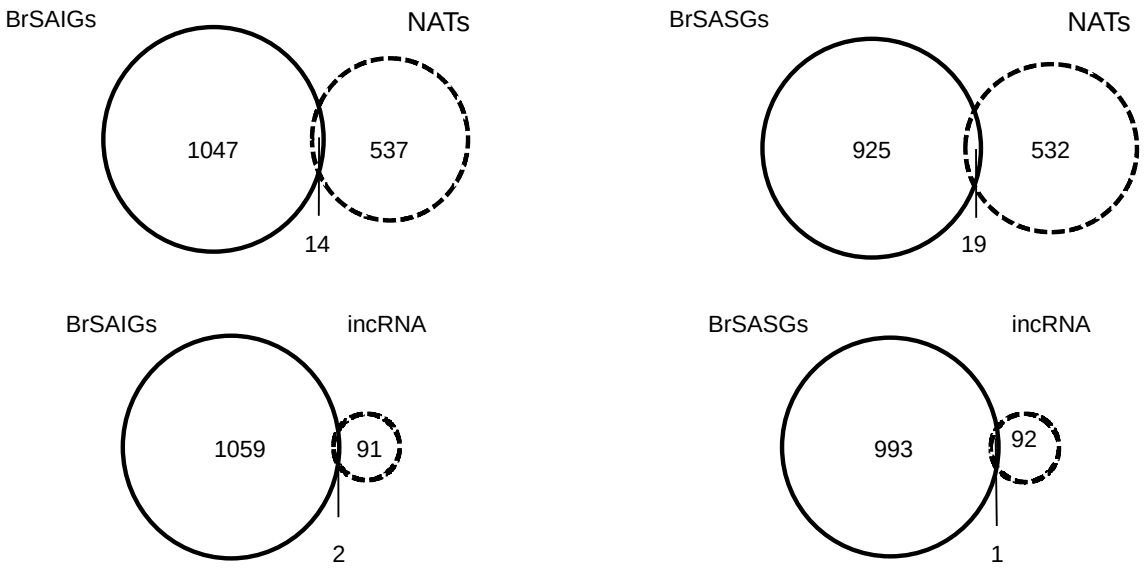

Figure IV-1. Venn diagrams between *B. rapa* SA-induced genes (BrSAIGs) or *B. rapa* SA-suppressed genes (BrSASGs) and paired genes overlapping NATs or incRNAs.

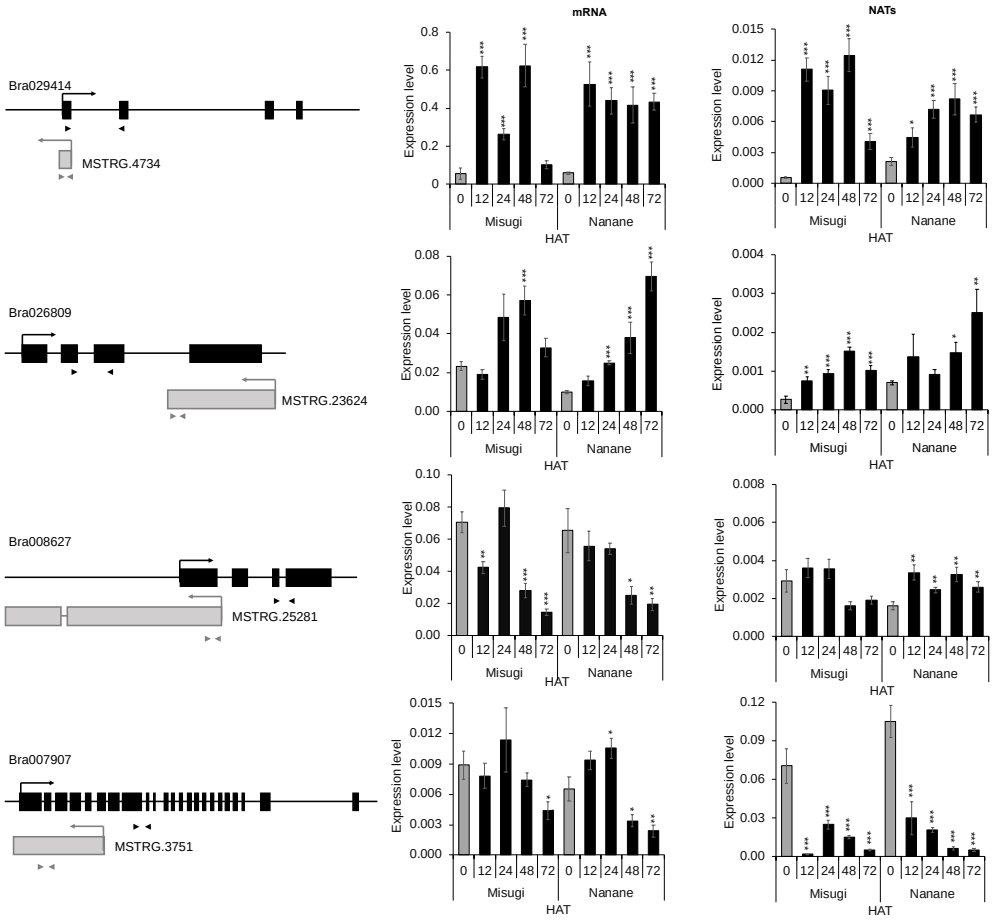

Figure IV-2. Expression levels in mRNAs and their paired NATs following salicylic acid (SA) treatment. Black and gray boxes represent the exon regions of genes or NATs, respectively. Arrows represent the direction of transcription. Black or gray arrowheads represent the position of primer sets for qPCR to detect the mRNAs or NATs, respectively. Bar graph represents values that are means standard error (s.e.; three biological and technical replicates) of relative *Bractin* expression levels. *, $p < 0.05$; **, $p < 0.01$; ***, $p < 0.001$ (Student's *t*-test). HAT, Hours after treatment.

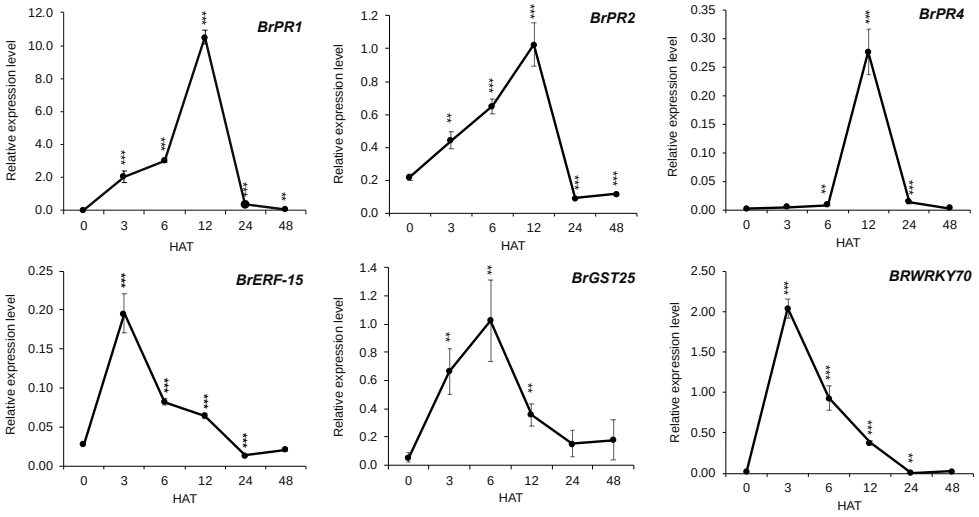

Figure IV-3. Gene expression levels in 'Misugi' after salicylic acid (SA) treatment by spraying. Gene expression levels of *BrPR1*, *BrGST25*, *BrERF15*, *BrPR2*, *BrPR4*, and *BrWRKY70*. Line graph represents values that are means standard error (s.e.; three biological and technical replicates) of relative *Bractin* expression levels. *, $p < 0.05$; **, $p < 0.01$; ***, $p < 0.001$ (Student's *t*-test). HAT, Hours after treatment.

Chapter V

Differences in the transcriptional immune response to *Albugo candida* between white rust resistant and susceptible cultivars in *Brassica rapa* L.

Abstract

Albugo candida causing white rust disease decreases the yield of *Brassica rapa* vegetables greatly. Resistant and susceptible cultivars in *B. rapa* vegetables have different immune responses against *A. candida* inoculation, however, the mechanism of how host plants respond to *A. candida* is still unknown. Using RNA sequencing, we identified differentially expressed genes (DEGs) between *A. candida* inoculated [48 and 72 h after inoculation (HAI)] and non-inoculated samples in resistant and susceptible cultivars of komatsuna (*B. rapa* var. *perviridis*). Functional DEGs differed between the resistant and susceptible cultivars in *A. candida* inoculated samples. Salicylic acid (SA) responsive genes tended to be changed in their expression levels by *A. candida* inoculation in both resistant and susceptible cultivars, but different genes were identified in the two cultivars. SA-dependent systemic acquired resistance (SAR) involving genes were upregulated following *A. candida* inoculation in the resistant cultivar. Particular genes categorized as SAR that changed expression levels overlapped between *A. candida* and *Fusarium oxysporum* f. sp. *conglutinans* (*Foc*) inoculated samples in resistant cultivars suggesting a role for SAR in defense response to both pathogens particularly in the effector-triggered immunity (ETI) downstream pathway. These findings will be useful for understanding white rust resistance mechanisms in *B. rapa*.

Keywords: Defense response, Systemic acquired resistance, Biotrophic pathogen**,** Komatsuna, Transcriptome.

Introduction

The genus *Brassica* provides vegetables, oilseeds, condiments, and fodder crops that are significant sources of nutrition and health-promoting substances such as vitamins, minerals, dietary fiber, and phytochemicals (Cheng, et al. 2016, Neik et al. 2017, Lv et al. 2020a). This genus includes *Brassica rapa* L., *Brassica oleracea* L., *Brassica napus* L., and *Brassica juncea* (L.) Czern & Coss. *B. rapa* contains leafy vegetables such as Chinese cabbage (var. *pekinensis*), pak choi (var. *chinensis*), and komatsuna (var. *perviridis*), root vegetables such as turnip (var. *rapa*), and oilseed (var. *oleifera*). *B. oleracea* provides commercially important vegetable crops with morphological variations such as cabbage (var. *capitata*), broccoli (var. *italica*), kale (var. *acephala*), kohlrabi (var. *gongylode*s), and cauliflower (var. *botrytis*) (Lv et al. 2020a). The oilseed crop, canola/rapeseed is included in *B. napus*, and in *B. juncea*, Indian mustard, brown and leaf mustards, and Sarepta mustard are included (Lv et al. 2020a, Zhang, et al. 2021). *B. rapa* (AA genome) is one of the ancestral species of *B. juncea* (AABB genome) and *B. napus* (AACC genome). Other ancestral species are *Brassica nigra* (BB genome) and *B. oleracea* (CC genome) (U 1935).

Most *B. rapa* vegetables are F_1 hybrid cultivars (Fujimoto et al. 2018), and disease resistance is a high priority for developing new F_1 hybrid cultivars (Lv et al. 2020b, Mehraj et al. 2020). Pathogens such as fungi, bacteria, and viruses reduce production in *B. rapa* vegetables (Lv et al. 2020b, Mehraj et al. 2020), and white rust is a major disease. White rust is caused by an obligate biotrophic oomycete pathogen, *Albugo candida*, and the symptoms of this disease appear as white to cream-colored zoosporangial pustules on cotyledons, leaves, and stems (Saharan et al. 2014). This disease spreads to the leaf surface, stem, or inflorescences, and the pustules become more prominent as the disease progresses (Meena et al. 2014). White rust infection damages the value of products and reduces seed formation leading to significant yield losses not only in *B. rapa* vegetables but also in *B. juncea* (Indian mustard) and *B. napus* (canola/rapeseed) (Neik et al. 2017, Singh et al. 2021).

There are two types of plant immunity, pathogen/microbe-associated molecular pattern (PAMP/MAMP)-triggered immunity (PTI) and effector-triggered immunity (ETI) (Jones and Dangl 2006, Dodds and Rathjen, 2010). Basically, PTI is the first barrier and stimulates defense gene expression such as the mitogen-associated protein kinase (MAPK) cascade or WRKY transcription factors to protect against pathogen invasion. Pathogens supply avirulence (AVR) molecules / proteins called effectors to suppress PTI. The failure of PTI defense helps to activate an immune response, which is called effector-triggered immunity (ETI). PTI is governed by cell

surface-localized pattern recognition receptors by the recognition of PAMPs/MAMPs, and effector-triggered immunity is activated by host resistance (R) proteins. This recognition of specific effectors by R proteins is termed “gene-for-gene resistance” or “gene for gene theory” (Jones and Dangl 2006). PTI is comparatively weaker than ETI against newly adapted pathogens in host plants (Dodds and Rathjen 2010). ETI leads to hypersensitive responses (HR) including programmed cell death, synthesis of plant hormones, and expression of defense-related genes. Recently it was reported that ETI and PTI cross talked and shared the same downstream responses (Lu and Tsuda 2021, Yuan, et al. 2021a, Yuan et al. 2021b). In general, the salicylic acid (SA) signaling pathway contributes to resistance against biotrophic and hemibiotrophic pathogens, while the jasmonic acid (JA) and ethylene (ET) signaling pathways contribute to resistance against necrotrophic pathogens (Glazebrook 2005, Bari and Jones 2009, Pieterse et al. 2012, Klessig et al. 2018). Basically, the SA pathway and the JA/ET pathway act antagonistically, but there are some reports that these pathways interact synergistically (Bari and Jones 2009, Pieterse et al. 2012, Caarls et al. 2015, Shigenaga and Argueso 2016, Shigenaga et al. 2017, Klessig et al. 2018, Zhang et al. 2018).

RNA-sequencing (RNA-seq) gives accurate global expression profiling not only of protein-coding genes but also of noncoding RNAs. It also can be applied to detect allele-specific expression and alternative splicing variants (Garber et al. 2011, Saeki et al. 2016, Shea et al. 2019, Stark et al. 2019, Wang et al. 2021). RNA-seq can monitor expression of pathogen responsive genes in host plants and provide insights into the network, pathways, or genes involved in the plant immune response against the pathogen (Neik et al. 2020, Campos et al. 2021). In *B. rapa*, the transcriptional response against *Plasmodiophora brassicae* that causes clubroot (Chen et al. 2016, Yuan et al 2021c), *Fusarium oxysporum* f. sp. *conglutinans* (*Foc*) that causes Fusarium yellows (Miyaji et al. 2017), *Pectobacterium carotovorum* ssp. *carotovorum* that causes soft rot (Liu et al. 2019), or *Hyaloperonospora brassicae* that causes downy mildew (Zheng et al. 2020) have been examined by RNA-seq and important pathways or candidate genes involved in the resistance mechanisms have been identified. SA responsive genes have also been identified by RNA-seq and combined with the transcriptome analyses of SA treatment and *Foc* infection has shown that SA-responsive genes [i.e., genes involved in systemic acquired resistance (SAR)] induced by *Foc* infection may play an important role in the defense response to *Foc* (Miyaji et al. 2021a).

The aim of this study was to gain insights into the immune responses of host plants against *A. candida* infection in *B. rapa* vegetables. We performed RNA-seq at 48 and 72 h after *A. candida* inoculation in resistant and susceptible komatsuna cultivars to examine the broad

disease responses. Genes differentially expressed between non-inoculated and inoculated plants and between white rust resistant and susceptible cultivars were identified. Our study will be useful for identifying pathways or genes associated with the defense response to *A. candida* and contribute to understanding the resistance mechanism.

Materials and Methods

Plant materials and fungal materials

Two commercial F_1 hybrid cultivars of komatsuna (*B. rapa* var. *perviridis*), 'Nanane' (Takii & Co., Ltd., Kyoto, Japan) and 'Misugi' (Sakata Seed Corporation, Yokohama, Japan), were used as plant materials. Research carried out on plant material is comply with relevant institutional, national, and international guidelines and legislation.

A. candida of Mibuna isolate WMB01 was originally isolated from Mibuna (*B. rapa* var. *lacinofolia*) in a field in Higashi-ohmi, Shiga, Japan in 2013. Another turnip isolates WKB01 was originally isolated from a turnip (*B. rapa* var. *rapa*) in a field in Kobe, Hyogo, Japan in 2018. For maintaining WMB01 and WKB01, seedling of 'Misugi' was used. Seven-day old plants were inoculated through spraying WMB01 or WKB01 with the concentration of 1×10^5 zoosporangia/ml, then incubated in a moist chamber for 24 h at 22 °C under dark condition and the plants were moved to a growth chamber and kept under growth conditions of 16 h light and 8 h dark at 21°C, with regular irrigation. Every three to four weeks inoculation, above process was repeated for maintaining. WMB01 and WKB01 were maintained at laboratory of horticultural crop propagation, Kobe University.

Inoculation test

Seeds of 'Nanane' and 'Misugi' cultivars were sown on soil and kept under 16 h light and 8 h dark at 21°C. Seven-day old plants were inoculated through spraying WMB01 or WKB01 with the concentration of 1×10^5 zoosporangia/ml. To confirm successful inoculation, plants were incubated in a dark growth chamber for 24 h at 22 °C with 100% humidity and the plants were moved to a growth chamber and kept under growth conditions of 16 h light and 8 h dark at 21°C, with regular irrigation. Ten days after inoculation, 'Misugi' showed many white-colored zoosporangial pustules on the adaxial and abaxial side of cotyledons, while 'Nanane' did not show any pustules on both sides of cotyledons (Figure V-1), indicating that 'Nanane' and 'Misugi' are resistant and susceptible to *A. candida*, respectively. For gene expression studies, one cotyledon of each plant was harvested after 24, 48, or 72 h inoculation of *A. candida*, and frozen in liquid nitrogen.

For gene expression study using true leaves, 14-day-old seedlings were inoculated through spraying WKB01 with the concentration of 1×10^5 zoosporangia/ml. The resistance of 'Nanane' and the susceptibility of 'Misugi' were confirmed by maintaining the plants in a dark

growth chamber for 24 h at 22 °C with 100% humidity, and the plants were moved to a growth chamber and kept under growth conditions of 16 h light and 8 h dark at 21°C, with regular irrigation. The first true leaf of each seedling was harvested after 72 h inoculation of WKB01, and frozen in liquid nitrogen.

RNA-sequencing

Total RNA from cotyledons was extracted by SV Total RNA Isolation System (Promega Co., Madison, WI, USA). Twelve sequence libraries were prepared for RNA-sequencing (RNA-seq), (1) N_0HAI, samples without *A. candida* inoculation (WMB01) in 'Nanane' (two replicates); (2) N_48HAI, samples with *A. candida* (WMB01) inoculation at 48 h after inoculation (HAI) in 'Nanane' (two replicates); (3) N_72HAI, samples with *A. candida* (WMB01) inoculation at 72 HAI in 'Nanane' (two biological replicates); (4) M_0HAI, samples without *A. candida* (WMB01) inoculation in 'Misugi' (two replicates); (5) M_48HAI, samples with *A. candida* (WMB01) inoculation at 48 h after inoculation in 'Misugi' (two replicates); (6) M _72HAI, samples with *A. candida* (WMB01) inoculation at 72 HAI in 'Misugi' (two replicates). 1 μg of total RNA was used to prepare each sequencing library with an RNA Sample Prep Kit v.2 (Illumina, San Diego, CA, USA).

Differentially expressed genes (DEGs) detection and gene ontology analysis

RNA-seq was performed using Nextseq500 (75 bp read length, paired-end). Sequenced reads were quality checked by FastQC version 0.11.8 and low-quality reads were trimmed using Trimmomatic version 0.36 (Bolger et al. 2014). HISAT2 version 2.1.0 (Kim et al. 2019) was used to align the trimmed reads to the *B. rapa* reference genome version 1.5 (http://brassicadb.cn). The number of clean reads and the percentage of mapped reads are shown in Table V-1. Gene expression levels (fragments per kilo-base per million (FPKM)) were scored using cuffdiff v.2.2.1 (Trapnell et al. 2012). Differentially expressed genes (DEGs) with and without *A. candida* inoculation were identified based on two criteria of two-fold difference ($|\log 2 \text{ ratio}| \geq 1.0$) and 95% confidence. The gene ontology (GO) tool, agriGO (Du et al. 2010), was used for enrichment analysis of gene functional ontology term following the methods described by Shimizu et al. (2014).

Gene expression analysis

For validation of RNA-seq analysis by real-time RT-PCR (qPCR), we used total RNA isolated from cotyledons with and without inoculation with *A. candida* (WMB01) independently

harvested from RNA-seq. Using *A. candida* (WKB01) isolate, total RNA isolated from cotyledons or true leaves with and without inoculation was used. cDNA was synthesized from 500 ng total RNA using ReverTra Ace® qPCR RT Master Mix with gDNA Remover (TOYOBO Co., Ltd., Osaka, Japan). The specificity of the primer set of each gene was first tested by electrophoresis of RT-PCR amplified products using QuickTaq®HS DyeMix (TOYOBO) on 1.5% agarose gel in which single products were observed. RT-PCR conditions were 94 °C for 2 min followed by 35 cycles of 94 °C for 30 s, 55 °C for 30 s, and 68 °C for 30 s. The absence of genomic DNA contamination was confirmed by the PCR of no RT control (Akter et al. 2020, Miyaji et al. 2021b).

qPCR was performed using a LightCycler 96 (Roche Molecular Systems, Inc., Pleasanton, CA, USA). cDNA was amplified using FastStart Essential DNA Green Master (Roche). qPCR conditions were 95 °C for 10 min followed by 40 cycles of 95 °C for 10 s, 60 °C for 10 s, and 72 °C for 10 s, and Melting program (65–97 °C at 0.1 °C/s) (Akter et al. 2020). After amplification cycles, each reaction was subjected to melt temperature analysis to confirm the presence of single amplified products. The relative expression level of each gene relative to *ACTIN* (*Bractin*) was automatically calculated using automatic CQ calling according to the manufacture's instruction (Roche) (Fujimoto et al. 2006). Data presented are the average and standard error of three biological and technical replicates and statistically analyzed using Dunnett's test or Student's *t* test, p value < 0.05 or 0.01. The primer sets are listed in Table V-2.

Results

Determination of time points for detecting differentially expressed genes following *A. candida* inoculation

The komatsuna white rust resistant cultivar 'Nanane' and susceptible cultivar 'Misugi' were used. To determine the time points for detecting differentially expressed genes (DEGs) following *A. candida* inoculation, we inoculated seven-day seedlings WMB01 and harvested cotyledons at 0, 24, 48, and 72 h after *A. candida* inoculation (HAI). The phytohormone SA contributes to activation of the defense response against biotrophic pathogens such as *A. candida* (Glazebrook, 2005, Bari and Jones, 2009, Pieterse et al. 2012, Klessig et al. 2018), so the transcriptional response following *A. candida* inoculation in three SA-induced genes, *PATHOGENESIS-RELATED 1* (*BrPR1*), *BrPR2*, and *BETA-1,3-GLUCANASE 3* (*BrBG3*) (Miyaji et al. 2021a), was examined. In the resistant cultivar, 'Nanane', the expression levels of *BrPR1*, *BrPR2*, and *BrBG3* were highest at 48 HAI, then decreased at 72 HAI, but the expression levels at 72 HAI were higher than at 0 or 24 HAI (Figure V-2). In contrast, the susceptible cultivar, 'Misugi', showed a low level of expression of the three genes at all times following *A. candida* inoculation (Figure V-2). These results indicate that 48 and 72 HAI are suitable times for detecting the differences in transcription between resistant and susceptible cultivars following *A. candida* inoculation.

Identification of differentially expressed genes following *A. candida* inoculation

RNA-seq was performed at 0, 48, and 72 HAI in 'Nanane' and 'Misugi'. From 8.3 M to 11.3 M reads were mapped to the reference genome, and from 5.8 M to 9.2 M reads (about 70-80% of total reads) were uniquely mapped to the reference genome (Table V-1). DEGs between with and without *A. candida* inoculation were identified using the following criteria, two-fold difference ($|\log2|$ ratio ≥ 1) and 95% FDR. At 48 HAI, 1,735 DEGs including 1,002 up-regulated (N_48HAI_up) and 733 down-regulated genes (N_48HAI _down) were identified in 'Nanane'. In 'Misugi', 1,363 DEGs including 865 up-regulated (M_48HAI _up) and 498 down-regulated DEGs (M_48HAI _down) were identified (Table V-3). At 72 HAI, 1,459 DEGs including 716 up-regulated (N_72HAI _up) and 743 down-regulated genes (N_72HAI _down) were identified in 'Nanane', and in 'Misugi', 1,409 DEGs including 722 up-regulated (M_72HAI _up) and 687 down-regulated DEGs (M_72HAI _down) were identified (Table V-3). Hierarchical clustering analysis revealed that the two cultivars were separated; 48 HAI and 72 HAI samples were clustered (Figure V-3a). More genes overlapped between two time points in the same cultivar

(44.4%-77.7%) than between the two cultivars at the same time point (36.8%-57.5%) (Figure V-3b, Table V-3).

Six genes, *BrPR1*, *BrPR2*, *BrBG3*, *ADENOSINE-5'-PHOSPHOSULFATE KINASE 1* (*BrAPK1*), *GLUTATHIONE S-TRANSFERASE F9* (*BrGSTF9*), and *SUPERROOT 1* (*BrSUR1*), were selected for validation of RNA-seq analysis by qPCR. The expression pattern determined by qPCR corresponded to the RNA-seq patterns in all six genes of both lines, except for the expression of *BrAPK1* in 'Nanane' (Figure V-4).

The expression pattern of six genes following inoculation by a different isolate, WKB01, was examined by qPCR. Seven-day seedlings were inoculated with WKB01 and cotyledons harvested at 0 and 72 HAI. The expression of all six genes was induced by WKB01 inoculation in both lines, except for *BrAPK1* and *BrSUR1* in 'Nanane' (Figure V-5). The expression pattern of all genes following WKB01 inoculation corresponds to that following WMB01 inoculation (Figures V-4 and V-5). The expression pattern of six genes in true leaves was also examined. Fourteen-days seedlings were inoculated with WKB01 and first leaves were harvested at 0 and 72 HAI. The expression of all six genes was induced by WKB01 inoculation in both lines (Figure V-5). The expression pattern of all genes in true leaves corresponded to that of cotyledons except for *BrAPK1* and *BrBG3* in 'Nanane' (Figure V-5).

Gene ontology analysis of differentially expressed genes following inoculation of *A. candida*

The up- and down-regulated genes at 48 or 72 HAI in the resistant or susceptible cultivars were categorized into GO cellular component (CC), GO molecular function (MF), and GO biological process (BP). 80 and 87 categories were overrepresented in up-regulated DEGs at 48 HAI in 'Nanane' and 'Misugi', respectively (FDR < 0.001), and 71 categories overlapped (Figure V-6, Tables V-4 and V-5). Genes categorized into 'structural constituent of ribosome' and 'chloroplast' in CC were overrepresented in both cultivars (Figure V-7, Tables V-4 and V-5). Five and 103 categories were overrepresented in down-regulated DEGs at 48 HAI in 'Nanane' and 'Misugi', respectively (FDR < 0.001), and one category overlapped (Figure V-6, Tables V-6 and V-7). In 'Misugi', stress response or stimulus-related terms and secondary metabolic process-related terms were overrepresented. The genes categorized into 'transcription regulator activity' in MF tended to be overrepresented in the downregulated genes at 48 HAI of 'Nanane' (Figure V-7, Tables V-6 and V-7).

379 and 367 categories were overrepresented in upregulated DEGs at 72 HAI in 'Nanane' and 'Misugi', respectively (FDR < 0.001), and 290 categories overlapped (Figure V-6, Tables

V-8 and V-9). In ‘Misugi’, stress response or stimulus-related terms and secondary metabolic process-related terms tended to be overrepresented (Figure V-7, Tables V-8 and V-9). Defense response-related terms such as ‘systemic acquired resistance’, ‘programmed cell death’, and ‘regulation of defense response’, SA-related terms such as ‘salicylic acid metabolic process’ and ‘salicylic acid mediated signaling pathway’, and photosynthesis-related terms tended to be overrepresented in ‘Nanane’ (Figure V-7, Tables V-8 and V-9). 201 and 116 categories were overrepresented in downregulated DEGs at 72 HAI in ‘Nanane’ and ‘Misugi’, respectively (FDR < 0.001), of which 58 categories overlapped (Figure V-6, Tables V-10 and V-11). Genes categorized into ‘secondary metabolic process’ in BP was overrepresented in both cultivars. In ‘Misugi’, genes categorized into ‘transporter activity’ in MF was overrepresented (Figure V-7, Tables V-10 and V-11). The genes categorized into ‘transcription regulator activity’ in MF were overrepresented and stress response or stimulus-related terms tended to be overrepresented in ‘Nanane’ (Figure V- 7, Tables V-10 and V-11).

Comparison between differentially expressed genes by *A. candida* inoculation and SA-responsive genes

We identified 3,780 and 3,423 SA-responsive genes in ‘Nanane’ and ‘Misugi’, respectively (Miyaji et al. 2021). Genes categorized into ‘salicylic acid mediated signaling pathway’ were overrepresented in up and downregulated genes at 72 HAI following *A. candida* inoculation in ‘Nanane’ (Figure V-7). It was predicted that some SA-responsive genes would overlap with DEGs following *A. candida* inoculation. Of 3,780 SA-responsive genes in ‘Nanane’, 572 of 1,735 (33.0%) DEGs at 48 HAI and 549 of 1,459 (37.6%) DEGs at 72 HAI overlapped (Figure V-8, Table V-3). Of 3,423 SA-responsive genes in ‘Misugi’, 463 of 1,363 (34.0%) DEGs at 48 HAI and 518 of 1,409 (36.8%) DEGs at 72 HAI overlapped (Figure V- 8, Table V-3). These results showed that in both cultivars, DEGs following *A. candida* inoculation accounted for a high proportion of SA-responsive genes at both 48 and 72 HAI.

Of 59 genes that showed upregulation by SA treatment in both *B. rapa* and *A. thaliana* (Miyaji et al. 2021a), 12 and nine genes were upregulated at 48 and 72 HAI in ‘Nanane’, and eight genes were common between two time points, including *DOWNY MILDEW RESISTANT 6* (*DMR6*) and *WRKY DNA-BINDING PROTEIN 54* (*WRKY54*) (Table V-12). Only a few genes were upregulated at 48 HAI or 72 HAI in ‘Misugi’ (Table V-12). Of 19 *BrPR* genes identified previously (Miyaji et al. 2021a), one of two *BrPR1* genes and two of nine *BrPR2* genes were upregulated at both 48 and 72 HAI in ‘Nanane’, and one of three *BrPR4* genes was downregulated at 72 HAI in ‘Nanane’. One of the five *BrPR3* gene was downregulated at 72

HAI in ‘Nanane’ (Figure V-9). In ‘Misugi’, none of the 19 *BrPR* genes showed any change in expression levels (Figure V-9). Two *BrPR2* and two *BrPR4* in ‘Nanane’ and one *BrPR3* gene in ‘Misugi’ tended to be upregulated, although they were not identified as DEGs in the RNA-seq analysis (Figure V-9). Genes categorized into ‘systemic acquired resistance’ also tended to show differential expression following *A. candida* inoculation in ‘Nanane’ but not in ‘Misugi’ (Table V-13).

Comparison between differentially expressed genes following inoculation by *A. candida* and *Fusarium oxysporum* inoculation

Previously, we performed RNA-seq using *B. rapa* Fusarium yellows resistant and susceptible lines with and without *F. oxysporum* f. sp. *conglutinans* (*Foc*) inoculation at 24 and 72 HAI and identified DEGs between inoculated and non-inoculated samples (DRA005538 and DRA005976) (Miyaji et al. 2017). Gene ontology analysis using upregulated genes in inoculated samples at 24 HAI showed an overrepresentation of one category, systemic acquired resistance, in resistant lines (Miyaji et al. 2017). Later, we identified upregulated genes following *Foc* inoculation that overlapped with SA-induced genes (Miyaji et al. 2021a). From these studies, we suggested that the defense response to *Foc* is mediated by SA-induced genes at 24 HAI in *B. rapa* (Miyaji et al. 2017, Miyaji et al. 2021a). Of 245 upregulated genes after *Foc* inoculation in the Fusarium yellows resistant line (RJKB-T23) in *B. rapa*, 47 (19%) and 25 genes (10%) were also upregulated after *A. candida* inoculation at 48 and 72 HAI in ‘Nanane’, and 19 genes overlapped between two time points (Table V-3). In ‘Misugi’, 18 (7%) and 26 genes (11%) were also upregulated after *A. candida* inoculation at 48 and 72 HAI, and 16 genes overlapped between two time points (Table V-3). However, between cultivars at the same time points, only a few upregulated genes overlapped (one at 48 HAI and four at 72 HAI) (Table V-3). Some SAR-related genes and *BrPR* genes overlapped between upregulated genes in both Fusarium yellows resistant line and white rust resistant cultivar (Figure V-9, Table V-13), while no gene overlapped between upregulated genes in both Fusarium yellows resistant line and white rust susceptible cultivar (Figure 9, Table V-13). Previously, we identified 39 SA-induced genes specific to Fusarium yellows resistant lines (Miyaji et al. 2021a). Of these 39 genes, 24 (61.5%) and 13 (33.3%) genes were upregulated by *A. candida* inoculation at 48 and 72 HAI, respectively, in ‘Nanane’, while a few genes were upregulated at 48 and 72 HAI in ‘Misugi’ (Figure V-10), suggesting a similar defense response mediated by SA occurred in resistant cultivar/line between two different pathogens, especially at 48 HAI by *A. candida* inoculation and 24 HAI with *Foc* inoculation.

Discussion

In this study, we used two *A. candida* isolates; WMB01 was isolated from Mibuna and WKB01 was isolated from a turnip, in a different year and in a different field. Pathogenicity was confirmed by repeated inoculation tests in the controlled condition (using a growth chamber), and it was not changed by seasons or repeated inoculation. Because *A. candida* has some host specificity (Petkowski et al. 2008), we compared the pathogenicity of WMB01 and WKB01 to *B. rapa*, and there was no difference in pathogenicity between the two isolates, suggesting that WMB01 and WKB01 are the same race. In cotyledons, all six genes showed similar expression patterns between WMB01 and WKB01 inoculation at 72 HAI. We also compared the expression pattern following WKB01 inoculation between cotyledons and true leaves, and most genes showed similar expression patterns between these two tissues. These results suggest that our RNA-seq data using single tissue and single isolate could reflect the transcriptional change following *A. candida* inoculation. However, race or tissue-specific transcriptional change following *A. candida* inoculation could be included in our RNA-seq data, and RNA-seq data using multiple isolates and tissues will be able to exclude these effects.

We identified DEGs at 48 and 72 HAI following *A. candida* inoculation. About 3-4% of total genes showed changed gene expression following *A. candida* inoculation in the white rust resistant ('Nanane') and susceptible ('Misugi') cultivars. Nearly half of the DEGs (40-55%) overlapped between the resistant and susceptible cultivars at 48 and 72 HAI. Most overrepresented GO terms in upregulated genes overlapped between the resistant and susceptible cultivars at 48 HAI, and three-quarters of overrepresented GO terms in upregulated genes at 72 HAI overlapped between them. In contrast, overrepresented GO terms in downregulated genes at 48 and 72 HAI were cultivar specific; more than 100 cultivar specific GO terms were identified in 'Misugi' at 48 HAI and in 'Nanane' at 72 HAI. These results suggest that the function of transcriptionally responsive genes following *A. candida* inoculation differs between the resistant and susceptible cultivars at 48 and 72 HAI, particularly for downregulated genes. Similar differences in the function of transcriptional responsive genes between the resistant and susceptible inbred lines have been observed in *Foc* inoculation (Miyaji et al. 2017). In the case of *Foc* inoculation, 50% of the upregulated genes at 24 HAI overlapped between resistant and susceptible inbred lines, but at 72 HAI only 10% overlapped making the difference between the resistant and susceptible lines clear. The percentage of overlapped downregulated genes between resistant and susceptible inbred lines was low at both 24 and 72 HAI (Miyaji et al. 2017).

In the *A. candida* response, some overrepresented GO terms were cultivar specific at 48 or 72 HAI. At 48 HAI, a small number of cultivar-specific GO terms were present in upregulated genes. Genes involved in the GO terms related to abiotic stress response or 'secondary metabolic process' tended to be downregulated at 48 HAI in the susceptible cultivar, while these GO terms were overrepresented in upregulated and downregulated genes at 72 HAI in both resistant and susceptible cultivars. This difference might be due to the different degrees of pathogen infection between resistant and susceptible cultivars at 48 HAI. At 72 HAI, the expression of genes categorized into SA response-related terms or 'program cell death' tended to be up and downregulated in the resistant cultivars. The genes categorized into 'systemic acquired resistance' tended to be upregulated in the resistant cultivar. These results also reflect different degrees of pathogen infection and suggest that hypersensitive reactions could occur in the resistant cultivar. The expression of genes categorized into 'auxin biosynthetic process' tended to be up-regulated in the susceptible cultivar. Upregulation of genes categorized into 'auxin biosynthetic process' by *Foc* inoculation was also observed in the susceptible inbred line (Miyaji et al. 2017). The pathogens manipulate plant auxin biosynthesis and signaling that result in susceptibility of host plants; SA induced by biotrophic pathogen infection can reduce the biosynthesis of auxin to lessen susceptibility (Zhong et al. 2021). The maize pathogen effector of *Ustilago maydis* prevents transcriptional of a repressor of auxin signaling to upregulate auxin signaling and promote susceptibility (Navarrete et al. 2022). Upregulation of genes categorized into 'auxin biosynthetic process' by *A. candida* or *Foc* inoculation in the susceptible cultivar/inbred line is common, and ETI could suppress the upregulation of genes involved in 'auxin biosynthetic process' in the resistant cultivar/inbred line.

SA plays an essential role in defense response, and genes categorized into SA response-related terms were overrepresented in upregulated genes at 72 HAI in the resistant cultivar. We identified SA responsive genes in 'Nanane' and 'Misugi' (Miyaji et al. 2021a), and 30-40% of DEGs overlapped with SA responsive genes in both cultivars. These percentages are higher than the percentages of SA-responsive genes in all genes (8-9%), and there was no difference in the percentages of SA-responsive genes in DEGs between resistant and susceptible cultivars, suggesting that expression of SA-responsive genes tended to be affected by *A. candida* inoculation in both cultivars. About 34% of DEGs overlapped with SA-responsive genes in both resistant and susceptible cultivars, these percentages were lower than the percentages of SA-responsive genes that were common in both cultivars (54-60%), suggesting that SA response genes with different roles in resistant and susceptible cultivars were changed in expression by *A. candida* inoculation. For *PR* genes and SAR-related genes, which are important for the defense response and are SA-responsive, the number of DEGs is higher in the resistant cultivar than in

the susceptible cultivar. Of SA-responsive genes conserved in *A. thaliana* and *B. rapa* that might have an important function in Brassicaceae, the number of DEGs is also higher in the resistant cultivar than in the susceptible cultivar. More genes related to the disease response may be identified as DEGs, which respond to SA in the resistant cultivar than in the susceptible cultivar.

Previous studies suggest that SA-dependent SAR plays a role in defense response in the hemibiotrophic pathogen, *Foc*, and 39 candidate genes that might function in defense response to *Foc* were identified (Miyaji et al.2017, Miyaji et al. 2021a). More of these 39 genes were identified as DEGs following *A. candida* inoculation in the resistant cultivar than in the susceptible cultivar, with 60% of DEGs overlapping at 48 HAI in the resistant cultivar. These results suggest that there may be some commonality in the defense response against the two different types of pathogens, *A. candida* and *Foc*. *BrPR2*, *BASIC PATHOGENESIS-RELATED PROTEIN 1* (*BrPRB1*), *BrDMR6*, *LUMINAL BINDING PROTEIN*, *SUPPRESSOR OF BIR1 1* (*BrSOBIR1*), and *MDIS1-INTERACTING RECEPTOR LIKE KINASE2* (*BrMIK2*) were upregulated by both *A. candida* and *Foc* inoculation in the resistant cultivar/inbred line. *DMR6* belongs to the superfamily of 2-oxoglutarate Fe (II)-dependent dioxygenases and is known as a susceptibility gene in *A. thaliana* (van Damme et al. 2005, van Damme et al. 2008). Inactivation of *DMR6* leads to resistance to different types of pathogens in *A. thaliana* (Zeilmaker et al. 2015). Loss of function of a *DMR6* ortholog in tomato and potato also showed disease resistance against different classes of pathogens (Kieu et al. 2021, Thomazella et al. 2021). *BrDMR6* genes were upregulated by *Foc* inoculation in both resistant and susceptible inbred lines, and coordinate upregulation of one *BrDMR6* genes and its paired natural antisense transcripts in the resistant inbred line was observed (Miyaji et al. 2017, Akter et al. 2022). Following *A. candida* inoculation, *BrDMR6* genes were upregulated at 48 HAI in the resistant cultivar and then decreased at 72 HAI to a level, which was still higher than in non-inoculated plants. *BrDMR6* genes were upregulated at 72 HAI in the susceptible cultivar, and the expression level of *BrDMR6* was eight times higher than in the resistant line. These results suggest that *BrDMR6* could be involved in susceptibility to *A. candida* in the susceptible line and the defense response to *A. candida* inoculation in the resistant line could repress *BrDMR6* expression. The leucine-rich repeat receptor protein, *SOBIR1*, which plays a role in PTI in *A. thaliana* (Pruitt et al. 2021), was upregulated by *A. candida* or *Foc* inoculation in the resistant cultivar/inbred line, suggesting that *BrSOBIR1* is involved in defense response against *A. candida* and *Foc*. In *A. thaliana*, the leucine-rich repeat receptor-like kinase *MIK2* is involved in resistance to *F. oxysporum* and may recognize elicitors of *F. oxysporum* extracts to induce PTI (Van der Does et al. 2017, Coleman *et* al. 2021, Rhodes et al. 2021). Although the *mik2* mutant in *A. thaliana* showed susceptibility to *F. oxysporum*, it did not show susceptibility to leaf pathogens, suggesting that *MIK2* is

involved in resistance to the specific pathogen in the root (Van der Does et al. 2017). However, *BrMIK2* was upregulated by both *A. candida* and *Foc* inoculation in the resistant cultivar/inbred line of *B. rapa*, suggesting that *BrMIK2* might be involved in deference response against these two pathogens.

Comparison among DEGs of *A. candida* inoculation, SA treatment, and *Foc* inoculation identified candidate genes involved in the defense response to *A. candida* in *B. rapa*. Transcriptome analysis following *A. candida* inoculation in the resistant and susceptible cultivars showed that activation of genes involved in defense responses such as SAR and programmed cell death was observed in the resistant cultivar. Similarly, transcriptome analysis following *Foc* inoculation in the resistant and susceptible inbred lines showed that activation of genes involved in defense responses such as SAR at 24 HAI was observed only in the resistant inbred line. *F. oxysporum* is a hemibiotrophic pathogen, and its infection cycle starts as a biotrophic phase and changes to a necrotrophic phage (Lyons et al. 2015). Our previous transcriptome suggested that *Foc* changes their phase from biotrophy to necrotrophy in susceptible lines from 24 to 72 HAI (Miyaji et al. 2017, Miyaji et al. 2021a). SAR plays a role in the defense response to biotrophic (*A. candida*) and biotrophic phase of hemibiotrophic (*Foc*) pathogens, and common SA-responsive genes were upregulated following *A. candida* and *Foc* inoculation in the resistant cultivar/inbred line. In the resistant cultivar/inbred line, resistance to these two pathogens is mediated by the immediate induction of SAR via biosynthesis of salicylic acid, which could be induced by the R protein recognizing AVR; the defense pathway downstream of ETI is shared between *A. candida* and *Foc*. Twenty-four SA-induced genes, which were also upregulated by *A. candida* and *Foc* inoculation in resistant cultivar/inbred line, including *BrPR2*, *BrPRB1*, *BrDMR6*, *BrSOBIR1*, and *BrMIK2*, are candidates for the defense response through SA by *A. candida* and *Foc* infection in *B. rapa*. This study will provide important data for future understanding of resistance mechanisms against *A. candida* in *B. rapa*.

In this study, we performed RNA-seq in a single-stage under-regulated growth condition. However, the actual growing environment in the field is more complex. To examine whether our results can apply to a real growing environment field condition, RNA-seq analysis in the field will be important and will enable us to understand the transcript overview of *B. rapa* by *A. candida* inoculation.

Figure V-1. Symptoms after *A. candida* inoculation in komatsuna cultivars 'Nanane' and 'Misugi'. Seven-days seedlings were inoculated by *A. candida*. Cotyledons were harvested at 10 days after inoculation, and both sides of cotyledons (left, adaxial; right, abaxial) were photographed.

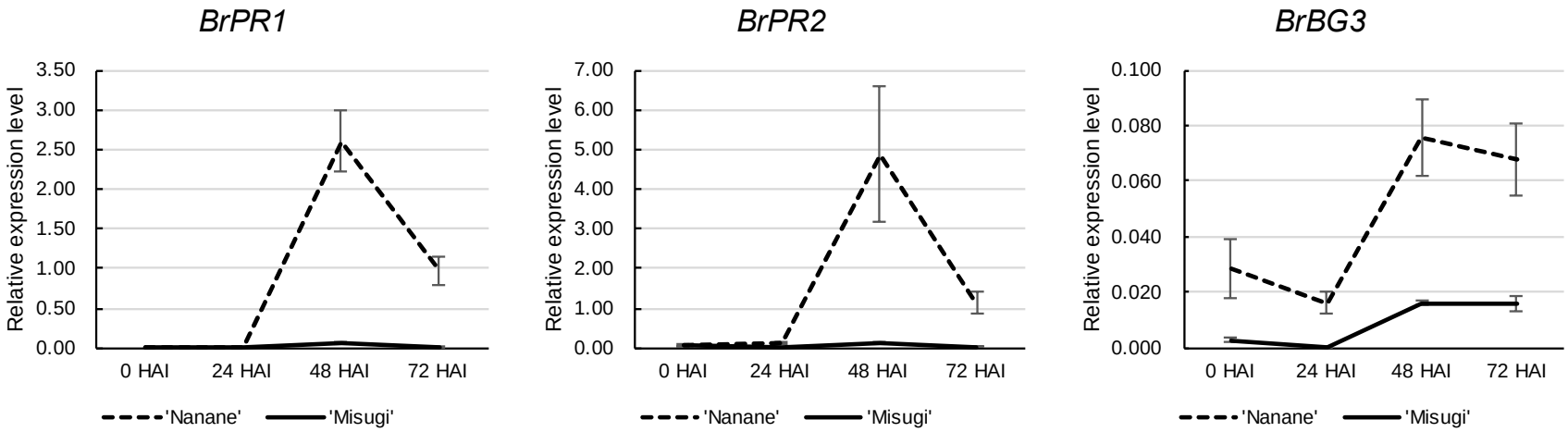

Figure V-2. Gene expression levels after *A. candida* inoculation. Expression levels of three genes were measured by real-time RT-PCR at 24, 48, and 72 h after *A. candida* inoculation (HAI). Values are mean ± SE (three biological and technical replicates) for relative expression levels compared with *Bractin*.

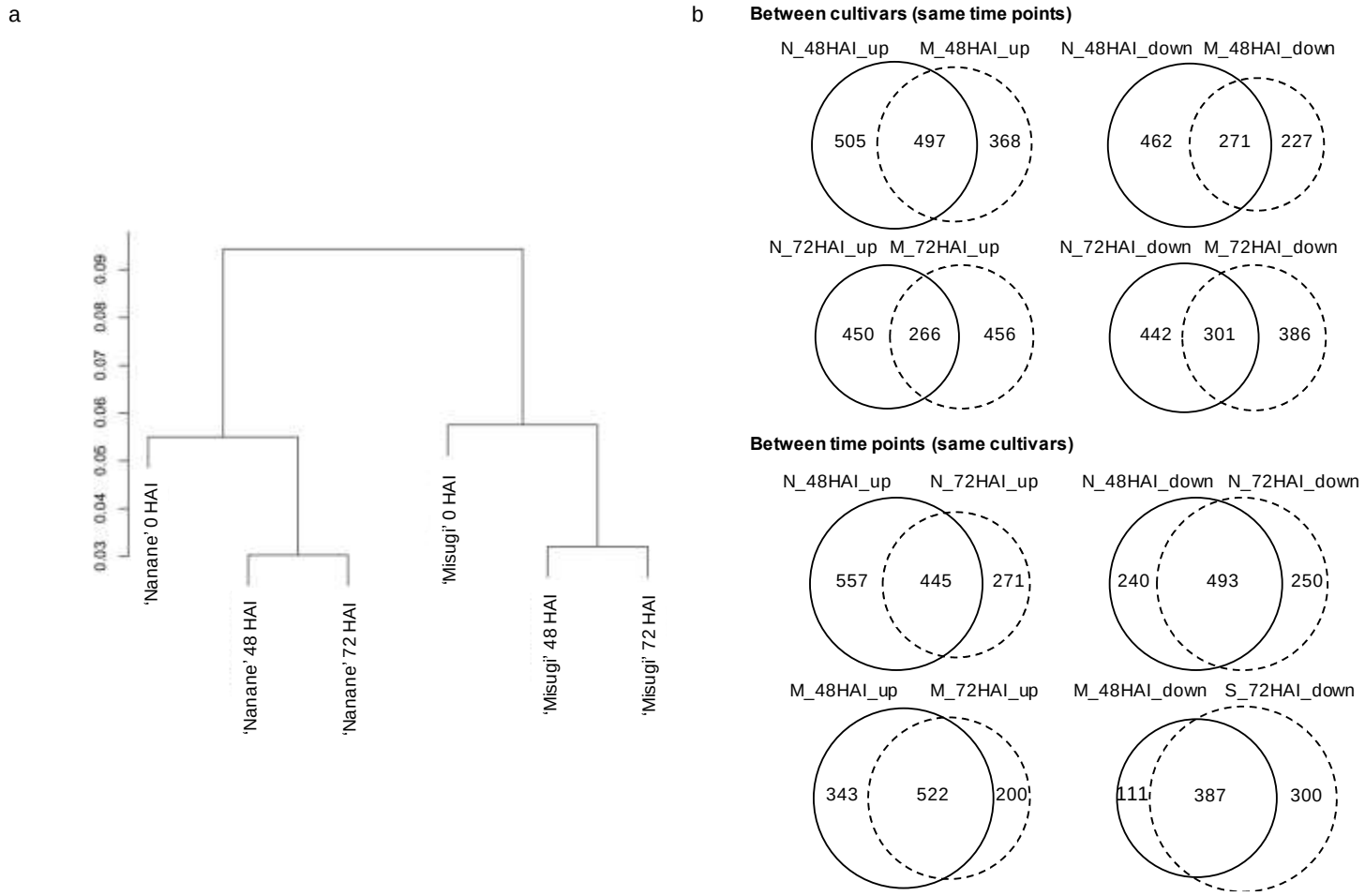

Figure V-3. Comparison of differentially expressed genes at 48 and 72 h after *A. candida* inoculation (HAI) in resistant ('Nanane', N) and susceptible ('Misugi', M) lines. (a) clustering analysis using fragments per kilobase per million (FPKM) values of all genes. (b) Venn diagram showing number of up or downregulated genes between lines or between time points.

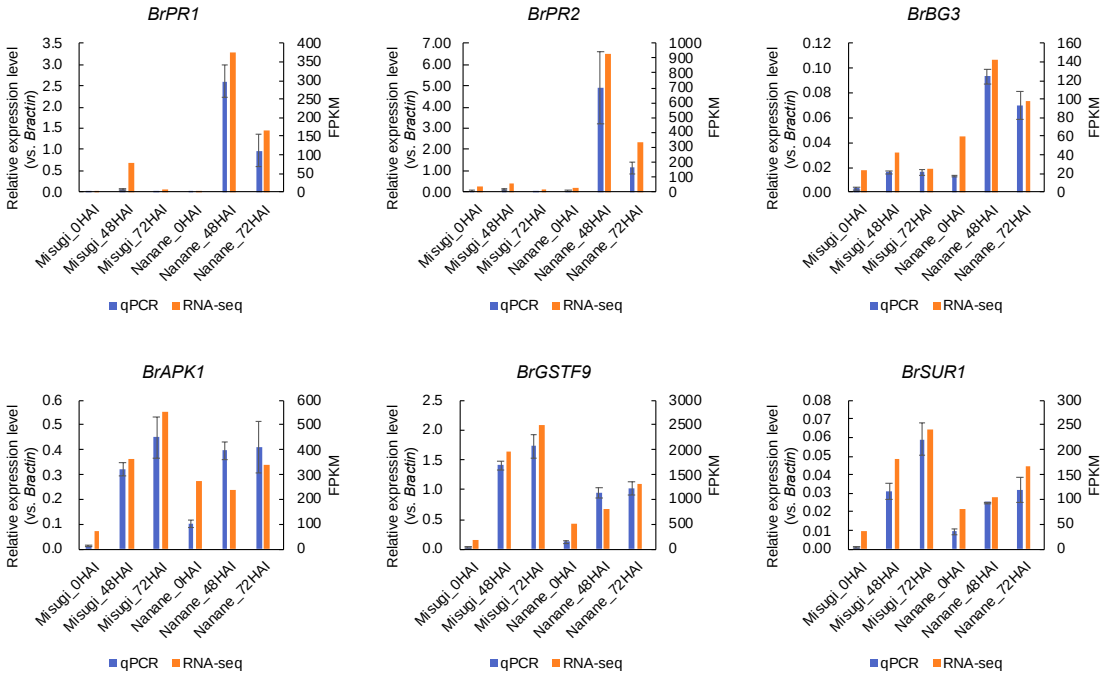

Figure V-4. Gene expression levels at 48 and 72 h after *A. candida* (WMB01) inoculation (HAI) measured by real time RT-PCR (qPCR) and RNA-seq. By qPCR, the values are means ± SE (three biological and technical replicates) of relative expression levels compared with *Bractin*. The values of fragments per kilobase per million (FPKM) were calculated by data from RNA-seq analysis.

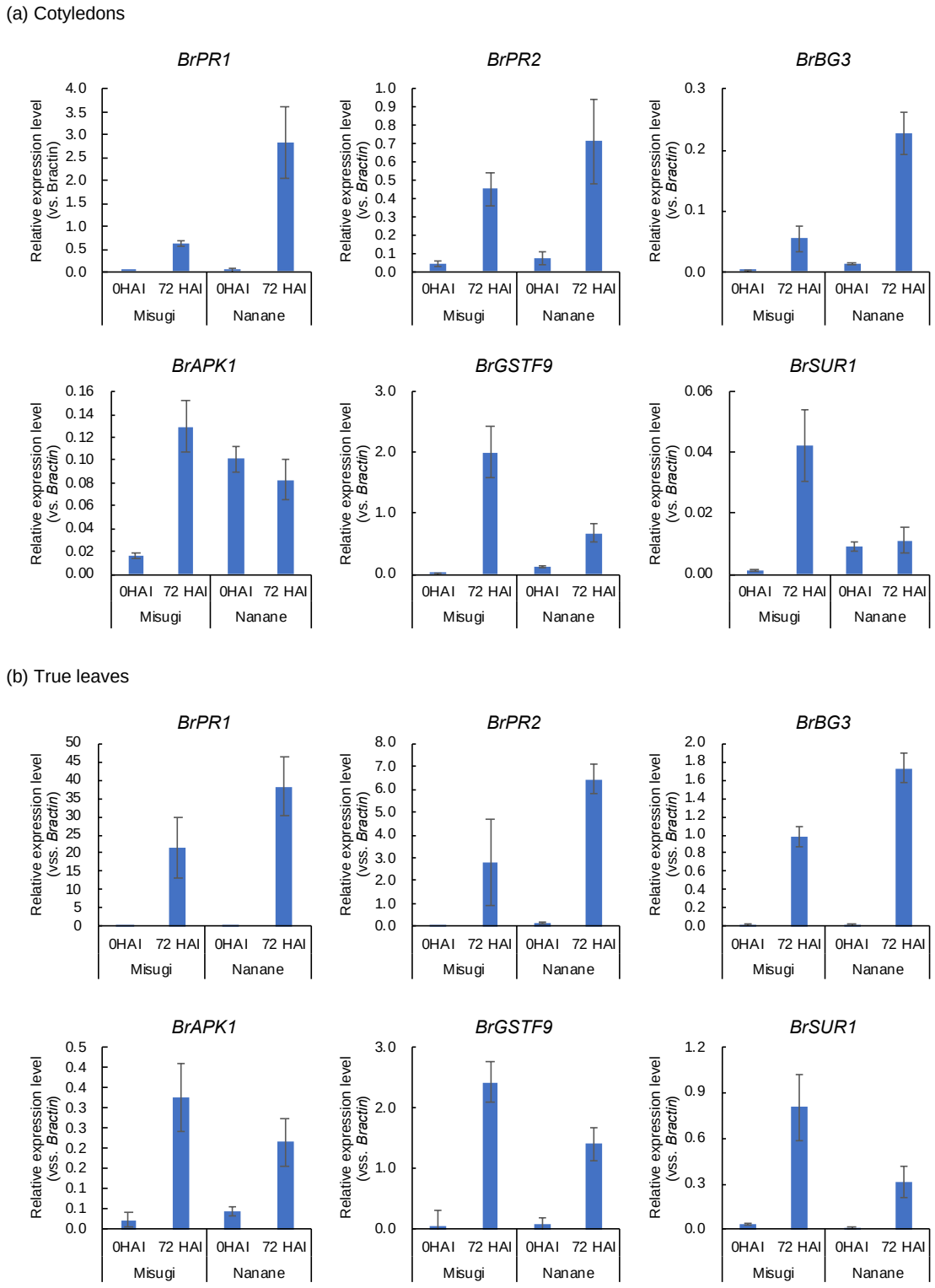

Figure V-5. Gene expression levels in cotyledons (a) and true leaves (b) at 72 h after *A. candida* (WKB01) inoculation (HAI) measured by real time RT-PCR (qPCR). The values are means ± SE (three biological and technical replicates) of relative expression levels compared with *Bractin*.

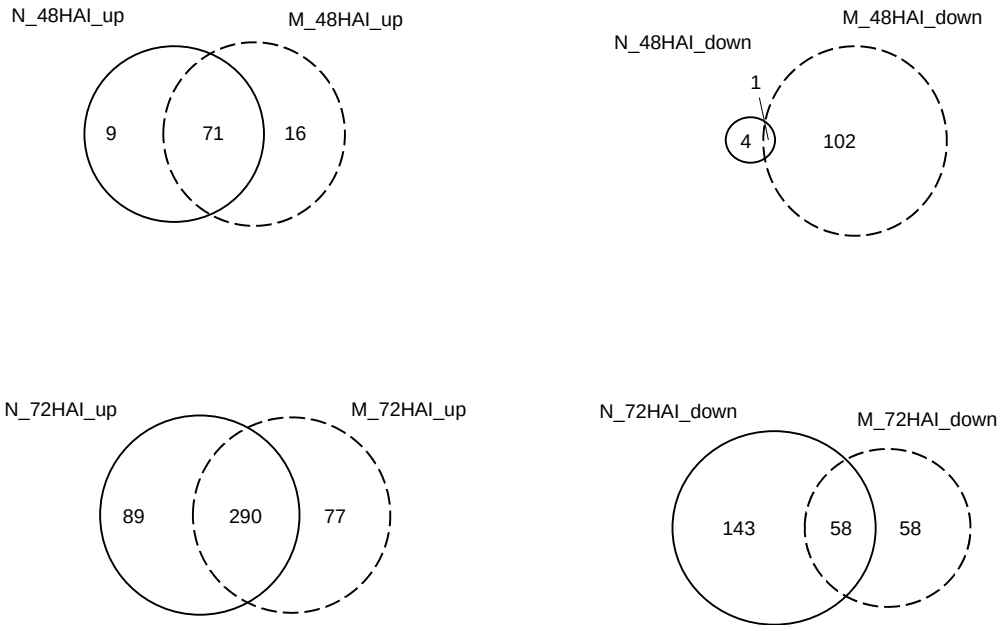

Figure V-6. Venn diagram showing number of GO terms overrepresented in up or downregulated genes following *A. candida* inoculation in 'Nanane' (N) and 'Misugi' (M). HAI, hours after *A. candida* inoculation.

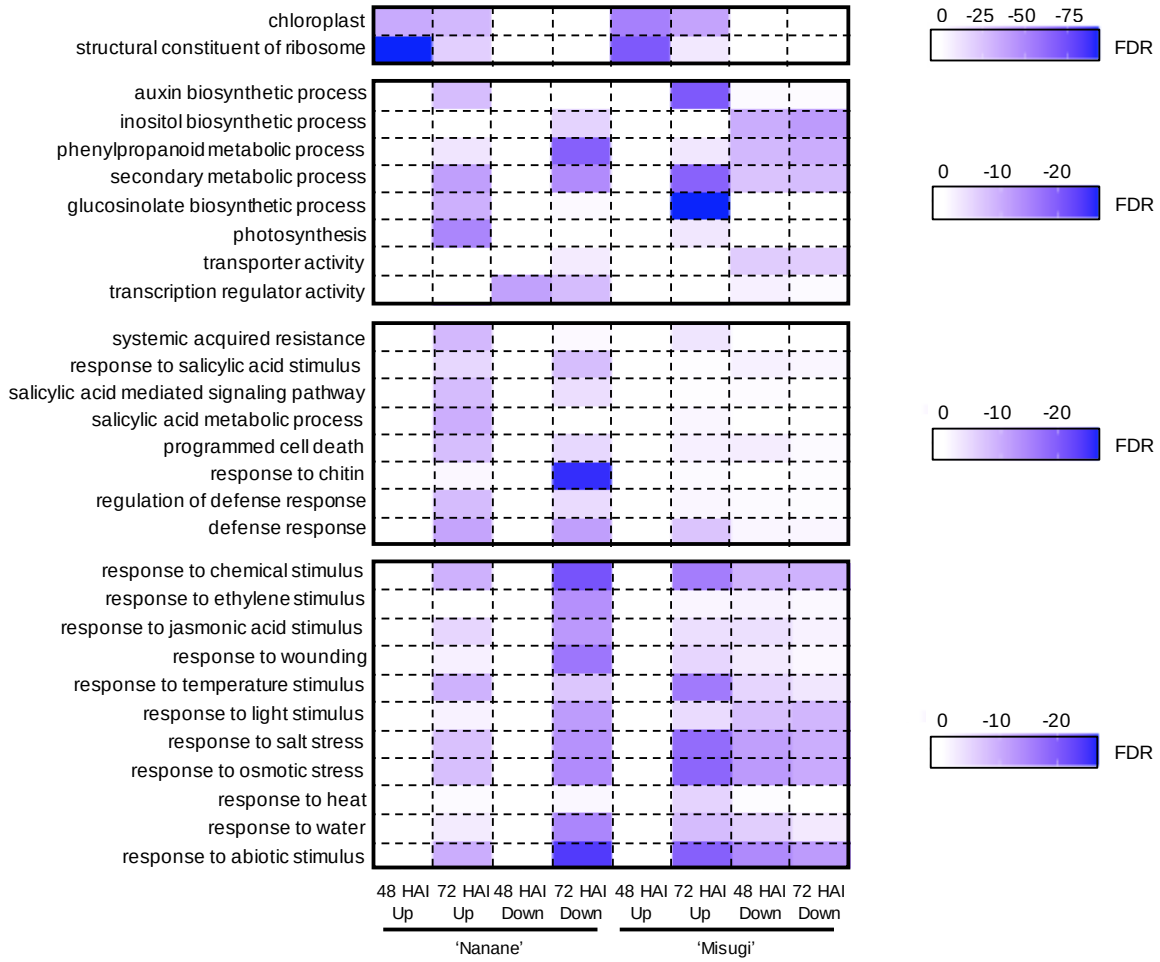

Figure V-7. GO terms overrepresented in up and downregulated genes following *A. candida* inoculation. Log_{10} value of FDR were shown with scale from white to purple. HAI, hours after *A. candida* inoculation.

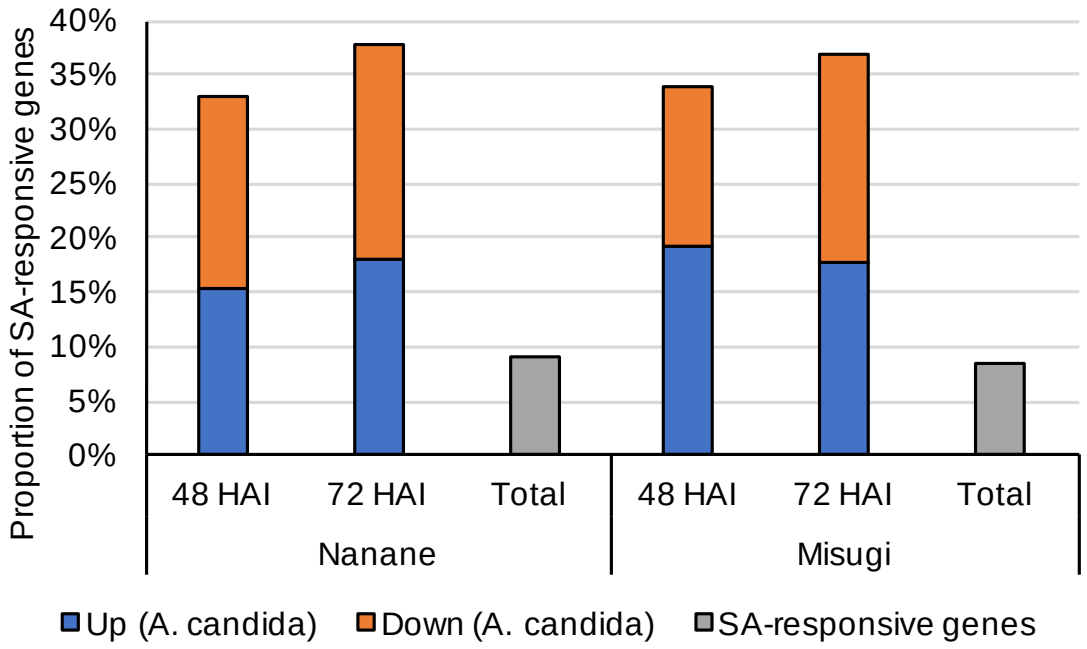

Figure V-8. Proportion of salicylic acid (SA)-responsive genes whose expression was up or downregulated by *A. candida* inoculation. "Total" represents the proportion of SA-responsive genes in all genes. HAI, hours after *A. candida* inoculation.

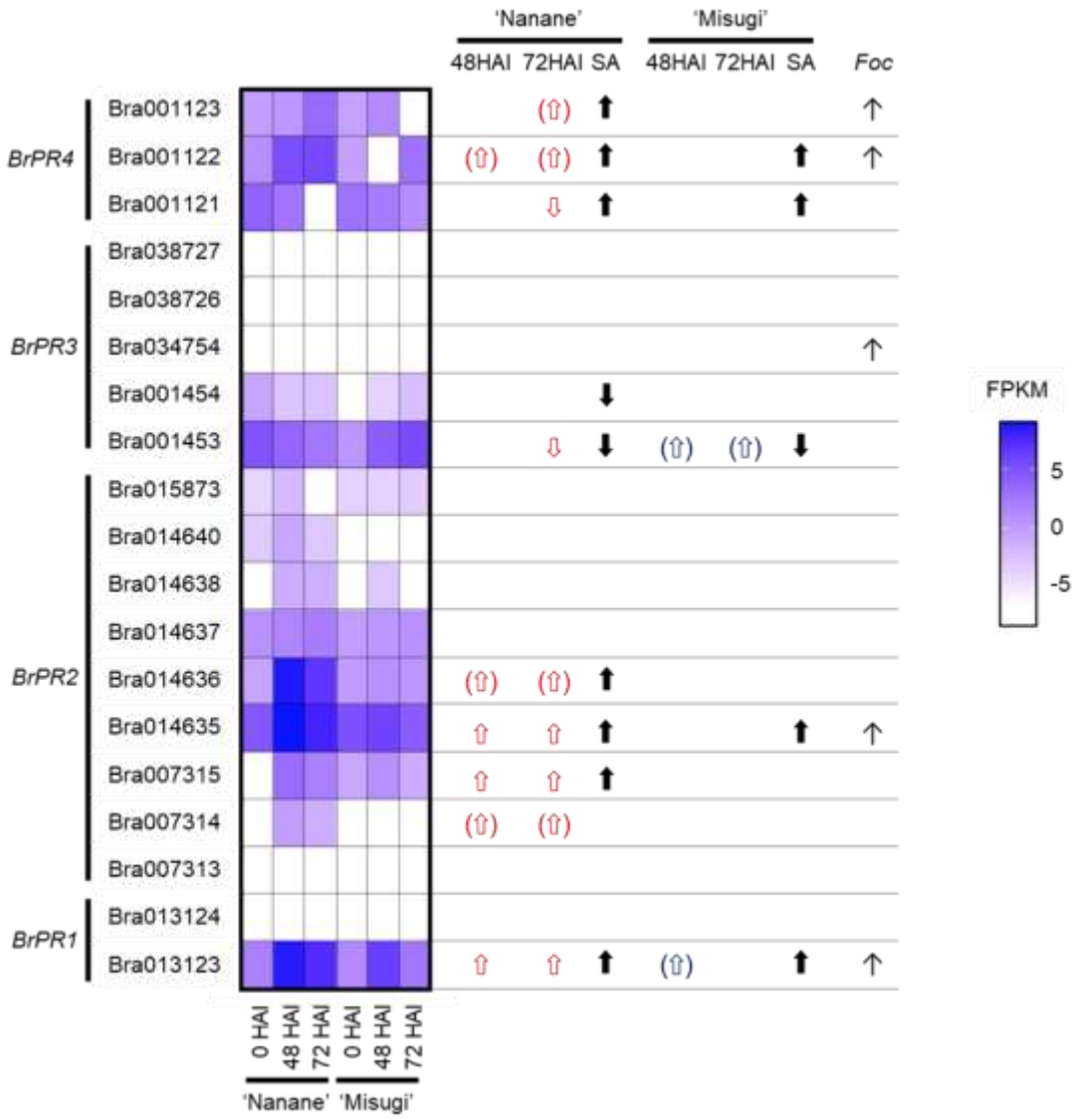

Figure V-9. Expression pattern of 19 *BrPR* genes following *A. candida* inoculation. Log_2 values of fragments per kilobase per million (FRKM) are shown with scale from white to purple. Parentheses indicates the upregulation but not significantly. "SA" represents up or downregulated at 72 h after salicylic acid (SA) treatments in 'Nanane' or 'Misugi' (Miyaji et al. 2021a). "*Foc*" represents upregulated after 24 h *Fusarium oxysporum* f. sp. *conglutinans* (*Foc*) inoculation in resistant line, RJKB-T23 (Miyaji et al. 2017). HAI, hours after *A. candida* inoculation.

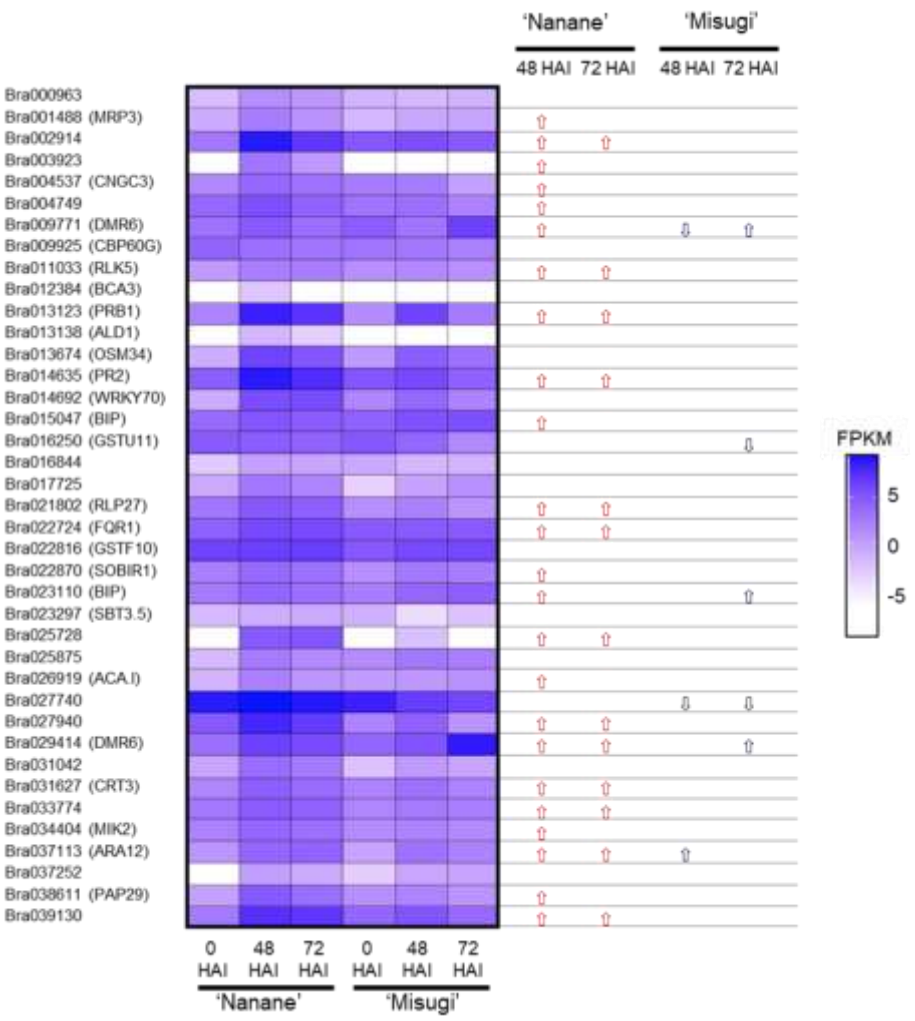

Figure V-10. Expression pattern following *A. candida* inoculation in 39 salicylic acid (SA)-induced genes specific to Fusarium yellows resistant lines. Log_2 values of fragments per kilobase per million (FRKM) are shown with scale from white to purple. HAI, hours after *A. candida* inoculation.

Table V-1. Mapped RNA-sequencing reads to reference genome

Sample name	Replicates	Total reads (paired)	Aligned concordantly exactly 1 time	
			mapped reads	%
'Nanane'				
N_0HAI	1	9,952,584	8,152,250	81.91
	2	8,589,666	7,011,745	81.63
N_48HAI	1	9,248,439	7,499,287	81.09
	2	11,250,675	9,168,899	81.50
N_72HAI	1	9,545,386	7,814,730	81.87
	2	9,154,361	7,506,450	82.00
M_0HAI	1	9,258,046	7,555,123	81.61
	2	9,262,704	7,573,097	81.76
M_48HAI	1	9,316,704	7,542,651	80.96
	2	8,560,565	6,892,061	80.51
M _72HAI	1	8,529,354	5,812,091	68.14
	2	8,303,426	6,509,247	78.39

Table V-2. Sequence of primers used in this study

Name	Forward primer (5'-3')	Reverse primer (5'-3')
BrAPK1	ACACAGGACAAAAACAAGGA	CTTCTGGTTCAAAGCACAAG
BrBG3	GCAGAACATCGATAGAGCGGT	TGAATGTCCCACTCGAAGGC
BrGSTF9	TCGAGACCGTCCCCGTCGAT	CCAAAAGGTCAGGTCCTTGT
BrPR1	CGAAAGCTCAAGACAGTCCA	GGCCAAGTTCTCTCCGTAAG
BrPR2	AATATCAAGGTCTCCACGAC	GTGTAGATATTCACGAGCAG
BrSUR1	TGAGCGAAGAAGAAGCACAC	AACGCCTCTCAGCGTTACGG
Bractin	CGGTCCAGCTTCGTCATACTCAGCC	AAATGTGATGTGGATATCAGGAAGG

Table V-3. Number of differentially expressed genes between with and without *A. candida* inoculation

	A. candida		SA			*F. oxysporum*		
			Up	Down	Total	Up	Down	Total
'Nanane'	48 HAI							
	Up	1002	146	118	264	47	0	47
	Down	733	101	207	308	7	1	8
	Total	1735	247	325	572	54	1	55
	72 HAI							
	Up	716	146	119	265	25	0	25
	Down	743	89	195	284	6	1	7
	Total	1459	235	314	549	31	1	32
'Misugi'	48 HAI							
	Up	865	93	170	263	18	0	18
	Down	498	127	73	200	7	1	8
	Total	1363	220	243	463	25	1	26
	72 HAI							
	Up	722	122	126	248	26	0	26
	Down	687	160	110	270	7	1	8
	Total	1409	282	236	518	33	1	34
'Nanane'	48 HAI							
&	Up	497	18	55	73	1	0	1
'Misugi'	Down	271	52	29	81	3	1	4
	Total	768	70	84	154	4	1	5
	72 HAI							
	Up	266	27	33	60	4	0	4
	Down	301	42	32	74	3	1	4
	Total	567	69	65	134	7	1	8

SA, number of overlapped genes with up or downregulated genes at 72 h after salicylic acid treatments (Miyaji et al. 2021a), *F. oxysporum*, number of overlapped genes with up or downregulated genes after 24h *Fusarium oxysporum* f. sp. *conglutinans* inoculation in resistant line, RJKB-T23 (Miyaji et al. 2017).

Table V-4. GO terms of up-regulated genes after 48 h *A. candida* inoculation in 'Nanane'

GO accession number	Term type	Term	FDR
GO:0022626	CC	cytosolic ribosome	2.40E-105
GO:0033279	CC	ribosomal subunit	9.80E-104
GO:0044445	CC	cytosolic part	3.80E-100
GO:0003735	MF	structural constituent of ribosome	6.00E-94
GO:0005840	CC	Ribosome	1.30E-86
GO:0043228	CC	non-membrane-bounded organelle	3.60E-85
GO:0043232	CC	intracellular non-membrane-bounded organelle	3.60E-85
GO:0030529	CC	ribonucleoprotein complex	5.30E-81
GO:0005198	MF	structural molecule activity	7.90E-73
GO:0022625	CC	cytosolic large ribosomal subunit	6.80E-71
GO:0044446	CC	intracellular organelle part	4.00E-70
GO:0044422	CC	organelle part	6.50E-70
GO:0015934	CC	large ribosomal subunit	7.50E-63
GO:0022627	CC	cytosolic small ribosomal subunit	7.30E-47
GO:0005730	CC	Nucleolus	1.60E-45
GO:0005829	CC	Cytosol	3.40E-43
GO:0015935	CC	small ribosomal subunit	3.80E-43
GO:0032991	CC	macromolecular complex	8.20E-41
GO:0044435	CC	plastid part	3.90E-37
GO:0044434	CC	chloroplast part	4.80E-36
GO:0031974	CC	membrane-enclosed lumen	4.90E-36
GO:0009507	CC	Chloroplast	1.20E-35
GO:0043233	CC	organelle lumen	1.50E-35
GO:0070013	CC	intracellular organelle lumen	1.50E-35
GO:0031981	CC	nuclear lumen	5.30E-35
GO:0009536	CC	Plastid	8.30E-35

GO:0044428	CC	nuclear part	8.50E-31
GO:0009532	CC	plastid stroma	1.70E-28
GO:0009570	CC	chloroplast stroma	2.90E-27
GO:0005773	CC	Vacuole	1.20E-20
GO:0044444	CC	cytoplasmic part	2.70E-20
GO:0055044	CC	Symplast	1.00E-19
GO:0009506	CC	Plasmodesma	1.00E-19
GO:0005911	CC	cell-cell junction	1.20E-19
GO:0030054	CC	cell junction	1.80E-19
GO:0009526	CC	plastid envelope	9.70E-19
GO:0031090	CC	organelle membrane	1.00E-18
GO:0009941	CC	chloroplast envelope	2.70E-18
GO:0009579	CC	Thylakoid	3.20E-18
GO:0005774	CC	vacuolar membrane	6.90E-18
GO:0044437	CC	vacuolar part	8.20E-18
GO:0003723	MF	RNA binding	1.60E-16
GO:0044459	CC	plasma membrane part	1.70E-16
GO:0005618	CC	cell wall	3.00E-16
GO:0030312	CC	external encapsulating structure	3.50E-16
GO:0031975	CC	Envelope	2.10E-14
GO:0031967	CC	organelle envelope	2.10E-14
GO:0005737	CC	Cytoplasm	1.70E-13
GO:0044436	CC	thylakoid part	6.20E-12
GO:0042651	CC	thylakoid membrane	8.70E-12
GO:0016020	CC	Membrane	1.20E-11
GO:0034357	CC	photosynthetic membrane	1.80E-11
GO:0055035	CC	plastid thylakoid membrane	2.50E-11
GO:0031976	CC	plastid thylakoid	6.60E-11
GO:0009534	CC	chloroplast thylakoid	6.60E-11
GO:0048046	CC	Apoplast	8.80E-11

GO:0009535	CC	chloroplast thylakoid membrane	8.80E-11
GO:0031984	CC	organelle subcompartment	1.00E-10
GO:0005886	CC	plasma membrane	7.40E-09
GO:0009295	CC	Nucleoid	3.20E-07
GO:0042623	MF	ATPase activity, coupled	7.00E-07
GO:0044425	CC	membrane part	1.80E-06
GO:0000790	CC	nuclear chromatin	2.40E-06
GO:0016887	MF	ATPase activity	1.90E-05
GO:0016853	MF	isomerase activity	2.90E-05
GO:0000166	MF	nucleotide binding	7.30E-05
GO:0016831	MF	carboxy-lyase activity	7.30E-05
GO:0008094	MF	DNA-dependent ATPase activity	9.70E-05
GO:0003746	MF	translation elongation factor activity	9.70E-05
GO:0042646	CC	plastid nucleoid	0.00015
GO:0019843	MF	rRNA binding	0.00021
GO:0005507	MF	copper ion binding	0.00038
GO:0005488	MF	Binding	0.00046
GO:0070035	MF	purine NTP-dependent helicase activity	0.00067
GO:0016830	MF	carbon-carbon lyase activity	0.00067
GO:0008026	MF	ATP-dependent helicase activity	0.00067
GO:0044454	CC	nuclear chromosome part	0.00073
GO:0016866	MF	intramolecular transferase activity	0.00092
GO:0016741	MF	transferase activity, transferring one-carbon groups	0.00099
GO:0008168	MF	methyltransferase activity	0.00099

MF; Molecular Function, CC; Cellular Component

Table V-5. GO terms of up-regulated genes after 48 h *A. candida* inoculation in 'Misugi'

GO accession number	Term type	Term	FDR
GO:0022626	CC	cytosolic ribosome	6.10E-81
GO:0044445	CC	cytosolic part	4.50E-71
GO:0003735	MF	structural constituent of ribosome	1.20E-70
GO:0033279	CC	ribosomal subunit	3.90E-70
GO:0043228	CC	non-membrane-bounded organelle	6.80E-70
GO:0005840	CC	Ribosome	6.80E-70
GO:0043232	CC	intracellular non-membrane-bounded organelle	6.80E-70
GO:0044446	CC	intracellular organelle part	6.80E-70
GO:0044422	CC	organelle part	1.00E-69
GO:0030529	CC	ribonucleoprotein complex	5.30E-65
GO:0009532	CC	plastid stroma	2.20E-56
GO:0005198	MF	structural molecule activity	2.40E-56
GO:0009570	CC	chloroplast stroma	4.60E-56
GO:0044435	CC	plastid part	4.80E-54
GO:0044434	CC	chloroplast part	1.50E-53
GO:0022625	CC	cytosolic large ribosomal subunit	3.70E-52
GO:0005829	CC	Cytosol	6.90E-50
GO:0015934	CC	large ribosomal subunit	2.30E-48
GO:0009507	CC	Chloroplast	4.90E-46
GO:0009536	CC	Plastid	8.30E-46
GO:0005730	CC	Nucleolus	7.10E-39
GO:0032991	CC	macromolecular complex	1.60E-28
GO:0031981	CC	nuclear lumen	8.90E-27
GO:0043233	CC	organelle lumen	2.80E-26
GO:0070013	CC	intracellular organelle lumen	2.80E-26
GO:0031974	CC	membrane-enclosed lumen	4.20E-26
GO:0022627	CC	cytosolic small ribosomal subunit	7.90E-26

GO:0044444	CC	cytoplasmic part	1.60E-24
GO:0044428	CC	nuclear part	1.10E-23
GO:0015935	CC	small ribosomal subunit	1.30E-23
GO:0005773	CC	Vacuole	1.90E-23
GO:0009941	CC	chloroplast envelope	2.50E-21
GO:0009526	CC	plastid envelope	3.40E-21
GO:0055044	CC	Symplast	5.00E-20
GO:0009506	CC	Plasmodesma	5.00E-20
GO:0005911	CC	cell-cell junction	5.70E-20
GO:0030054	CC	cell junction	8.70E-20
GO:0009579	CC	Thylakoid	8.60E-18
GO:0044459	CC	plasma membrane part	1.70E-16
GO:0005737	CC	Cytoplasm	2.10E-16
GO:0031975	CC	Envelope	3.30E-16
GO:0031967	CC	organelle envelope	3.30E-16
GO:0005774	CC	vacuolar membrane	4.90E-16
GO:0031090	CC	organelle membrane	5.00E-16
GO:0044437	CC	vacuolar part	5.60E-16
GO:0003723	MF	RNA binding	1.60E-10
GO:0048046	CC	Apoplast	3.60E-09
GO:0031976	CC	plastid thylakoid	5.10E-09
GO:0009534	CC	chloroplast thylakoid	5.10E-09
GO:0055035	CC	plastid thylakoid membrane	5.50E-09
GO:0042651	CC	thylakoid membrane	6.30E-09
GO:0031984	CC	organelle subcompartment	7.20E-09
GO:0034357	CC	photosynthetic membrane	1.10E-08
GO:0005618	CC	cell wall	2.60E-08
GO:0030312	CC	external encapsulating structure	2.90E-08
GO:0044436	CC	thylakoid part	3.60E-08
GO:0009535	CC	chloroplast thylakoid membrane	7.00E-08

GO:0005507	MF	copper ion binding	1.90E-07
GO:0016829	MF	lyase activity	1.10E-06
GO:0016020	CC	Membrane	1.50E-06
GO:0009295	CC	Nucleoid	1.90E-06
GO:0044425	CC	membrane part	3.10E-06
GO:0042644	CC	chloroplast nucleoid	4.00E-06
GO:0030170	MF	pyridoxal phosphate binding	5.00E-06
GO:0070279	MF	vitamin B6 binding	5.00E-06
GO:0042646	CC	plastid nucleoid	5.40E-06
GO:0016741	MF	transferase activity, transferring one-carbon groups	1.20E-05
GO:0008168	MF	methyltransferase activity	1.20E-05
GO:0016853	MF	isomerase activity	1.60E-05
GO:0043229	CC	intracellular organelle	4.40E-05
GO:0043226	CC	Organelle	4.50E-05
GO:0005777	CC	Peroxisome	9.60E-05
GO:0042579	CC	Microbody	9.60E-05
GO:0019843	MF	rRNA binding	0.00012
GO:0019842	MF	vitamin binding	0.00020
GO:0016831	MF	carboxy-lyase activity	0.00028
GO:0016830	MF	carbon-carbon lyase activity	0.00031
GO:0005886	CC	plasma membrane	0.00032
GO:0016861	MF	intramolecular oxidoreductase activity, interconverting aldoses and ketoses	0.00042
GO:0003824	MF	catalytic activity	0.00045
GO:0048037	MF	cofactor binding	0.00045
GO:0044424	CC	intracellular part	0.00054
GO:0043231	CC	intracellular membrane-bounded organelle	0.00075
GO:0005622	CC	Intracellular	0.00075
GO:0043227	CC	membrane-bounded organelle	0.00075
GO:0000166	MF	nucleotide binding	0.00084

GO:0005488	MF	Binding	0.00094

MF; Molecular Function, CC; Cellular Component

Table V-6. GO terms of down-regulated genes after 48 h *A. candida* inoculation in 'Nanane'

GO accession number	Term type	Term	FDR
GO:0030528	MF	transcription regulator activity	4.20E-12
GO:0003700	MF	transcription factor activity	1.30E-11
GO:0003677	MF	DNA binding	2.90E-07
GO:0016758	MF	transferase activity, transferring hexosyl groups	2.10E-05
GO:0005515	MF	protein binding	2.10E-05

MF; Molecular Function

Table V-7. GO terms of down-regulated genes after 48 h *A. candida* inoculation in 'Misugi'

GO accession number	Term type	Term	FDR
GO:0009628	BP	response to abiotic stimulus	7.30E-15
GO:0006970	BP	response to osmotic stress	7.20E-13
GO:0009651	BP	response to salt stress	2.70E-12
GO:0010264	BP	myo-inositol hexakisphosphate biosynthetic process	1.40E-10
GO:0006021	BP	inositol biosynthetic process	1.40E-10
GO:0032958	BP	inositol phosphate biosynthetic process	1.40E-10
GO:0033517	BP	myo-inositol hexakisphosphate metabolic process	1.40E-10
GO:0044283	BP	small molecule biosynthetic process	6.50E-10
GO:0050896	BP	response to stimulus	7.80E-10
GO:0042221	BP	response to chemical stimulus	7.80E-10
GO:0010033	BP	response to organic substance	1.80E-09
GO:0043647	BP	inositol phosphate metabolic process	1.80E-09
GO:0009698	BP	phenylpropanoid metabolic process	2.90E-09
GO:0009813	BP	flavonoid biosynthetic process	5.20E-09
GO:0046173	BP	polyol biosynthetic process	5.20E-09
GO:0009812	BP	flavonoid metabolic process	6.40E-09
GO:0009719	BP	response to endogenous stimulus	6.80E-09
GO:0009737	BP	response to abscisic acid stimulus	6.90E-09
GO:0006020	BP	inositol metabolic process	8.80E-09
GO:0006950	BP	response to stress	1.40E-08
GO:0009411	BP	response to UV	1.60E-08
GO:0009416	BP	response to light stimulus	1.90E-08
GO:0009725	BP	response to hormone stimulus	3.30E-08
GO:0006833	BP	water transport	4.60E-08
GO:0042044	BP	fluid transport	4.60E-08
GO:0019748	BP	secondary metabolic process	8.40E-08

GO:0009314	BP	response to radiation	1.60E-07
GO:0006575	BP	cellular amino acid derivative metabolic process	2.20E-07
GO:0019751	BP	polyol metabolic process	2.20E-07
GO:0009699	BP	phenylpropanoid biosynthetic process	8.80E-07
GO:0005215	BP	transporter activity	8.90E-07
GO:0048511	BP	rhythmic process	1.20E-06
GO:0007623	BP	circadian rhythm	1.20E-06
GO:0050801	BP	ion homeostasis	1.20E-06
GO:0009414	BP	response to water deprivation	1.20E-06
GO:0042398	BP	cellular amino acid derivative biosynthetic process	1.30E-06
GO:0009415	BP	response to water	1.50E-06
GO:0006595	BP	polyamine metabolic process	1.70E-06
GO:0005372	BP	water transmembrane transporter activity	2.20E-06
GO:0015250	BP	water channel activity	2.20E-06
GO:0048878	BP	chemical homeostasis	2.30E-06
GO:0005886	CC	plasma membrane	2.50E-06
GO:0022857	MF	transmembrane transporter activity	3.20E-06
GO:0009963	BP	positive regulation of flavonoid biosynthetic process	5.40E-06
GO:0006725	BP	cellular aromatic compound metabolic process	8.00E-06
GO:0006598	BP	polyamine catabolic process	9.30E-06
GO:0022838	MF	substrate-specific channel activity	1.10E-05
GO:0015267	MF	channel activity	1.10E-05
GO:0022803	MF	passive transmembrane transporter activity	1.10E-05
GO:0009266	BP	response to temperature stimulus	1.20E-05
GO:0043455	BP	regulation of secondary metabolic process	1.20E-05
GO:0070838	BP	divalent metal ion transport	1.30E-05
GO:0046165	BP	alcohol biosynthetic process	1.40E-05
GO:0010224	BP	response to UV-B	1.50E-05
GO:0006972	BP	hyperosmotic response	1.70E-05
GO:0006519	BP	cellular amino acid and derivative metabolic process	2.20E-05

GO:0042402	BP	cellular biogenic amine catabolic process	2.20E-05
GO:0006873	BP	cellular ion homeostasis	2.50E-05
GO:0055082	BP	cellular chemical homeostasis	2.90E-05
GO:0055085	BP	transmembrane transport	3.00E-05
GO:0044281	BP	small molecule metabolic process	3.00E-05
GO:0006066	BP	alcohol metabolic process	3.40E-05
GO:0009962	BP	regulation of flavonoid biosynthetic process	3.60E-05
GO:0009755	BP	hormone-mediated signaling pathway	3.60E-05
GO:0006576	BP	cellular biogenic amine metabolic process	5.60E-05
GO:0022891	MF	substrate-specific transmembrane transporter activity	5.60E-05
GO:0015674	BP	di-, tri-valent inorganic cation transport	5.70E-05
GO:0009743	BP	response to carbohydrate stimulus	9.30E-05
GO:0071495	BP	cellular response to endogenous stimulus	0.0001
GO:0009409	BP	response to cold	0.00012
GO:0009310	BP	amine catabolic process	0.00013
GO:0042219	BP	cellular amino acid derivative catabolic process	0.00013
GO:0009605	BP	response to external stimulus	0.00013
GO:0009705	CC	plant-type vacuole membrane	0.00013
GO:0000325	CC	plant-type vacuole	0.00013
GO:0051716	BP	cellular response to stimulus	0.00014
GO:0022804	MF	active transmembrane transporter activity	0.00014
GO:0009739	BP	response to gibberellin stimulus	0.00015
GO:0032870	BP	cellular response to hormone stimulus	0.00015
GO:0009753	BP	response to jasmonic acid stimulus	0.00019
GO:0044437	CC	vacuolar part	0.00019
GO:0005774	CC	vacuolar membrane	0.00019
GO:0007242	BP	intracellular signaling cascade	0.00021
GO:0023052	BP	Signaling	0.00022
GO:0022892	MF	substrate-specific transporter activity	0.00023
GO:0055080	BP	cation homeostasis	0.00024

GO:0006816	BP	calcium ion transport	0.00028
GO:0090056	BP	regulation of chlorophyll metabolic process	0.00028
GO:0044282	BP	small molecule catabolic process	0.00030
GO:0030003	BP	cellular cation homeostasis	0.00039
GO:0005515	MF	protein binding	0.00043
GO:0042592	BP	homeostatic process	0.00049
GO:0009750	BP	response to fructose stimulus	0.00050
GO:0016020	CC	Membrane	0.00052
GO:0034284	BP	response to monosaccharide stimulus	0.00057
GO:0019725	BP	cellular homeostasis	0.00057
GO:0009746	BP	response to hexose stimulus	0.00057
GO:0051193	BP	regulation of cofactor metabolic process	0.00086
GO:0007030	BP	Golgi organization	0.00090
GO:0009805	BP	coumarin biosynthetic process	0.00090
GO:0009804	BP	coumarin metabolic process	0.00090
GO:0065007	BP	biological regulation	0.00090
GO:0048767	BP	root hair elongation	0.00096

MF; Molecular Function, CC; Cellular Component, BP; Biological Process

Table V-8. GO terms of up-regulated genes after 72 h *A. candida* inoculation in 'Nanane'

GO accession number	Term type	Term	FDR
GO:0044435	CC	plastid part	1.10E-34
GO:0044434	CC	chloroplast part	1.10E-33
GO:0044446	CC	intracellular organelle part	4.70E-30
GO:0044422	CC	organelle part	4.80E-30
GO:0009507	CC	Chloroplast	5.10E-30
GO:0009536	CC	Plastid	5.10E-30
GO:0009532	CC	plastid stroma	5.10E-30
GO:0009570	CC	chloroplast stroma	1.30E-28
GO:0009579	CC	Thylakoid	5.60E-26
GO:0022626	CC	cytosolic ribosome	1.80E-23
GO:0001510	BP	RNA methylation	4.40E-23
GO:0042254	BP	ribosome biogenesis	1.50E-22
GO:0022613	BP	ribonucleoprotein complex biogenesis	2.30E-22
GO:0005840	CC	Ribosome	7.60E-21
GO:0003735	MF	structural constituent of ribosome	4.00E-20
GO:0033279	CC	ribosomal subunit	5.80E-20
GO:0043228	CC	non-membrane-bounded organelle	5.90E-20
GO:0043232	CC	intracellular non-membrane-bounded organelle	5.90E-20
GO:0044281	BP	small molecule metabolic process	2.20E-19
GO:0055035	CC	plastid thylakoid membrane	2.50E-19
GO:0042651	CC	thylakoid membrane	4.40E-19
GO:0044445	CC	cytosolic part	5.50E-19
GO:0030529	CC	ribonucleoprotein complex	5.50E-19
GO:0034357	CC	photosynthetic membrane	1.00E-18
GO:0009535	CC	chloroplast thylakoid membrane	1.00E-18
GO:0031976	CC	plastid thylakoid	1.00E-18
GO:0009534	CC	chloroplast thylakoid	1.00E-18

GO:0031984	CC	organelle subcompartment	1.90E-18
GO:0044436	CC	thylakoid part	8.20E-18
GO:0005198	MF	structural molecule activity	6.50E-17
GO:0006412	BP	Translation	2.00E-16
GO:0009451	BP	RNA modification	2.20E-16
GO:0009941	CC	chloroplast envelope	1.30E-15
GO:0048046	CC	Apoplast	1.40E-15
GO:0015979	BP	Photosynthesis	2.10E-15
GO:0009526	CC	plastid envelope	4.80E-15
GO:0009657	BP	plastid organization	4.10E-14
GO:0006091	BP	generation of precursor metabolites and energy	1.10E-13
GO:0032787	BP	monocarboxylic acid metabolic process	1.10E-13
GO:0043436	BP	oxoacid metabolic process	1.40E-13
GO:0006082	BP	organic acid metabolic process	1.40E-13
GO:0042180	BP	cellular ketone metabolic process	1.40E-13
GO:0019752	BP	carboxylic acid metabolic process	1.40E-13
GO:0006364	BP	rRNA processing	2.40E-13
GO:0006950	BP	response to stress	2.60E-13
GO:0016072	BP	rRNA metabolic process	2.70E-13
GO:0015934	CC	large ribosomal subunit	3.60E-13
GO:0005829	CC	Cytosol	3.90E-13
GO:0044282	BP	small molecule catabolic process	4.30E-13
GO:0051707	BP	response to other organism	4.60E-13
GO:0019252	BP	starch biosynthetic process	6.10E-13
GO:0006725	BP	cellular aromatic compound metabolic process	6.10E-13
GO:0010035	BP	response to inorganic substance	7.60E-13
GO:0005982	BP	starch metabolic process	7.60E-13
GO:0031090	CC	organelle membrane	1.60E-12
GO:0005975	BP	carbohydrate metabolic process	1.70E-12
GO:0044262	BP	cellular carbohydrate metabolic process	1.90E-12

GO:0034641	BP	cellular nitrogen compound metabolic process	2.10E-12
GO:0019748	BP	secondary metabolic process	2.60E-12
GO:0005996	BP	monosaccharide metabolic process	3.50E-12
GO:0044283	BP	small molecule biosynthetic process	5.10E-12
GO:0006090	BP	pyruvate metabolic process	5.90E-12
GO:0019684	BP	photosynthesis, light reaction	7.00E-12
GO:0044275	BP	cellular carbohydrate catabolic process	1.40E-11
GO:0034660	BP	ncRNA metabolic process	1.40E-11
GO:0006952	BP	defense response	1.50E-11
GO:0050896	BP	response to stimulus	1.50E-11
GO:0016052	BP	carbohydrate catabolic process	1.60E-11
GO:0042742	BP	defense response to bacterium	1.60E-11
GO:0009607	BP	response to biotic stimulus	1.90E-11
GO:0022625	CC	cytosolic large ribosomal subunit	2.10E-11
GO:0034637	BP	cellular carbohydrate biosynthetic process	2.20E-11
GO:0045087	BP	innate immune response	2.80E-11
GO:0009617	BP	response to bacterium	2.80E-11
GO:0005730	CC	Nucleolus	4.40E-11
GO:0034470	BP	ncRNA processing	5.90E-11
GO:0019288	BP	isopentenyl diphosphate biosynthetic process, mevalonate-independent pathway	6.10E-11
GO:0044271	BP	cellular nitrogen compound biosynthetic process	6.20E-11
GO:0044249	BP	cellular biosynthetic process	7.20E-11
GO:0002376	BP	immune system process	7.20E-11
GO:0006955	BP	immune response	7.20E-11
GO:0009240	BP	isopentenyl diphosphate biosynthetic process	8.70E-11
GO:0046490	BP	isopentenyl diphosphate metabolic process	8.70E-11
GO:0000023	BP	maltose metabolic process	9.10E-11
GO:0044237	BP	cellular metabolic process	9.20E-11
GO:0019682	BP	glyceraldehyde-3-phosphate metabolic process	1.00E-10

GO:0044444	CC	cytoplasmic part	1.00E-10
GO:0016143	BP	S-glycoside metabolic process	1.20E-10
GO:0019757	BP	glycosinolate metabolic process	1.20E-10
GO:0019760	BP	glucosinolate metabolic process	1.20E-10
GO:0016051	BP	carbohydrate biosynthetic process	1.50E-10
GO:0009628	BP	response to abiotic stimulus	1.50E-10
GO:0005618	CC	cell wall	1.70E-10
GO:0019725	BP	cellular homeostasis	1.80E-10
GO:0006066	BP	alcohol metabolic process	1.90E-10
GO:0009658	BP	chloroplast organization	1.90E-10
GO:0030312	CC	external encapsulating structure	1.90E-10
GO:0009058	BP	biosynthetic process	2.00E-10
GO:0009696	BP	salicylic acid metabolic process	2.20E-10
GO:0046164	BP	alcohol catabolic process	2.20E-10
GO:0019320	BP	hexose catabolic process	2.50E-10
GO:0006007	BP	glucose catabolic process	2.50E-10
GO:0042402	BP	cellular biogenic amine catabolic process	2.60E-10
GO:0046394	BP	carboxylic acid biosynthetic process	2.70E-10
GO:0016053	BP	organic acid biosynthetic process	2.70E-10
GO:0006576	BP	cellular biogenic amine metabolic process	2.80E-10
GO:0046365	BP	monosaccharide catabolic process	3.40E-10
GO:0031975	CC	Envelope	3.60E-10
GO:0031967	CC	organelle envelope	3.60E-10
GO:0019761	BP	glucosinolate biosynthetic process	3.80E-10
GO:0016144	BP	S-glycoside biosynthetic process	3.80E-10
GO:0019758	BP	glycosinolate biosynthetic process	3.80E-10
GO:0009814	BP	defense response, incompatible interaction	4.40E-10
GO:0042221	BP	response to chemical stimulus	5.20E-10
GO:0009310	BP	amine catabolic process	6.00E-10
GO:0009266	BP	response to temperature stimulus	6.50E-10

GO:0006995	BP	cellular response to nitrogen starvation	6.50E-10
GO:0006006	BP	glucose metabolic process	8.30E-10
GO:0042219	BP	cellular amino acid derivative catabolic process	9.20E-10
GO:0051704	BP	multi-organism process	9.20E-10
GO:0046686	BP	response to cadmium ion	1.00E-09
GO:0044272	BP	sulfur compound biosynthetic process	1.10E-09
GO:0008152	BP	metabolic process	1.20E-09
GO:0019318	BP	hexose metabolic process	1.30E-09
GO:0033554	BP	cellular response to stress	1.30E-09
GO:0043414	BP	macromolecule methylation	1.50E-09
GO:0016138	BP	glycoside biosynthetic process	1.50E-09
GO:0006807	BP	nitrogen compound metabolic process	1.50E-09
GO:0010038	BP	response to metal ion	1.80E-09
GO:0016137	BP	glycoside metabolic process	1.80E-09
GO:0009683	BP	indoleacetic acid metabolic process	1.90E-09
GO:0009684	BP	indoleacetic acid biosynthetic process	1.90E-09
GO:0006081	BP	cellular aldehyde metabolic process	1.90E-09
GO:0042743	BP	hydrogen peroxide metabolic process	2.00E-09
GO:0032259	BP	Methylation	2.40E-09
GO:0070013	CC	intracellular organelle lumen	2.80E-09
GO:0043233	CC	organelle lumen	2.80E-09
GO:0055082	BP	cellular chemical homeostasis	2.90E-09
GO:0045088	BP	regulation of innate immune response	3.20E-09
GO:0009627	BP	systemic acquired resistance	3.40E-09
GO:0031974	CC	membrane-enclosed lumen	3.40E-09
GO:0002682	BP	regulation of immune system process	3.60E-09
GO:0050776	BP	regulation of immune response	3.60E-09
GO:0005984	BP	disaccharide metabolic process	4.80E-09
GO:0009056	BP	catabolic process	4.80E-09
GO:0032991	CC	macromolecular complex	5.10E-09

GO:0006800	BP	oxygen and reactive oxygen species metabolic process	5.30E-09
GO:0044248	BP	cellular catabolic process	5.60E-09
GO:0043562	BP	cellular response to nitrogen levels	5.70E-09
GO:0010363	BP	regulation of plant-type hypersensitive response	5.80E-09
GO:0009311	BP	oligosaccharide metabolic process	5.80E-09
GO:0044042	BP	glucan metabolic process	5.90E-09
GO:0080134	BP	regulation of response to stress	6.50E-09
GO:0030003	BP	cellular cation homeostasis	6.70E-09
GO:0044238	BP	primary metabolic process	6.90E-09
GO:0009626	BP	plant-type hypersensitive response	6.90E-09
GO:0034050	BP	host programmed cell death induced by symbiont	7.80E-09
GO:0080010	BP	regulation of oxygen and reactive oxygen species metabolic process	8.10E-09
GO:0010310	BP	regulation of hydrogen peroxide metabolic process	8.10E-09
GO:0031347	BP	regulation of defense response	8.60E-09
GO:0006612	BP	protein targeting to membrane	9.10E-09
GO:0009074	BP	aromatic amino acid family catabolic process	1.00E-08
GO:0006730	BP	one-carbon metabolic process	1.00E-08
GO:0009697	BP	salicylic acid biosynthetic process	1.00E-08
GO:0016020	CC	Membrane	1.10E-08
GO:0080135	BP	regulation of cellular response to stress	1.20E-08
GO:0043067	BP	regulation of programmed cell death	1.20E-08
GO:0006519	BP	cellular amino acid and derivative metabolic process	1.20E-08
GO:0044106	BP	cellular amine metabolic process	1.30E-08
GO:0006873	BP	cellular ion homeostasis	1.30E-08
GO:0009851	BP	auxin biosynthetic process	1.30E-08
GO:0022627	CC	cytosolic small ribosomal subunit	1.30E-08
GO:0044085	BP	cellular component biogenesis	1.60E-08
GO:0042434	BP	indole derivative metabolic process	1.60E-08

GO:0042430	BP	indole and derivative metabolic process	1.60E-08
GO:0051234	BP	establishment of localization	1.60E-08
GO:0012501	BP	programmed cell death	1.60E-08
GO:0009308	BP	amine metabolic process	1.60E-08
GO:0019438	BP	aromatic compound biosynthetic process	1.60E-08
GO:0070838	BP	divalent metal ion transport	1.80E-08
GO:0055080	BP	cation homeostasis	1.80E-08
GO:0006970	BP	response to osmotic stress	1.90E-08
GO:0042592	BP	homeostatic process	2.00E-08
GO:0009250	BP	glucan biosynthetic process	2.00E-08
GO:0010941	BP	regulation of cell death	2.00E-08
GO:0042435	BP	indole derivative biosynthetic process	2.30E-08
GO:0006605	BP	protein targeting	2.80E-08
GO:0042436	BP	indole derivative catabolic process	2.90E-08
GO:0019439	BP	aromatic compound catabolic process	2.90E-08
GO:0006073	BP	cellular glucan metabolic process	3.30E-08
GO:0055044	CC	Symplast	3.40E-08
GO:0009506	CC	Plasmodesma	3.40E-08
GO:0005911	CC	cell-cell junction	3.60E-08
GO:0050832	BP	defense response to fungus	4.00E-08
GO:0051179	BP	Localization	4.00E-08
GO:0030054	CC	cell junction	4.40E-08
GO:0006811	BP	ion transport	4.70E-08
GO:0048878	BP	chemical homeostasis	4.70E-08
GO:0009651	BP	response to salt stress	5.10E-08
GO:0050801	BP	ion homeostasis	5.50E-08
GO:0008299	BP	isoprenoid biosynthetic process	6.80E-08
GO:0015935	CC	small ribosomal subunit	7.10E-08
GO:0048583	BP	regulation of response to stimulus	7.40E-08
GO:0005773	CC	Vacuole	7.40E-08

GO:0031981	CC	nuclear lumen	7.50E-08
GO:0005737	CC	Cytoplasm	7.60E-08
GO:0051649	BP	establishment of localization in cell	8.20E-08
GO:0008219	BP	cell death	8.40E-08
GO:0016265	BP	Death	8.40E-08
GO:0009850	BP	auxin metabolic process	9.00E-08
GO:0006790	BP	sulfur metabolic process	1.10E-07
GO:0043170	BP	macromolecule metabolic process	1.10E-07
GO:0006569	BP	tryptophan catabolic process	1.40E-07
GO:0046218	BP	indolalkylamine catabolic process	1.40E-07
GO:0016168	MF	chlorophyll binding	1.50E-07
GO:0009620	BP	response to fungus	1.60E-07
GO:0009117	BP	nucleotide metabolic process	1.60E-07
GO:0009765	BP	photosynthesis, light harvesting	1.80E-07
GO:0006753	BP	nucleoside phosphate metabolic process	1.90E-07
GO:0046483	BP	heterocycle metabolic process	2.10E-07
GO:0009063	BP	cellular amino acid catabolic process	2.50E-07
GO:0006720	BP	isoprenoid metabolic process	2.70E-07
GO:0044260	BP	cellular macromolecule metabolic process	2.70E-07
GO:0009987	BP	cellular process	3.50E-07
GO:0051641	BP	cellular localization	3.60E-07
GO:0008654	BP	phospholipid biosynthetic process	3.90E-07
GO:0010467	BP	gene expression	4.00E-07
GO:0006979	BP	response to oxidative stress	4.80E-07
GO:0019538	BP	protein metabolic process	6.00E-07
GO:0010287	CC	Plastoglobuli	7.40E-07
GO:0044093	BP	positive regulation of molecular function	8.70E-07
GO:0043085	BP	positive regulation of catalytic activity	8.70E-07
GO:0006575	BP	cellular amino acid derivative metabolic process	8.90E-07
GO:0030076	CC	light-harvesting complex	9.10E-07

GO:0015674	BP	di-, tri-valent inorganic cation transport	9.30E-07
GO:0051186	BP	cofactor metabolic process	1.00E-06
GO:0034754	BP	cellular hormone metabolic process	1.10E-06
GO:0051667	BP	establishment of plastid localization	1.40E-06
GO:0051644	BP	plastid localization	1.40E-06
GO:0009902	BP	chloroplast relocation	1.40E-06
GO:0055086	BP	nucleobase, nucleoside and nucleotide metabolic process	1.40E-06
GO:0009072	BP	aromatic amino acid family metabolic process	1.50E-06
GO:0009409	BP	response to cold	1.70E-06
GO:0006520	BP	cellular amino acid metabolic process	1.80E-06
GO:0044267	BP	cellular protein metabolic process	1.80E-06
GO:0010027	BP	thylakoid membrane organization	2.10E-06
GO:0009668	BP	plastid membrane organization	2.10E-06
GO:0009595	BP	detection of biotic stimulus	2.20E-06
GO:0006098	BP	pentose-phosphate shunt	2.20E-06
GO:0006740	BP	NADPH regeneration	2.20E-06
GO:0051716	BP	cellular response to stimulus	2.20E-06
GO:0009862	BP	systemic acquired resistance, salicylic acid mediated signaling pathway	2.40E-06
GO:0009069	BP	serine family amino acid metabolic process	2.40E-06
GO:0034613	BP	cellular protein localization	2.50E-06
GO:0006644	BP	phospholipid metabolic process	2.60E-06
GO:0051656	BP	establishment of organelle localization	2.70E-06
GO:0000165	BP	MAPKKK cascade	2.80E-06
GO:0006739	BP	NADP metabolic process	3.00E-06
GO:0006810	BP	Transport	3.20E-06
GO:0006886	BP	intracellular protein transport	3.60E-06
GO:0009863	BP	salicylic acid mediated signaling pathway	3.80E-06
GO:0071446	BP	cellular response to salicylic acid stimulus	3.80E-06

GO:0005976	BP	polysaccharide metabolic process	3.90E-06
GO:0009867	BP	jasmonic acid mediated signaling pathway	4.20E-06
GO:0071395	BP	cellular response to jasmonic acid stimulus	4.20E-06
GO:0006996	BP	organelle organization	4.70E-06
GO:0006414	BP	translational elongation	4.70E-06
GO:0019344	BP	cysteine biosynthetic process	4.90E-06
GO:0042274	BP	ribosomal small subunit biogenesis	5.00E-06
GO:0006568	BP	tryptophan metabolic process	5.00E-06
GO:0006586	BP	indolalkylamine metabolic process	5.00E-06
GO:0006534	BP	cysteine metabolic process	5.60E-06
GO:0019637	BP	organophosphate metabolic process	5.80E-06
GO:0006733	BP	oxidoreduction coenzyme metabolic process	6.00E-06
GO:0009220	BP	pyrimidine ribonucleotide biosynthetic process	6.30E-06
GO:0046496	BP	nicotinamide nucleotide metabolic process	6.30E-06
GO:0006769	BP	nicotinamide metabolic process	6.30E-06
GO:0006812	BP	cation transport	6.30E-06
GO:0070727	BP	cellular macromolecule localization	6.60E-06
GO:0019362	BP	pyridine nucleotide metabolic process	7.30E-06
GO:0007243	BP	protein kinase cascade	8.10E-06
GO:0006396	BP	RNA processing	8.50E-06
GO:0051188	BP	cofactor biosynthetic process	1.10E-05
GO:0031399	BP	regulation of protein modification process	1.10E-05
GO:0009218	BP	pyrimidine ribonucleotide metabolic process	1.10E-05
GO:0009070	BP	serine family amino acid biosynthetic process	1.10E-05
GO:0043603	BP	cellular amide metabolic process	1.30E-05
GO:0043900	BP	regulation of multi-organism process	1.30E-05
GO:0009991	BP	response to extracellular stimulus	1.40E-05
GO:0009753	BP	response to jasmonic acid stimulus	1.40E-05
GO:0009820	BP	alkaloid metabolic process	1.50E-05
GO:0006221	BP	pyrimidine nucleotide biosynthetic process	1.50E-05

GO:0031668	BP	cellular response to extracellular stimulus	1.60E-05
GO:0071496	BP	cellular response to external stimulus	1.80E-05
GO:0006220	BP	pyrimidine nucleotide metabolic process	1.80E-05
GO:0009751	BP	response to salicylic acid stimulus	1.90E-05
GO:0016070	BP	RNA metabolic process	2.00E-05
GO:0046906	MF	tetrapyrrole binding	2.00E-05
GO:0009309	BP	amine biosynthetic process	2.10E-05
GO:0008104	BP	protein localization	2.40E-05
GO:0044428	CC	nuclear part	2.40E-05
GO:0031348	BP	negative regulation of defense response	2.50E-05
GO:0033036	BP	macromolecule localization	2.50E-05
GO:0046148	BP	pigment biosynthetic process	2.50E-05
GO:0035304	BP	regulation of protein amino acid dephosphorylation	2.60E-05
GO:0035303	BP	regulation of dephosphorylation	3.10E-05
GO:0044264	BP	cellular polysaccharide metabolic process	3.20E-05
GO:0044459	CC	plasma membrane part	3.30E-05
GO:0009891	BP	positive regulation of biosynthetic process	3.40E-05
GO:0031328	BP	positive regulation of cellular biosynthetic process	3.40E-05
GO:0018198	BP	peptidyl-cysteine modification	3.50E-05
GO:0045036	BP	protein targeting to chloroplast	3.90E-05
GO:0032268	BP	regulation of cellular protein metabolic process	5.80E-05
GO:0030001	BP	metal ion transport	6.20E-05
GO:0044265	BP	cellular macromolecule catabolic process	6.40E-05
GO:0009295	CC	Nucleoid	6.60E-05
GO:0005774	CC	vacuolar membrane	6.60E-05
GO:0005886	CC	plasma membrane	6.60E-05
GO:0044437	CC	vacuolar part	6.90E-05
GO:0045184	BP	establishment of protein localization	7.00E-05
GO:0015031	BP	protein transport	7.00E-05
GO:0031325	BP	positive regulation of cellular metabolic process	7.50E-05

GO:0031667	BP	response to nutrient levels	7.50E-05
GO:0031669	BP	cellular response to nutrient levels	8.60E-05
GO:0006096	BP	Glycolysis	8.70E-05
GO:0033692	BP	cellular polysaccharide biosynthetic process	8.70E-05
GO:0009165	BP	nucleotide biosynthetic process	9.00E-05
GO:0009893	BP	positive regulation of metabolic process	9.00E-05
GO:0046364	BP	monosaccharide biosynthetic process	9.50E-05
GO:0009057	BP	macromolecule catabolic process	9.90E-05
GO:0006139	BP	nucleobase, nucleoside, nucleotide and nucleic acid metabolic process	0.00010
GO:0051606	BP	detection of stimulus	0.00011
GO:0000271	BP	polysaccharide biosynthetic process	0.00012
GO:0070887	BP	cellular response to chemical stimulus	0.00013
GO:0046907	BP	intracellular transport	0.00013
GO:0009267	BP	cellular response to starvation	0.00013
GO:0042446	BP	hormone biosynthetic process	0.00013
GO:0031163	BP	metallo-sulfur cluster assembly	0.00013
GO:0016226	BP	iron-sulfur cluster assembly	0.00013
GO:0007030	BP	Golgi organization	0.00014
GO:0042440	BP	pigment metabolic process	0.00015
GO:0048585	BP	negative regulation of response to stimulus	0.00015
GO:0051640	BP	organelle localization	0.00016
GO:0051246	BP	regulation of protein metabolic process	0.00017
GO:0009059	BP	macromolecule biosynthetic process	0.00018
GO:0010167	BP	response to nitrate	0.00018
GO:0034645	BP	cellular macromolecule biosynthetic process	0.00018
GO:0008652	BP	cellular amino acid biosynthetic process	0.00019
GO:0061024	BP	membrane organization	0.00019
GO:0016044	BP	cellular membrane organization	0.00019
GO:0042594	BP	response to starvation	0.00020

GO:0010103	BP	stomatal complex morphogenesis	0.00022
GO:0006457	BP	protein folding	0.00022
GO:0009719	BP	response to endogenous stimulus	0.00022
GO:0009637	BP	response to blue light	0.00025
GO:0042793	BP	transcription from plastid promoter	0.00025
GO:0006820	BP	anion transport	0.00025
GO:0006094	BP	Gluconeogenesis	0.00026
GO:0048518	BP	positive regulation of biological process	0.00026
GO:0042542	BP	response to hydrogen peroxide	0.00036
GO:0015706	BP	nitrate transport	0.00037
GO:0009605	BP	response to external stimulus	0.00037
GO:0016491	MF	oxidoreductase activity	0.00037
GO:0000478	BP	endonucleolytic cleavages during rRNA processing	0.00038
GO:0000469	BP	cleavages during rRNA processing	0.00038
GO:0016043	BP	cellular component organization	0.00042
GO:0006595	BP	polyamine metabolic process	0.00049
GO:0042744	BP	hydrogen peroxide catabolic process	0.00051
GO:0010218	BP	response to far red light	0.00056
GO:0019319	BP	hexose biosynthetic process	0.00059
GO:0070301	BP	cellular response to hydrogen peroxide	0.00064
GO:0000097	BP	sulfur amino acid biosynthetic process	0.00071
GO:0006470	BP	protein amino acid dephosphorylation	0.00073
GO:0000302	BP	response to reactive oxygen species	0.00078
GO:0009521	CC	Photosystem	0.00080
GO:0009813	BP	flavonoid biosynthetic process	0.00081
GO:0009698	BP	phenylpropanoid metabolic process	0.00085
GO:0009812	BP	flavonoid metabolic process	0.00085
GO:0034599	BP	cellular response to oxidative stress	0.00099

MF; Molecular Function, CC; Cellular Component, BP; Biological Process

Table V-9. GO terms of up-regulated genes after 72 h *A. candida* inoculation in 'Misugi'

GO accession number	Term type	Term	FDR
GO:0044435	CC	plastid part	1.80E-46
GO:0009532	CC	plastid stroma	6.40E-46
GO:0044434	CC	chloroplast part	6.20E-45
GO:0009570	CC	chloroplast stroma	9.50E-45
GO:0044446	CC	intracellular organelle part	4.50E-39
GO:0044422	CC	organelle part	5.50E-39
GO:0009507	CC	Chloroplast	2.70E-38
GO:0009536	CC	Plastid	2.80E-38
GO:0044281	BP	small molecule metabolic process	2.00E-36
GO:0044272	BP	sulfur compound biosynthetic process	5.00E-33
GO:0006790	BP	sulfur metabolic process	1.60E-31
GO:0044271	BP	cellular nitrogen compound biosynthetic process	5.50E-31
GO:0009117	BP	nucleotide metabolic process	5.50E-31
GO:0006753	BP	nucleoside phosphate metabolic process	7.30E-31
GO:0009218	BP	pyrimidine ribonucleotide metabolic process	3.20E-30
GO:0006221	BP	pyrimidine nucleotide biosynthetic process	1.10E-29
GO:0044283	BP	small molecule biosynthetic process	1.50E-29
GO:0006220	BP	pyrimidine nucleotide metabolic process	1.70E-29
GO:0055086	BP	nucleobase, nucleoside and nucleotide metabolic process	2.10E-29
GO:0006520	BP	cellular amino acid metabolic process	2.50E-29
GO:0044106	BP	cellular amine metabolic process	5.80E-29
GO:0046483	BP	heterocycle metabolic process	7.30E-29
GO:0009220	BP	pyrimidine ribonucleotide biosynthetic process	8.30E-29
GO:0034641	BP	cellular nitrogen compound metabolic process	1.60E-28
GO:0006519	BP	cellular amino acid and derivative metabolic process	1.80E-28
GO:0019761	BP	glucosinolate biosynthetic process	6.90E-28

GO:0016144	BP	S-glycoside biosynthetic process	6.90E-28
GO:0019758	BP	glycosinolate biosynthetic process	6.90E-28
GO:0016143	BP	S-glycoside metabolic process	2.00E-27
GO:0019757	BP	glycosinolate metabolic process	2.00E-27
GO:0019760	BP	glucosinolate metabolic process	2.00E-27
GO:0016051	BP	carbohydrate biosynthetic process	5.90E-27
GO:0009308	BP	amine metabolic process	7.40E-27
GO:0008652	BP	cellular amino acid biosynthetic process	7.80E-27
GO:0034637	BP	cellular carbohydrate biosynthetic process	8.30E-27
GO:0009309	BP	amine biosynthetic process	1.00E-26
GO:0043436	BP	oxoacid metabolic process	5.10E-26
GO:0019752	BP	carboxylic acid metabolic process	5.10E-26
GO:0006082	BP	organic acid metabolic process	5.40E-26
GO:0042180	BP	cellular ketone metabolic process	1.40E-25
GO:0016138	BP	glycoside biosynthetic process	1.60E-25
GO:0005829	CC	Cytosol	1.80E-24
GO:0001510	BP	RNA methylation	2.80E-24
GO:0009069	BP	serine family amino acid metabolic process	3.60E-24
GO:0009165	BP	nucleotide biosynthetic process	3.90E-24
GO:0016137	BP	glycoside metabolic process	6.20E-24
GO:0010038	BP	response to metal ion	1.00E-23
GO:0006090	BP	pyruvate metabolic process	4.00E-23
GO:0046394	BP	carboxylic acid biosynthetic process	4.50E-23
GO:0016053	BP	organic acid biosynthetic process	4.50E-23
GO:0005773	CC	Vacuole	3.40E-22
GO:0046686	BP	response to cadmium ion	5.40E-22
GO:0006807	BP	nitrogen compound metabolic process	8.10E-22
GO:0009259	BP	ribonucleotide metabolic process	8.80E-22
GO:0044262	BP	cellular carbohydrate metabolic process	9.70E-22
GO:0009683	BP	indoleacetic acid metabolic process	9.80E-22

GO:0009684	BP	indoleacetic acid biosynthetic process	9.80E-22
GO:0009260	BP	ribonucleotide biosynthetic process	1.10E-21
GO:0043232	CC	intracellular non-membrane-bounded organelle	1.60E-21
GO:0043228	CC	non-membrane-bounded organelle	1.60E-21
GO:0009851	BP	auxin biosynthetic process	4.40E-21
GO:0009628	BP	response to abiotic stimulus	3.00E-20
GO:0044282	BP	small molecule catabolic process	3.00E-20
GO:0042254	BP	ribosome biogenesis	3.90E-20
GO:0005975	BP	carbohydrate metabolic process	4.20E-20
GO:0006006	BP	glucose metabolic process	5.70E-20
GO:0042435	BP	indole derivative biosynthetic process	5.90E-20
GO:0010035	BP	response to inorganic substance	5.90E-20
GO:0005996	BP	monosaccharide metabolic process	5.90E-20
GO:0022613	BP	ribonucleoprotein complex biogenesis	7.30E-20
GO:0042434	BP	indole derivative metabolic process	7.60E-20
GO:0042430	BP	indole and derivative metabolic process	7.60E-20
GO:0019748	BP	secondary metabolic process	7.60E-20
GO:0009451	BP	RNA modification	1.50E-19
GO:0006970	BP	response to osmotic stress	1.80E-19
GO:0009850	BP	auxin metabolic process	2.70E-19
GO:0044275	BP	cellular carbohydrate catabolic process	2.70E-19
GO:0044249	BP	cellular biosynthetic process	2.90E-19
GO:0042436	BP	indole derivative catabolic process	3.50E-19
GO:0016052	BP	carbohydrate catabolic process	4.60E-19
GO:0000096	BP	sulfur amino acid metabolic process	7.40E-19
GO:0009058	BP	biosynthetic process	7.40E-19
GO:0006950	BP	response to stress	8.40E-19
GO:0019318	BP	hexose metabolic process	1.00E-18
GO:0009651	BP	response to salt stress	1.30E-18
GO:0009070	BP	serine family amino acid biosynthetic process	1.30E-18

GO:0019344	BP	cysteine biosynthetic process	1.50E-18
GO:0006569	BP	tryptophan catabolic process	1.60E-18
GO:0046218	BP	indolalkylamine catabolic process	1.60E-18
GO:0005982	BP	starch metabolic process	1.70E-18
GO:0044444	CC	cytoplasmic part	1.90E-18
GO:0006534	BP	cysteine metabolic process	2.10E-18
GO:0005730	CC	Nucleolus	2.30E-18
GO:0009074	BP	aromatic amino acid family catabolic process	3.30E-18
GO:0019252	BP	starch biosynthetic process	5.60E-18
GO:0000097	BP	sulfur amino acid biosynthetic process	2.60E-17
GO:0019320	BP	hexose catabolic process	2.70E-17
GO:0006007	BP	glucose catabolic process	2.70E-17
GO:0006066	BP	alcohol metabolic process	3.60E-17
GO:0046365	BP	monosaccharide catabolic process	4.60E-17
GO:0009266	BP	response to temperature stimulus	6.50E-17
GO:0032787	BP	monocarboxylic acid metabolic process	1.10E-16
GO:0019439	BP	aromatic compound catabolic process	1.10E-16
GO:0044238	BP	primary metabolic process	1.20E-16
GO:0006725	BP	cellular aromatic compound metabolic process	1.20E-16
GO:0046164	BP	alcohol catabolic process	1.30E-16
GO:0050896	BP	response to stimulus	1.30E-16
GO:0044237	BP	cellular metabolic process	1.80E-16
GO:0042221	BP	response to chemical stimulus	2.00E-16
GO:0009579	CC	Thylakoid	4.40E-16
GO:0034754	BP	cellular hormone metabolic process	4.50E-16
GO:0009063	BP	cellular amino acid catabolic process	6.50E-16
GO:0042402	BP	cellular biogenic amine catabolic process	8.80E-16
GO:0009526	CC	plastid envelope	1.30E-15
GO:0044248	BP	cellular catabolic process	2.40E-15
GO:0009072	BP	aromatic amino acid family metabolic process	2.50E-15

GO:0009310	BP	amine catabolic process	4.70E-15
GO:0006568	BP	tryptophan metabolic process	4.90E-15
GO:0006586	BP	indolalkylamine metabolic process	4.90E-15
GO:0009941	CC	chloroplast envelope	5.00E-15
GO:0009056	BP	catabolic process	6.00E-15
GO:0042219	BP	cellular amino acid derivative catabolic process	1.00E-14
GO:0044042	BP	glucan metabolic process	2.10E-14
GO:0009250	BP	glucan biosynthetic process	2.60E-14
GO:0006364	BP	rRNA processing	6.70E-14
GO:0005737	CC	Cytoplasm	6.80E-14
GO:0016072	BP	rRNA metabolic process	8.50E-14
GO:0055044	CC	Symplast	8.60E-14
GO:0009506	CC	Plasmodesma	8.60E-14
GO:0005911	CC	cell-cell junction	9.10E-14
GO:0070013	CC	intracellular organelle lumen	9.10E-14
GO:0043233	CC	organelle lumen	9.10E-14
GO:0019288	BP	isopentenyl diphosphate biosynthetic process, mevalonate-independent pathway	1.10E-13
GO:0031974	CC	membrane-enclosed lumen	1.10E-13
GO:0048046	CC	Apoplast	1.10E-13
GO:0030054	CC	cell junction	1.10E-13
GO:0031090	CC	organelle membrane	1.10E-13
GO:0006094	BP	Gluconeogenesis	1.20E-13
GO:0006073	BP	cellular glucan metabolic process	1.40E-13
GO:0009240	BP	isopentenyl diphosphate biosynthetic process	1.90E-13
GO:0046490	BP	isopentenyl diphosphate metabolic process	1.90E-13
GO:0019682	BP	glyceraldehyde-3-phosphate metabolic process	2.50E-13
GO:0022626	CC	cytosolic ribosome	5.10E-13
GO:0046364	BP	monosaccharide biosynthetic process	5.50E-13
GO:0009657	BP	plastid organization	7.80E-13

GO:0006575	BP	cellular amino acid derivative metabolic process	8.00E-13
GO:0019319	BP	hexose biosynthetic process	8.00E-13
GO:0000023	BP	maltose metabolic process	8.30E-13
GO:0031981	CC	nuclear lumen	1.10E-12
GO:0050801	BP	ion homeostasis	1.50E-12
GO:0051707	BP	response to other organism	1.60E-12
GO:0034660	BP	ncRNA metabolic process	1.70E-12
GO:0055080	BP	cation homeostasis	2.10E-12
GO:0048878	BP	chemical homeostasis	2.30E-12
GO:0046165	BP	alcohol biosynthetic process	2.80E-12
GO:0005840	CC	Ribosome	3.00E-12
GO:0044265	BP	cellular macromolecule catabolic process	3.70E-12
GO:0006576	BP	cellular biogenic amine metabolic process	3.90E-12
GO:0006081	BP	cellular aldehyde metabolic process	4.00E-12
GO:0008152	BP	metabolic process	4.90E-12
GO:0031975	CC	Envelope	5.30E-12
GO:0031967	CC	organelle envelope	5.30E-12
GO:0006096	BP	Glycolysis	5.70E-12
GO:0034470	BP	ncRNA processing	7.00E-12
GO:0042742	BP	defense response to bacterium	9.20E-12
GO:0009057	BP	macromolecule catabolic process	1.00E-11
GO:0044459	CC	plasma membrane part	1.10E-11
GO:0042446	BP	hormone biosynthetic process	1.40E-11
GO:0009607	BP	response to biotic stimulus	1.60E-11
GO:0033279	CC	ribosomal subunit	2.10E-11
GO:0009658	BP	chloroplast organization	2.60E-11
GO:0009987	BP	cellular process	3.00E-11
GO:0006730	BP	one-carbon metabolic process	3.40E-11
GO:0030529	CC	ribonucleoprotein complex	4.50E-11

GO:0006139	BP	nucleobase, nucleoside, nucleotide and nucleic acid metabolic process	4.60E-11
GO:0044445	CC	cytosolic part	5.20E-11
GO:0009617	BP	response to bacterium	6.60E-11
GO:0005774	CC	vacuolar membrane	1.00E-10
GO:0044437	CC	vacuolar part	1.20E-10
GO:0043414	BP	macromolecule methylation	1.40E-10
GO:0005984	BP	disaccharide metabolic process	1.70E-10
GO:0009311	BP	oligosaccharide metabolic process	2.40E-10
GO:0032259	BP	Methylation	2.50E-10
GO:0006412	BP	Translation	3.10E-10
GO:0006873	BP	cellular ion homeostasis	3.10E-10
GO:0055082	BP	cellular chemical homeostasis	4.10E-10
GO:0065008	BP	regulation of biological quality	5.50E-10
GO:0042592	BP	homeostatic process	6.10E-10
GO:0008299	BP	isoprenoid biosynthetic process	6.10E-10
GO:0019725	BP	cellular homeostasis	6.70E-10
GO:0003735	MF	structural constituent of ribosome	8.10E-10
GO:0006720	BP	isoprenoid metabolic process	8.70E-10
GO:0030003	BP	cellular cation homeostasis	1.00E-09
GO:0051716	BP	cellular response to stimulus	1.10E-09
GO:0006091	BP	generation of precursor metabolites and energy	1.10E-09
GO:0042445	BP	hormone metabolic process	1.30E-09
GO:0006733	BP	oxidoreduction coenzyme metabolic process	1.30E-09
GO:0043170	BP	macromolecule metabolic process	1.40E-09
GO:0044428	CC	nuclear part	1.60E-09
GO:0033554	BP	cellular response to stress	1.90E-09
GO:0005976	BP	polysaccharide metabolic process	2.10E-09
GO:0044093	BP	positive regulation of molecular function	2.40E-09
GO:0043085	BP	positive regulation of catalytic activity	2.40E-09

GO:0044085	BP	cellular component biogenesis	2.40E-09
GO:0046700	BP	heterocycle catabolic process	2.60E-09
GO:0044260	BP	cellular macromolecule metabolic process	2.80E-09
GO:0006457	BP	protein folding	3.70E-09
GO:0006098	BP	pentose-phosphate shunt	3.80E-09
GO:0006740	BP	NADPH regeneration	3.80E-09
GO:0006739	BP	NADP metabolic process	5.90E-09
GO:0010817	BP	regulation of hormone levels	7.20E-09
GO:0000271	BP	polysaccharide biosynthetic process	8.20E-09
GO:0055035	CC	plastid thylakoid membrane	8.80E-09
GO:0042651	CC	thylakoid membrane	8.80E-09
GO:0009414	BP	response to water deprivation	1.00E-08
GO:0044436	CC	thylakoid part	1.10E-08
GO:0051704	BP	multi-organism process	1.20E-08
GO:0006996	BP	organelle organization	1.20E-08
GO:0031976	CC	plastid thylakoid	1.40E-08
GO:0009534	CC	chloroplast thylakoid	1.40E-08
GO:0034357	CC	photosynthetic membrane	1.40E-08
GO:0009415	BP	response to water	1.50E-08
GO:0046496	BP	nicotinamide nucleotide metabolic process	1.60E-08
GO:0006769	BP	nicotinamide metabolic process	1.60E-08
GO:0043648	BP	dicarboxylic acid metabolic process	1.70E-08
GO:0005983	BP	starch catabolic process	1.70E-08
GO:0019362	BP	pyridine nucleotide metabolic process	2.00E-08
GO:0031984	CC	organelle subcompartment	2.00E-08
GO:0019438	BP	aromatic compound biosynthetic process	2.50E-08
GO:0009535	CC	chloroplast thylakoid membrane	2.80E-08
GO:0033692	BP	cellular polysaccharide biosynthetic process	3.30E-08
GO:0005618	CC	cell wall	3.40E-08
GO:0030312	CC	external encapsulating structure	3.70E-08

GO:0043603	BP	cellular amide metabolic process	4.30E-08
GO:0008654	BP	phospholipid biosynthetic process	4.40E-08
GO:0044264	BP	cellular polysaccharide metabolic process	5.00E-08
GO:0016829	MF	lyase activity	5.00E-08
GO:0009820	BP	alkaloid metabolic process	5.10E-08
GO:0005198	MF	structural molecule activity	5.70E-08
GO:0015934	CC	large ribosomal subunit	6.80E-08
GO:0051186	BP	cofactor metabolic process	9.90E-08
GO:0045036	BP	protein targeting to chloroplast	1.00E-07
GO:0006605	BP	protein targeting	1.20E-07
GO:0006952	BP	defense response	1.20E-07
GO:0070838	BP	divalent metal ion transport	1.20E-07
GO:0009251	BP	glucan catabolic process	1.20E-07
GO:0009409	BP	response to cold	1.20E-07
GO:0046395	BP	carboxylic acid catabolic process	1.30E-07
GO:0016054	BP	organic acid catabolic process	1.30E-07
GO:0006544	BP	glycine metabolic process	3.40E-07
GO:0051188	BP	cofactor biosynthetic process	5.30E-07
GO:0007030	BP	Golgi organization	5.30E-07
GO:0009719	BP	response to endogenous stimulus	5.50E-07
GO:0006972	BP	hyperosmotic response	5.50E-07
GO:0048037	MF	cofactor binding	6.40E-07
GO:0009295	CC	Nucleoid	7.00E-07
GO:0032991	CC	macromolecular complex	7.20E-07
GO:0051169	BP	nuclear transport	7.40E-07
GO:0006913	BP	nucleocytoplasmic transport	7.40E-07
GO:0006979	BP	response to oxidative stress	7.40E-07
GO:0022625	CC	cytosolic large ribosomal subunit	9.00E-07
GO:0009605	BP	response to external stimulus	1.00E-06
GO:0016853	MF	isomerase activity	1.00E-06

GO:0006546	BP	glycine catabolic process	1.10E-06
GO:0006396	BP	RNA processing	1.30E-06
GO:0006644	BP	phospholipid metabolic process	1.30E-06
GO:0009066	BP	aspartate family amino acid metabolic process	1.60E-06
GO:0009071	BP	serine family amino acid catabolic process	1.70E-06
GO:0000272	BP	polysaccharide catabolic process	2.80E-06
GO:0070727	BP	cellular macromolecule localization	2.90E-06
GO:0019637	BP	organophosphate metabolic process	3.30E-06
GO:0009814	BP	defense response, incompatible interaction	3.80E-06
GO:0044247	BP	cellular polysaccharide catabolic process	4.00E-06
GO:0042398	BP	cellular amino acid derivative biosynthetic process	5.40E-06
GO:0051641	BP	cellular localization	5.40E-06
GO:0008104	BP	protein localization	6.10E-06
GO:0009408	BP	response to heat	6.40E-06
GO:0034599	BP	cellular response to oxidative stress	7.00E-06
GO:0006833	BP	water transport	7.80E-06
GO:0042044	BP	fluid transport	7.80E-06
GO:0005507	MF	copper ion binding	7.90E-06
GO:0045087	BP	innate immune response	8.30E-06
GO:0030170	MF	pyridoxal phosphate binding	8.40E-06
GO:0070279	MF	vitamin B6 binding	8.40E-06
GO:0016020	CC	Membrane	9.20E-06
GO:0034613	BP	cellular protein localization	1.00E-05
GO:0046148	BP	pigment biosynthetic process	1.10E-05
GO:0009611	BP	response to wounding	1.40E-05
GO:0006886	BP	intracellular protein transport	1.50E-05
GO:0002376	BP	immune system process	1.50E-05
GO:0006955	BP	immune response	1.50E-05
GO:0006606	BP	protein import into nucleus	1.50E-05
GO:0051649	BP	establishment of localization in cell	1.80E-05

GO:0051170	BP	nuclear import	1.90E-05
GO:0006163	BP	purine nucleotide metabolic process	1.90E-05
GO:0009620	BP	response to fungus	1.90E-05
GO:0034504	BP	protein localization in nucleus	2.20E-05
GO:0006732	BP	coenzyme metabolic process	2.70E-05
GO:0003824	MF	catalytic activity	2.70E-05
GO:0033036	BP	macromolecule localization	2.90E-05
GO:0010467	BP	gene expression	3.20E-05
GO:0042646	CC	plastid nucleoid	4.30E-05
GO:0006800	BP	oxygen and reactive oxygen species metabolic process	4.50E-05
GO:0009416	BP	response to light stimulus	5.90E-05
GO:0010033	BP	response to organic substance	5.90E-05
GO:0015674	BP	di-, tri-valent inorganic cation transport	6.20E-05
GO:0006414	BP	translational elongation	6.30E-05
GO:0045184	BP	establishment of protein localization	7.10E-05
GO:0015031	BP	protein transport	7.10E-05
GO:0046417	BP	chorismate metabolic process	7.10E-05
GO:0009073	BP	aromatic amino acid family biosynthetic process	7.10E-05
GO:0044425	CC	membrane part	7.90E-05
GO:0070887	BP	cellular response to chemical stimulus	8.00E-05
GO:0042440	BP	pigment metabolic process	8.70E-05
GO:0065007	BP	biological regulation	9.30E-05
GO:0009067	BP	aspartate family amino acid biosynthetic process	9.50E-05
GO:0016043	BP	cellular component organization	9.60E-05
GO:0022627	CC	cytosolic small ribosomal subunit	0.0001
GO:0006164	BP	purine nucleotide biosynthetic process	0.00011
GO:0016860	MF	intramolecular oxidoreductase activity	0.00011
GO:0034614	BP	cellular response to reactive oxygen species	0.00012
GO:0016070	BP	RNA metabolic process	0.00012

GO:0009725	BP	response to hormone stimulus	0.00014
GO:0055066	BP	di-, tri-valent inorganic cation homeostasis	0.00014
GO:0009269	BP	response to desiccation	0.00015
GO:0009753	BP	response to jasmonic acid stimulus	0.00017
GO:0009314	BP	response to radiation	0.00018
GO:0042743	BP	hydrogen peroxide metabolic process	0.00021
GO:0009791	BP	post-embryonic development	0.00024
GO:0046907	BP	intracellular transport	0.00027
GO:0051082	MF	unfolded protein binding	0.0003
GO:0019842	MF	vitamin binding	0.0003
GO:0015935	CC	small ribosomal subunit	0.00032
GO:0071495	BP	cellular response to endogenous stimulus	0.00035
GO:0032502	BP	developmental process	0.00042
GO:0000302	BP	response to reactive oxygen species	0.00044
GO:0007275	BP	multicellular organismal development	0.00044
GO:0008610	BP	lipid biosynthetic process	0.00048
GO:0016109	BP	tetraterpenoid biosynthetic process	0.00049
GO:0016117	BP	carotenoid biosynthetic process	0.00049
GO:0003723	MF	RNA binding	0.0005
GO:0009737	BP	response to abscisic acid stimulus	0.00051
GO:0071489	BP	cellular response to red or far red light	0.00051
GO:0000478	BP	endonucleolytic cleavages during rRNA processing	0.00052
GO:0000469	BP	cleavages during rRNA processing	0.00052
GO:0016491	MF	oxidoreductase activity	0.00054
GO:0005777	CC	Peroxisome	0.00055
GO:0042579	CC	Microbody	0.00055
GO:0005886	CC	plasma membrane	0.00055
GO:0010043	BP	response to zinc ion	0.00059
GO:0019538	BP	protein metabolic process	0.00062
GO:0033365	BP	protein localization in organelle	0.00063

GO:0051179	BP	Localization	0.00066
GO:0009627	BP	systemic acquired resistance	0.00069
GO:0051094	BP	positive regulation of developmental process	0.00069
GO:0031407	BP	oxylipin metabolic process	0.00071
GO:0010027	BP	thylakoid membrane organization	0.00072
GO:0009668	BP	plastid membrane organization	0.00072
GO:0042744	BP	hydrogen peroxide catabolic process	0.00073
GO:0051234	BP	establishment of localization	0.00074
GO:0032501	BP	multicellular organismal process	0.00077
GO:0016108	BP	tetraterpenoid metabolic process	0.00081
GO:0016116	BP	carotenoid metabolic process	0.00081
GO:0070301	BP	cellular response to hydrogen peroxide	0.0009
GO:0031163	BP	metallo-sulfur cluster assembly	0.00096
GO:0016226	BP	iron-sulfur cluster assembly	0.00096
GO:0048518	BP	positive regulation of biological process	0.00098

MF; Molecular Function, CC; Cellular Component, BP; Biological Process

Table V-10. GO terms of down-regulated genes after 72 h *A. candida* inoculation in 'Nanane'

GO accession number	Term type	Term	FDR
GO:0010033	BP	response to organic substance	1.10E-28
GO:0009743	BP	response to carbohydrate stimulus	1.10E-28
GO:0010200	BP	response to chitin	8.90E-27
GO:0009628	BP	response to abiotic stimulus	4.70E-25
GO:0009719	BP	response to endogenous stimulus	8.30E-23
GO:0042398	BP	cellular amino acid derivative biosynthetic process	2.20E-22
GO:0009605	BP	response to external stimulus	4.30E-22
GO:0006575	BP	cellular amino acid derivative metabolic process	7.20E-22
GO:0042221	BP	response to chemical stimulus	8.00E-22
GO:0009725	BP	response to hormone stimulus	9.70E-22
GO:0050896	BP	response to stimulus	1.30E-21
GO:0009698	BP	phenylpropanoid metabolic process	2.80E-20
GO:0009812	BP	flavonoid metabolic process	9.10E-19
GO:0044283	BP	small molecule biosynthetic process	1.30E-17
GO:0009611	BP	response to wounding	1.90E-17
GO:0006950	BP	response to stress	2.20E-17
GO:0009813	BP	flavonoid biosynthetic process	7.90E-17
GO:0009737	BP	response to abscisic acid stimulus	1.30E-16
GO:0009755	BP	hormone-mediated signaling pathway	1.40E-16
GO:0023052	BP	Signaling	1.00E-15
GO:0071495	BP	cellular response to endogenous stimulus	1.20E-15
GO:0009414	BP	response to water deprivation	1.20E-15
GO:0023033	BP	signaling pathway	1.30E-15
GO:0032870	BP	cellular response to hormone stimulus	1.40E-15
GO:0009415	BP	response to water	2.00E-15
GO:0002679	BP	respiratory burst during defense response	4.10E-15

GO:0045730	BP	respiratory burst	4.10E-15
GO:0009699	BP	phenylpropanoid biosynthetic process	8.10E-15
GO:0006970	BP	response to osmotic stress	1.20E-14
GO:0019748	BP	secondary metabolic process	1.20E-14
GO:0023034	BP	intracellular signaling pathway	2.10E-14
GO:0009411	BP	response to UV	3.30E-14
GO:0009723	BP	response to ethylene stimulus	4.70E-14
GO:0006519	BP	cellular amino acid and derivative metabolic process	8.00E-14
GO:0009651	BP	response to salt stress	8.00E-14
GO:0000160	BP	two-component signal transduction system (phosphorelay)	1.10E-13
GO:0007242	BP	intracellular signaling cascade	2.40E-13
GO:0009753	BP	response to jasmonic acid stimulus	3.90E-13
GO:0071310	BP	cellular response to organic substance	6.30E-13
GO:0007165	BP	signal transduction	6.90E-13
GO:0009416	BP	response to light stimulus	1.10E-12
GO:0023046	BP	signaling process	2.70E-12
GO:0023060	BP	signal transmission	2.70E-12
GO:0006952	BP	defense response	3.00E-12
GO:0002252	BP	immune effector process	3.50E-12
GO:0051716	BP	cellular response to stimulus	1.60E-11
GO:0070887	BP	cellular response to chemical stimulus	2.70E-11
GO:0009314	BP	response to radiation	2.80E-11
GO:0050789	BP	regulation of biological process	3.30E-11
GO:0006725	BP	cellular aromatic compound metabolic process	4.10E-11
GO:0065007	BP	biological regulation	4.50E-11
GO:0009873	BP	ethylene mediated signaling pathway	1.10E-10
GO:0010224	BP	response to UV-B	3.30E-10
GO:0071369	BP	cellular response to ethylene stimulus	6.50E-10
GO:0002376	BP	immune system process	9.20E-10

GO:0006955	BP	immune response	9.20E-10
GO:0050794	BP	regulation of cellular process	1.30E-09
GO:0009409	BP	response to cold	2.30E-09
GO:0045087	BP	innate immune response	2.30E-09
GO:0030528	MF	transcription regulator activity	8.40E-09
GO:0051707	BP	response to other organism	9.50E-09
GO:0019438	BP	aromatic compound biosynthetic process	1.50E-08
GO:0042538	BP	hyperosmotic salinity response	1.50E-08
GO:0043455	BP	regulation of secondary metabolic process	1.50E-08
GO:0009751	BP	response to salicylic acid stimulus	1.60E-08
GO:0009607	BP	response to biotic stimulus	2.40E-08
GO:0003700	MF	transcription factor activity	1.10E-07
GO:0009266	BP	response to temperature stimulus	1.70E-07
GO:0009612	BP	response to mechanical stimulus	1.70E-07
GO:0046283	BP	anthocyanin metabolic process	1.70E-07
GO:0031326	BP	regulation of cellular biosynthetic process	3.80E-07
GO:0009889	BP	regulation of biosynthetic process	3.90E-07
GO:0006972	BP	hyperosmotic response	4.60E-07
GO:0009733	BP	response to auxin stimulus	5.70E-07
GO:0080090	BP	regulation of primary metabolic process	1.00E-06
GO:0044281	BP	small molecule metabolic process	1.40E-06
GO:0031323	BP	regulation of cellular metabolic process	2.20E-06
GO:0033554	BP	cellular response to stress	2.30E-06
GO:0019222	BP	regulation of metabolic process	2.40E-06
GO:0009620	BP	response to fungus	3.00E-06
GO:0009963	BP	positive regulation of flavonoid biosynthetic process	3.10E-06
GO:0009626	BP	plant-type hypersensitive response	4.80E-06
GO:0034050	BP	host programmed cell death induced by symbiont	5.30E-06
GO:0010264	BP	myo-inositol hexakisphosphate biosynthetic process	5.50E-06
GO:0006021	BP	inositol biosynthetic process	5.50E-06

GO:0032958	BP	inositol phosphate biosynthetic process	5.50E-06
GO:0033517	BP	myo-inositol hexakisphosphate metabolic process	5.50E-06
GO:0051704	BP	multi-organism process	6.80E-06
GO:0080135	BP	regulation of cellular response to stress	7.70E-06
GO:0030968	BP	endoplasmic reticulum unfolded protein response	9.80E-06
GO:0070838	BP	divalent metal ion transport	9.80E-06
GO:0034620	BP	cellular response to unfolded protein	1.10E-05
GO:0006986	BP	response to unfolded protein	1.10E-05
GO:0071215	BP	cellular response to abscisic acid stimulus	1.20E-05
GO:0046173	BP	polyol biosynthetic process	1.20E-05
GO:0010363	BP	regulation of plant-type hypersensitive response	1.20E-05
GO:0009888	BP	tissue development	1.30E-05
GO:0032559	MF	adenyl ribonucleotide binding	1.30E-05
GO:0001883	MF	purine nucleoside binding	1.30E-05
GO:0030554	MF	adenyl nucleotide binding	1.30E-05
GO:0001882	MF	nucleoside binding	1.30E-05
GO:0006355	BP	regulation of transcription, DNA-dependent	1.50E-05
GO:0006633	BP	fatty acid biosynthetic process	1.50E-05
GO:0071445	BP	cellular response to protein stimulus	1.50E-05
GO:0015674	BP	di-, tri-valent inorganic cation transport	1.50E-05
GO:0045449	BP	regulation of transcription	1.50E-05
GO:0009738	BP	abscisic acid mediated signaling pathway	1.60E-05
GO:0009718	BP	anthocyanin biosynthetic process	1.60E-05
GO:0051252	BP	regulation of RNA metabolic process	1.60E-05
GO:0006984	BP	ER-nuclear signaling pathway	1.70E-05
GO:0006612	BP	protein targeting to membrane	1.70E-05
GO:0044238	BP	primary metabolic process	1.80E-05
GO:0071216	BP	cellular response to biotic stimulus	1.90E-05
GO:0043067	BP	regulation of programmed cell death	1.90E-05
GO:0005886	CC	plasma membrane	1.90E-05

GO:0012501	BP	programmed cell death	2.10E-05
GO:0006595	BP	polyamine metabolic process	2.20E-05
GO:0008219	BP	cell death	2.90E-05
GO:0009962	BP	regulation of flavonoid biosynthetic process	2.90E-05
GO:0016265	BP	Death	2.90E-05
GO:0010941	BP	regulation of cell death	3.00E-05
GO:0043647	BP	inositol phosphate metabolic process	3.40E-05
GO:0010468	BP	regulation of gene expression	3.60E-05
GO:0009058	BP	biosynthetic process	3.80E-05
GO:0045088	BP	regulation of innate immune response	4.20E-05
GO:0006816	BP	calcium ion transport	4.20E-05
GO:0080134	BP	regulation of response to stress	4.30E-05
GO:0048583	BP	regulation of response to stimulus	4.30E-05
GO:0002682	BP	regulation of immune system process	4.40E-05
GO:0050776	BP	regulation of immune response	4.40E-05
GO:0010556	BP	regulation of macromolecule biosynthetic process	4.60E-05
GO:0044249	BP	cellular biosynthetic process	5.20E-05
GO:0009744	BP	response to sucrose stimulus	5.40E-05
GO:0048856	BP	anatomical structure development	5.40E-05
GO:0009867	BP	jasmonic acid mediated signaling pathway	5.50E-05
GO:0071395	BP	cellular response to jasmonic acid stimulus	5.50E-05
GO:0031347	BP	regulation of defense response	5.70E-05
GO:0032501	BP	multicellular organismal process	5.90E-05
GO:0006598	BP	polyamine catabolic process	6.10E-05
GO:0048768	BP	root hair cell tip growth	6.30E-05
GO:0034285	BP	response to disaccharide stimulus	6.70E-05
GO:0019219	BP	regulation of nucleobase, nucleoside, nucleotide and nucleic acid metabolic process	7.40E-05
GO:0009805	BP	coumarin biosynthetic process	9.00E-05
GO:0009804	BP	coumarin metabolic process	9.00E-05

GO:0017076	MF	purine nucleotide binding	9.00E-05
GO:0032555	MF	purine ribonucleotide binding	9.00E-05
GO:0032553	MF	ribonucleotide binding	9.00E-05
GO:0051171	BP	regulation of nitrogen compound metabolic process	0.00010
GO:0044459	CC	plasma membrane part	0.00010
GO:0009692	BP	ethylene metabolic process	0.00011
GO:0009693	BP	ethylene biosynthetic process	0.00011
GO:0048731	BP	system development	0.00011
GO:0048513	BP	organ development	0.00011
GO:0006020	BP	inositol metabolic process	0.00011
GO:0007275	BP	multicellular organismal development	0.00012
GO:0043449	BP	cellular alkene metabolic process	0.00013
GO:0043450	BP	alkene biosynthetic process	0.00013
GO:0009863	BP	salicylic acid mediated signaling pathway	0.00013
GO:0071446	BP	cellular response to salicylic acid stimulus	0.00013
GO:0016740	MF	transferase activity	0.00013
GO:0003824	MF	catalytic activity	0.00013
GO:0003677	MF	DNA binding	0.00014
GO:0006631	BP	fatty acid metabolic process	0.00016
GO:0006351	BP	transcription, DNA-dependent	0.00016
GO:0006350	BP	transcription	0.00016
GO:0032774	BP	RNA biosynthetic process	0.00017
GO:0009987	BP	cellular process	0.00017
GO:0002213	BP	defense response to insect	0.00018
GO:0032502	BP	developmental process	0.00018
GO:0060255	BP	regulation of macromolecule metabolic process	0.00018
GO:0042440	BP	pigment metabolic process	0.00019
GO:0005524	MF	ATP binding	0.00019
GO:0048509	BP	regulation of meristem development	0.00021
GO:0019751	BP	polyol metabolic process	0.00022

GO:0044237	BP	cellular metabolic process	0.00022
GO:0048507	BP	meristem development	0.00023
GO:0016301	MF	kinase activity	0.00023
GO:0005488	MF	binding	0.00025
GO:0034976	BP	response to endoplasmic reticulum stress	0.00026
GO:0008152	BP	metabolic process	0.00029
GO:0009625	BP	response to insect	0.00034
GO:0004428	MF	inositol or phosphatidylinositol kinase activity	0.00036
GO:0006576	BP	cellular biogenic amine metabolic process	0.00037
GO:0040007	BP	growth	0.00039
GO:0022622	BP	root system development	0.00046
GO:0048364	BP	root development	0.00046
GO:0016773	MF	phosphotransferase activity, alcohol group as acceptor	0.00047
GO:0044106	BP	cellular amine metabolic process	0.00048
GO:0006468	BP	protein amino acid phosphorylation	0.00059
GO:0071496	BP	cellular response to external stimulus	0.00060
GO:0006790	BP	sulfur metabolic process	0.00063
GO:0051179	BP	localization	0.00074
GO:0016758	MF	transferase activity, transferring hexosyl groups	0.00078
GO:0004672	MF	protein kinase activity	0.00078
GO:0034641	BP	cellular nitrogen compound metabolic process	0.00080
GO:0009694	BP	jasmonic acid metabolic process	0.00082
GO:0007623	BP	circadian rhythm	0.00083
GO:0046148	BP	pigment biosynthetic process	0.00083
GO:0048511	BP	rhythmic process	0.00083
GO:0005515	MF	protein binding	0.00085
GO:0000166	MF	nucleotide binding	0.00095

MF; Molecular Function, CC; Cellular Component, BP; Biological Process

Table V-11. GO terms of down-regulated genes after 72 h *A. candida* inoculation in 'Misugi'

GO accession number	Term type	Term	FDR
GO:0010264	BP	myo-inositol hexakisphosphate biosynthetic process	1.00E-12
GO:0006021	BP	inositol biosynthetic process	1.00E-12
GO:0032958	BP	inositol phosphate biosynthetic process	1.00E-12
GO:0033517	BP	myo-inositol hexakisphosphate metabolic process	1.00E-12
GO:0009628	BP	response to abiotic stimulus	1.00E-12
GO:0044283	BP	small molecule biosynthetic process	1.10E-12
GO:0009411	BP	response to UV	6.80E-12
GO:0046173	BP	polyol biosynthetic process	1.10E-11
GO:0043647	BP	inositol phosphate metabolic process	3.20E-11
GO:0006970	BP	response to osmotic stress	8.00E-11
GO:0009698	BP	phenylpropanoid metabolic process	1.80E-10
GO:0009651	BP	response to salt stress	2.00E-10
GO:0050896	BP	response to stimulus	2.20E-10
GO:0006020	BP	inositol metabolic process	2.90E-10
GO:0042221	BP	response to chemical stimulus	5.50E-10
GO:0005886	CC	plasma membrane	5.90E-10
GO:0006575	BP	cellular amino acid derivative metabolic process	1.20E-09
GO:0009416	BP	response to light stimulus	1.70E-09
GO:0010033	BP	response to organic substance	2.50E-09
GO:0019751	BP	polyol metabolic process	3.90E-09
GO:0019748	BP	secondary metabolic process	1.10E-08
GO:0009314	BP	response to radiation	2.30E-08
GO:0042398	BP	cellular amino acid derivative biosynthetic process	2.90E-08
GO:0016020	CC	membrane	3.20E-08
GO:0009812	BP	flavonoid metabolic process	4.80E-08
GO:0006833	BP	water transport	1.20E-07

GO:0042044	BP	fluid transport	1.20E-07
GO:0009813	BP	flavonoid biosynthetic process	1.40E-07
GO:0005975	BP	carbohydrate metabolic process	2.20E-07
GO:0009699	BP	phenylpropanoid biosynthetic process	2.50E-07
GO:0016740	MF	transferase activity	2.70E-07
GO:0042335	BP	cuticle development	4.00E-07
GO:0009725	BP	response to hormone stimulus	9.50E-07
GO:0006950	BP	response to stress	1.20E-06
GO:0044459	CC	plasma membrane part	1.30E-06
GO:0009719	BP	response to endogenous stimulus	1.40E-06
GO:0005372	MF	water transmembrane transporter activity	1.40E-06
GO:0005215	MF	transporter activity	1.40E-06
GO:0015250	MF	water channel activity	1.40E-06
GO:0006066	BP	alcohol metabolic process	2.10E-06
GO:0006595	BP	polyamine metabolic process	2.50E-06
GO:0022857	MF	transmembrane transporter activity	2.50E-06
GO:0055085	BP	transmembrane transport	2.60E-06
GO:0006519	BP	cellular amino acid and derivative metabolic process	3.40E-06
GO:0009605	BP	response to external stimulus	4.60E-06
GO:0006725	BP	cellular aromatic compound metabolic process	5.00E-06
GO:0016051	BP	carbohydrate biosynthetic process	8.40E-06
GO:0007623	BP	circadian rhythm	9.60E-06
GO:0048511	BP	rhythmic process	9.60E-06
GO:0046165	BP	alcohol biosynthetic process	9.60E-06
GO:0044281	BP	small molecule metabolic process	1.10E-05
GO:0009805	BP	coumarin biosynthetic process	1.10E-05
GO:0009804	BP	coumarin metabolic process	1.10E-05
GO:0043455	BP	regulation of secondary metabolic process	1.30E-05
GO:0009963	BP	positive regulation of flavonoid biosynthetic process	1.50E-05
GO:0009737	BP	response to abscisic acid stimulus	1.50E-05

GO:0006576	BP	cellular biogenic amine metabolic process	1.70E-05
GO:0005976	BP	polysaccharide metabolic process	1.70E-05
GO:0031226	CC	intrinsic to plasma membrane	2.00E-05
GO:0006631	BP	fatty acid metabolic process	3.00E-05
GO:0044262	BP	cellular carbohydrate metabolic process	3.00E-05
GO:0044042	BP	glucan metabolic process	3.50E-05
GO:0010817	BP	regulation of hormone levels	3.50E-05
GO:0000038	BP	very-long-chain fatty acid metabolic process	4.10E-05
GO:0043481	BP	anthocyanin accumulation in tissues in response to UV light	4.10E-05
GO:0043480	BP	pigment accumulation in tissues	4.10E-05
GO:0010224	BP	response to UV-B	4.10E-05
GO:0043473	BP	pigmentation	4.10E-05
GO:0043478	BP	pigment accumulation in response to UV light	4.10E-05
GO:0043476	BP	pigment accumulation	4.10E-05
GO:0043479	BP	pigment accumulation in tissues in response to UV light	4.10E-05
GO:0031224	CC	intrinsic to membrane	5.90E-05
GO:0005773	CC	vacuole	5.90E-05
GO:0006598	BP	polyamine catabolic process	6.60E-05
GO:0006633	BP	fatty acid biosynthetic process	6.70E-05
GO:0003824	MF	catalytic activity	7.10E-05
GO:0022891	MF	substrate-specific transmembrane transporter activity	7.70E-05
GO:0044425	CC	membrane part	8.50E-05
GO:0009505	CC	plant-type cell wall	8.50E-05
GO:0046658	CC	anchored to plasma membrane	8.50E-05
GO:0006629	BP	lipid metabolic process	8.90E-05
GO:0048767	BP	root hair elongation	9.50E-05
GO:0030243	BP	cellulose metabolic process	0.00011
GO:0009962	BP	regulation of flavonoid biosynthetic process	0.00011
GO:0016747	MF	transferase activity, transferring acyl groups other than amino-acyl groups	0.00011

GO:0023052	BP	signaling	0.00012
GO:0006810	BP	transport	0.00014
GO:0051234	BP	establishment of localization	0.00016
GO:0009755	BP	hormone-mediated signaling pathway	0.00017
GO:0030312	CC	external encapsulating structure	0.00018
GO:0008202	BP	steroid metabolic process	0.00019
GO:0051179	BP	localization	0.00019
GO:0034637	BP	cellular carbohydrate biosynthetic process	0.00020
GO:0022804	MF	active transmembrane transporter activity	0.00024
GO:0016126	BP	sterol biosynthetic process	0.00030
GO:0042402	BP	cellular biogenic amine catabolic process	0.00034
GO:0005911	CC	cell-cell junction	0.00035
GO:0005618	CC	cell wall	0.00035
GO:0055044	CC	symplast	0.00035
GO:0044437	CC	vacuolar part	0.00035
GO:0005774	CC	vacuolar membrane	0.00035
GO:0009506	CC	plasmodesma	0.00035
GO:0030054	CC	cell junction	0.00037
GO:0016758	MF	transferase activity, transferring hexosyl groups	0.00042
GO:0016125	BP	sterol metabolic process	0.00045
GO:0065008	BP	regulation of biological quality	0.00045
GO:0019438	BP	aromatic compound biosynthetic process	0.00057
GO:0009743	BP	response to carbohydrate stimulus	0.00057
GO:0023033	BP	signaling pathway	0.00058
GO:0032870	BP	cellular response to hormone stimulus	0.00082
GO:0009739	BP	response to gibberellin stimulus	0.00086
GO:0022892	MF	substrate-specific transporter activity	0.00091
GO:0022838	MF	substrate-specific channel activity	0.00091
GO:0015267	MF	channel activity	0.00091
GO:0004553	MF	hydrolase activity, hydrolyzing O-glycosyl compounds	0.00091
GO:0022803	MF	passive transmembrane transporter activity	0.00091

MF; Molecular Function, CC; Cellular Component, BP; Biological Process

Table V-12. List to genes whose expression is up or downregulated by *A. candida* inoculation among species conserved SA response genes

ID				'Nanane'		'Misugi'	
B. rapa	*A. thaliana*	Gene	Annotation	48 HAI	72 HAI	48 HAI	72 HAI
Bra000124	AT2G39210	.	Major facilitator superfamily protein				
Bra000889	AT2G46450	CNGC12	cyclic nucleotide-gated channel 12				
Bra002021	AT2G17120	LYM2	lysm domain GPI-anchored protein 2 precursor				
Bra003047	AT5G53550	YSL3	YELLOW STRIPE like 3				
Bra004130	AT1G65800	RK2	receptor kinase 2				
Bra004537	AT2G46430	CNGC3	cyclic nucleotide gated channel 3	up			
Bra004540	AT2G46400	WRKY46	WRKY DNA-binding protein 46				
Bra005059	AT2G39210	.	Major facilitator superfamily protein				
Bra006178	AT5G13080	WRKY75	WRKY DNA-binding protein 75				
Bra007265	AT3G56710	SIB1	sigma factor binding protein 1				
Bra008264	AT1G76520	.	Auxin efflux carrier family protein				

Bra009660	AT2G17120	LYM2	lysm domain GPI-anchored protein 2 precursor				
Bra009771	AT5G24530	DMR6	2-oxoglutarate (2OG) and Fe(II)-dependent oxygenase superfamily protein	up		down	up
Bra009925	AT5G26920	CBP60G	Cam-binding protein 60-like G				
Bra010220	AT4G31800	WRKY18	WRKY DNA-binding protein 18				
Bra010740	AT4G38550	.	Arabidopsis phospholipase-like protein (PEARLI 4) family				
Bra010752	AT4G14220	RHF1A	RING-H2 group F1A				
Bra011033	AT4G28490	RLK5 // HAE	Leucine-rich receptor-like protein kinase family protein	up	up		
Bra011299	AT4G31800	WRKY18	WRKY DNA-binding protein 18				
Bra012008	AT2G27660	.	Cysteine/Histidine-rich C1 domain family protein	up	up		
Bra012780	AT4G15550	IAGLU	indole-3-acetate beta-D-glucosyltransferase				
Bra013445	AT4G20110	VSR7	VACUOLAR SORTING RECEPTOR 7	up			
Bra013579	AT4G21990	APS3	APS reductase 3	down	down	down	down
Bra013934	AT4G25940	.	ENTH/ANTH/VHS superfamily protein				
Bra014674	AT3G56710	SIB1	sigma factor binding protein 1	up	up		

Bra015375	AT1G04980	PDI10 // PDIL2-2	PDI-like 2-2				up
Bra015543	AT1G07000	EXO70B2	exocyst subunit exo70 family protein B2				
Bra015693	AT1G77120	ADH1	alcohol dehydrogenase 1				
Bra016962	AT5G42440	.	Protein kinase superfamily protein				
Bra016974	AT2G40750	WRKY54	WRKY DNA-binding protein 54	up	up	up	
Bra017085	AT2G39210	.	Major facilitator superfamily protein				
Bra018988	AT1G52780	.	Protein of unknown function (DUF2921)				
Bra019301	AT4G23470	.	PLAC8 family protein				
Bra019406	AT4G21990	APS3	APS reductase 3	down	down	down	down
Bra020196	AT5G22570	WRKY38	WRKY DNA-binding protein 38				
Bra020820	AT4G23260	CRK18	cysteine-rich RLK (RECEPTOR-like protein kinase) 18				
Bra021164	AT3G16150	.	N-terminal nucleophile aminohydrolases (Ntn hydrolases) superfamily protein	down			
Bra022870	AT2G31880	SOBIR1 // EVR	Leucine-rich repeat protein kinase family protein	up			
Bra024304	AT5G64510	TIN1	unknown protein				

Bra026187	AT1G14790	RDR1	RNA-dependent RNA polymerase 1				
Bra027286	AT3G14990	.	Class I glutamine amidotransferase-like superfamily protein				
Bra027306	AT3G14840	.	Leucine-rich repeat transmembrane protein kinase	up	up	up	
Bra028132	AT5G37600	GLN1;1 // GSR 1	glutamine synthase clone R1		up	up	
Bra028224	AT5G39050	.	HXXXD-type acyl-transferase family protein				
Bra028660	AT5G08380	AGAL1	alpha-galactosidase 1				
Bra029201	AT5G63790	NAC102	NAC domain containing protein 102				
Bra029414	AT5G24530	DMR6	2-oxoglutarate (2OG) and Fe(II)-dependent oxygenase superfamily protein	up	up		up
Bra031293	AT3G21630	CERK1 // LYSM RLK1	chitin elicitor receptor kinase 1				
Bra033382	AT1G03290	.	unknown protein				
Bra033480	AT3G14990	.	Class I glutamine amidotransferase-like superfamily protein				
Bra033494	AT4G15550	IAGLU	indole-3-acetate beta-D-glucosyltransferase				
Bra034243	AT3G26600	ARO4	armadillo repeat only 4				

Bra038080	AT4G15550	IAGLU	indole-3-acetate beta-D-glucosyltransferase				
Bra039130	AT3G01290	.	SPFH/Band 7/PHB domain-containing membrane-associated protein family	up	up		
Bra039539	AT4G15530	PPDK	pyruvate orthophosphate dikinase				
Bra039540	AT4G15530	PPDK	pyruvate orthophosphate dikinase				
Bra039980	AT2G29420	GST25 // GSTU7	glutathione S-transferase tau 7				
Bra040152	AT3G04070	anac047 // NAC047	NAC domain containing protein 47				down
Bra040801	AT4G13510	AMT1;1	ammonium transporter 1;1	up	up		

Table V-13. List to genes whose expression was up or downregulated by *A. candida* inoculation among genes categorized into GO term 'systemic acquired resistance'

ID		Annotation	'Nanane'			'Misugi'			*F. oxysporum*
			A. candida		SA	*A. candida*		SA	
B. rapa	*A. thaliana*		48 HAI	72 HAI		48 HAI	72 HAI		
Bra000064	AT2G38470	WRKY DNA-binding protein 33	down	down	down				up
Bra000310	AT2G43570	chitinase, putative	up		up			up	up
Bra000421	AT2G46370	Auxin-responsive GH3 family protein						down	
Bra001121	AT3G04720	pathogenesis-related 4		down	up			up	
Bra001122	AT3G04720	pathogenesis-related 4			up			up	up
Bra001123	AT3G04720	pathogenesis-related 4			up				up
Bra002906	AT5G55460	Bifunctional inhibitor/lipid-transfer protein/seed storage 2S albumin superfamily protein						up	

Bra002914	AT5G55410	Bifunctional inhibitor/lipid-transfer protein/seed storage 2S albumin superfamily protein	up	up	up			up	up
Bra003527	AT1G59870	ABC-2 and Plant PDR ABC-type transporter family protein	up	up	down	up	up		
Bra003789	AT1G74710	ADC synthase superfamily protein	up	up				up	
Bra004543	AT2G46370	Auxin-responsive GH3 family protein			up			up	
Bra004771	AT2G43570	chitinase, putative	up	up	up			up	up
Bra005104	AT2G38470	WRKY DNA-binding protein 33						up	
Bra007315	AT3G57260	beta-1,3-glucanase 2	up	up	up				
Bra008165	AT1G74710	ADC synthase superfamily protein	up		up			up	up
Bra010475	AT4G25050	acyl carrier protein 4			down			down	
Bra010821	AT1G29660	GDSL-like Lipase/Acylhydrolase superfamily protein			down		down	down	
Bra011919	AT1G55490	chaperonin 60 beta	up	up	down	up	up	down	
Bra013137	AT2G13810	AGD2-like defense response protein 1			up				
Bra013138	AT2G13810	AGD2-like defense response protein 1			up				up

Bra013859	AT4G25050	acyl carrier protein 4			down		down	
Bra014635	AT3G57260	beta-1,3-glucanase 2	up	up	up		up	up
Bra014636	AT3G57260	beta-1,3-glucanase 2			up			
Bra014853	AT3G53980	Bifunctional inhibitor/lipid-transfer protein/seed storage 2S albumin superfamily protein			down	up		
Bra016977	AT2G40690	NAD-dependent glycerol-3-phosphate dehydrogenase family protein			down		down	
Bra017117	AT2G38470	WRKY DNA-binding protein 33			down			up
Bra019193	AT4G25050	acyl carrier protein 4			down		down	
Bra022325	AT3G18490	Eukaryotic aspartyl protease family protein			up		up	
Bra025093	AT5G45110	NPR1-like protein 3			up		up	
Bra028091	AT2G18660	plant natriuretic peptide A			up		up	up
Bra028838	AT5G03350	Legume lectin family protein					up	
Bra028980	AT5G55450	Bifunctional inhibitor/lipid-transfer protein/seed storage 2S albumin superfamily protein	up	up			up	

Bra030155	AT1G29660	GDSL-like Lipase/Acylhydrolase superfamily protein		down			down
Bra030796	AT1G09750	Eukaryotic aspartyl protease family protein		down			down
Bra030858	AT1G55490	chaperonin 60 beta	up		up	up	down
Bra031912	AT5G64570	beta-D-xylosidase 4		down			down
Bra032155	AT2G23620	methyl esterase 1		up			up
Bra033431	AT3G52430	alpha/beta-Hydrolases superfamily protein		up			
Bra035574	AT5G55450	Bifunctional inhibitor/lipid-transfer protein/seed storage 2S albumin superfamily protein		up			up
Bra039284	AT2G46370	Auxin-responsive GH3 family protein		up			up
Bra039455	AT3G05180	GDSL-like Lipase/Acylhydrolase superfamily protein		up			no

SA, number of overlapped genes with up or downregulated genes at 72 h after salicylic acid treatments

F. oxysporum, number of overlapped genes with up or downregulated genes after 24 h *Fusarium oxysporum* f. sp. *conglutinance* inoculation in resistant line, RJKB-T23

Chapter VI

General discussion

In this dissertation, we performed QTL-seq analysis using F2 populations derived from crosses between *For* resistant and susceptible lines for the identification of *For* resistance gene. Previously, we identified the Fusarium yellows *R* gene against *Foc* and *focbr1-1* allele (a 35 kb deletion of *FocBr1*) in *B. rapa* (*FocBr1*) and *B. oleracea* (*FocBo1*) but no one identified the *R* gene against *For.* In this study, we identified the single causative locus for *For* resistance, which covered *FocBr1*. There was no difference in expression levels of *FocBr1* between resistant and susceptible lines, but there were some amino acid sequence differences between *For* susceptible allele (*focbr1-2*) and resistant alleles (*FocBr1* and *FocBo1*), suggesting that changes in amino acid sequence result in loss of function. We also developed the codominant DNA marker, focbr1-2m, in the case of *focbr1-2* that can distinguish the heterozygosity of *FocBr1* and *focbr1-2* alleles. This new allele is need to be removed to use for breeding, which will be useful for breeding stable Fusarium yellows resistant cultivars. Using this new DNA marker, we screened genotypes of *B. rapa* breeding including 157 Chinese cabbage, 35 turnips, 40 pak choi, and 73 komatsuna lines and cultivars. In Chinese cabbage cultivars, a few lines have *focbr1-2* alleles. There was complete agreement between the DNA marker-based prediction and the inoculation test in Chinese cabbage lines using the Bra012688m marker (Kawamura et al. 2016). So, the presence of the *focbr1-2* allele may have a chance to cause susceptibility during the breeding of Fusarium yellows-resistant cultivars in Chinese cabbage. In the case of turnip, most cultivars (about 85%) did not have *focbr1-2* alleles, suggesting that this allele will not be a problem for breeding. However, in pak choi, 40% of cultivars have *focbr1-2* alleles. In komatsuna, about 30% of cultivars have *focbr1-2* alleles and about 7% of cultivars were homozygous for the *focbr1-2* allele or heterozygous for *focbr1-2* and *focbr1-1* alleles. For the breeding of Fusarium yellows resistant cultivars in pak choi or komatsuna, the presence of the *focbr1-2* allele should be mapped in breeding lines, and the DNA marker, focbr1-2m, developed in this study will be useful for DNA marker-assisted selection **(Chapter II).**

We examined the association of transcriptional changes between six mRNAs and their paired NATs following *Foc* inoculation at 24 and 72 HAI in Fusarium yellows resistant and susceptible lines. A strong association between mRNA and their paired NATs was found, especially in Bra033549-MSTRG.1355 and Bra029414-MSTRG.4734 pairs. Noncoding RNA (ncRNA) including NATs regulates mRNAs, which plays a role in defense response. The Bra029414-MSTRG.4734 pair was clearly upregulated following *Foc* inoculation in the resistant

line. The *A. thaliana* ortholog of Bra029414 (*DMR6*) belongs to the superfamily of 2-oxoglutarate Fe (II)-dependent dioxygenases that is upregulated by pathogen infection or SA treatment and encodes a salicylic acid 5-hydroxylase that fine-tunes SA homeostasis. In *B. rapa*, *DMR6* was upregulated by salicylic acid treatment, *Foc* infection, and was more induced in the susceptible line than in the resistant line. In *A. thaliana*, knocking down the expression of a NAT resulted in a decreased expression level of its paired mRNA, suggesting that this NAT regulates the expression of its paired mRNA. In tomatoes, overexpression of a NAT induced its paired mRNA and enhanced resistance to *Phytophthora infestans* infection. Negative regulators also showed resistance after the knockout of the *DMR6* gene **(Chapter III).**

We found that not only pathogen inoculation but also SA treatment found transcriptional coordination between mRNAs and paired NATs on two commercial komatsuna cultivars 'Misugi' and 'Nanane'. We performed RNA-seq analysis with and without SA treatment in two komatsuna cultivars and identified SA-responsive genes at the whole genome level. We identified *B. rapa* SA-induced genes (BrSAIGs) and *B. rapa* SA-suppressed genes (BrSASGs), respectively. In this study, we identified genes overlapping between BrSAIGs/BrSASGs and paired genes overlapping NATs or incRNAs in their encoding regions. The transcriptional relationship between mRNAs and their paired NATs following SA treatment was examined, and two pairs Bra029414/MSTRG.4734 (r=0.80, p<0.01) and Bra026809/MSTRG.23624 (r=0.74, p<0.05) pairs showed a positive association of expression levels between mRNAs and their paired NATs. The transcriptional association of mRNAs and their paired NATs plays a role in SA response. In this study, we sprayed SA on the samples, which is more high-throughput compared to previously performed SA treatment on the solid medium, because it has limitations on the number of samples that can be assayed simultaneously. Six SA-induced genes were shown to be upregulated following SA treatments following spraying. Transcriptional induction was faster with SA spraying than by adding SA into the medium indicating that SA spraying is applicable for further experiments **(Chapter IV).**

We performed an inoculation test with the *A. candida* pathogen at 48 and 72 h in resistant and susceptible komatsuna cultivars and gained insights into the immune responses of the host plant. We identified differentially expressed genes (DEGs) between *A. candida* inoculated [48 and 72 h after inoculation (HAI)] and non-inoculated samples in resistant and susceptible cultivars of komatsuna using RNA-seq. The expression pattern of six genes following inoculation by two different isolates, WMB01 and WKB01, were examined by qPCR. Most of the six genes showed similar patterns of induction of expression following *A. candida* inoculation both in cotyledons and true leaves but we identified different genes in the two

cultivars. Following *A. candida* inoculation, we identified DEGs at 48 and 72 HAI, and functional DEGs differed between the resistant and susceptible cultivars in *A. candida* inoculated samples. We performed GO analysis and observed the *A. candida* response, some overrepresented GO terms were cultivar specific at 48 or 72 HAI. Genes involved in SA-dependent SAR involving GO terms or 'program cell death', and 'regulation of defense response' tended to be up and downregulated in the resistant cultivars at 72 HAI. Resistance or immunity-related GO terms 'systemic acquired resistance' tended to be upregulated in the resistant cultivar but not in the susceptible cultivar reflecting different degrees of pathogen infection, and suggesting that hypersensitive reactions could occur in the resistant cultivar. Common SA-responsive genes categorized as SAR overlapped between DEGs following *A. candida* or *Foc* inoculation in the resistant cultivar/inbred lines. These results suggest the role of SAR in the defense response to both pathogens particularly in the effector-triggered immunity (ETI) downstream pathway. These findings will be useful for understanding white rust resistance mechanisms in *B. rapa* (**Chapter V).**

In conclusion, we identified a resistant (*R*) gene for Fusarium yellows in *B. rapa* and developed a new DNA marker, which has already been incorporated in breeding for resistance in Fusarium yellows in komatsuna. Non-coding RNA also plays an important role in defense response by regulating mRNAs following *F. oxysporum* inoculation, which is important for understanding the resistance mechanisms of Fusarium yellows disease. It was the first report on the role of non-coding RNA in plant defense related to these diseases. We determined transcriptional response to *A. candida* inoculation varied between resistant and susceptible cultivars, which is also potential output to know resistance mechanisms. We also detected that the resistance mechanism to *A. candida* and *F. oxysporum* in *B. rapa* is similar.

Publications List

Original research articles

1. Naomi Miyaji, **Mst Arjina Akter#**, Chizuko Suzukamo, Hasan Mehraj, Tomoe Shindo, Takeru Itabashi, Keiichi Okazaki, Motoki Shimizu, Makoto Kaji, Masahiko Katsumata, Elizabeth S. Dennis and Ryo Fujimoto. Development of a new DNA marker for Fusarium yellows resistance in *Brassica rapa* vegetables. *Plants* 10(6), 1082. [May, 2021] **[doi]** 10.3390/plants10061082 **#Co-first author**

2. **Mst. Arjina Akter**, Hasan Mehraj, Naomi Miyaji, Satoshi Takahashi, Takeshi Takasaki-Yasuda, Motoaki Seki, Elizabeth S. Dennis, Ryo Fujimoto, Kenji Osabe. Transcriptional association between mRNAs and their paired natural antisense transcripts following *Fusarium oxysporum* inoculation in *Brassica rapa* L. *Horticulturae*, 8(1), 17. [January, 2022] [**doi**] 10.3390/horticulturae8010017

3. **Mst Arjina Akter**, Naomi Miyaji, Motoki Shimizu, Takeshi Takasaki-Yasuda, Elizabeth S. Dennis, and Ryo Fujimoto. The role of salicylic acid-responsive genes in disease resistance in *Brassica rapa* vegetables. *Acta Horticulturae*, 1362, 305-312. [April, 2023] [**doi**] 10.17660/ActaHortic.2023.1362.41

4. Naomi Miyaji, **Mst. Arjina Akter#**, Motoki Shimizu, Hasan Mehraj, Md Asad-Ud Doullah, Elizabeth S. Dennis, Izumi Chuma, Ryo Fujimoto. Differences in the transcriptional immune response to *Albugo candida* between white rust resistant and susceptible cultivars in *Brassica rapa* L. *Scientific Reports*, 13, 8599. [May, 2023] **[doi]** 10.1038/s41598-023-35205-5 **#Co-first author.**

Review article

1. Shiraki S, Fujiwara K, Kamiya Y, **Mst Arjina Akter**, Dennis ES, Fujimoto R, Mehraj H. Molecular basis of heterosis in *Arabidopsis thaliana* and vegetable crops. *Horticulturae*, 9(3), 366. [March, 2023]. [**doi**] 10.3390/horticulturae9030366

Book chapters

1. **Mst Arjina Akter**, Hasan Mehraj, Takeru Itabashi, Tomoe Shindo, Masaaki Osaka, Ayasha Akter, Naomi Miyaji, Naoki Chiba, Junji Miyazaki, Ryo Fujimoto. Breeding for disease resistance in brassica vegetables using DNA marker selection. In Brassica breeding and biotechnology. IntechOpen, London, pp 1-16. [February, 2021]. [**doi**] 10.5772/intechopen.96263

2. Yoshiki Kamiya, Saaya Shiraki, Kazumasa Fujiwara, **Mst Arjina Akter**, Ayasha Akter, Ryo Fujimoto, Hasan Mehraj. The role of epigenetic transcriptional regulation in *Brassica* vegetables: a potential resource for epigenetic breeding**.** In Smart Plant Breeding for Vegetable Crops in Post-genomics Era. Springer, Singapore, pp 1-24. [January, 2023]. **[doi]** 10.1007/978-981-19-5367-5_1

Acknowledgments

I, Akter Mst. Arjina, would like to express my profound gratitude to Dr. Ryo Fujimoto, Associate Professor at Kobe University, my esteemed supervisor, for giving me a chance to work with his research team, and for all the outstanding guidance, keen support, encouragement, and instruction he provided me throughout my doctoral studies. I would like to acknowledge cordially and give my warmest thank to him who made this work possible giving his time, effort, and understanding in helping me succeed in my studies.

My thanks and gratefulness to my co-supervisors and dissertation committee members Professor Takeshi Takasaki-Yasuda and Professor Yuichi Uno for their kind review of this thesis and for their valuable comments, and suggestions to research work.

I would like to thank the Ministry of Education, Culture, Sports, Science and Technology of Japan for financial support.

I would like to express my deepest appreciation to my co-authors, Dr. Naomi Miyaji, Dr. Ayasha Akter, Dr. Hasan Mehraj, Dr. Motoki Shimizu, Dr. Kenji Osabe, Dr. Satoshi Takahashi, Dr. Motoaki Seki, Dr. Elizabeth S Dennis, Dr. Chizuko Suzukamo, Dr. Tomoe Shindo, Dr. Takeru Itabashi, Dr. Keiichi Okazaki, Dr. Makoto Kaji, Dr. Masahiko Katsumata, Dr. Md Asad-Ud Doullah, Dr. Izumi Chuma.

I am thankful to my lab members (Mr. Kodai Matsuo, Ms. Terumi Murakami, Ms. Moe Yamashita, Mr. Yoshiki Kamiya, Mr. Kazumasa Fujiwara, Ms. Saaya Shiraki. Mr. Kohei Kunita, Mr. Keita Nishimura, Ms. Yuki Kawamoto, Mr. Shuta Yano, Mr. Miharu Yamada and others) for their kind assistance in my PhD journey.

I thank Ms. Yumiko Arai for her technical assistance. I also thank the staff of the Graduate School of Agricultural Science, Kobe University for their kind support. Special thanks to Bangladesh Agricultural University, Bangladesh for giving me study leave.

I would like to give my heartfelt and special thanks to my husband Md. Anwar Hoshain who sacrifice the most during this journey, and my family including my beloved parents, sisters, grandmother, uncle-aunts, and my In-laws as a whole for their continuous support by inspiring and understanding when undertaking my research. All of your prayer for me was what sustained me this far.

References

Agrios, G.N. *Plant Pathology*, 5th Edition, Elsevier. **2005**; pp.887–901.

Akter, A.; Miyazaki, J.; Shea, D.J.; Nishida, N.; Takada, S.; Miyaji, N.; Mehraj, H.; Shimizu, M.; Doullah, M.A.U.; Takasaki-Yasuda, T.; Okazaki, K. Gene expression analysis in response to vernalization in Chinese cabbage (*Brassica rapa* L.). *Hort. J.* **2020**, *89*, 268–277.

Akter, A.; Itabashi, E.; Kakizaki, T.; Okazaki, K.; Dennis, E.S.; Fujimoto, R. Genome triplication leads to transcriptional divergence of *FLOWERING LOCUS C* genes during vernalization in the genus *Brassica*. *Front. Plant Sci.* **2021a**, *11*, 619417.

Akter, M.A.; Mehraj, H.; Itabashi, T.; Shindo, T.; Osaka, M.; Akter, A.; Miyaji, N.; Chiba, N.; Miyazaki, J.; Fujimoto, R. Breeding for disease resistance in *Brassica* vegetables using DNA marker selection. In Aminul Islam, A.K.M.; Hossain, M.A.; and Mominul Islam, A.K.M. (Eds.) *Brassica Breeding and Biotechnology*. IntechOpen: London, UK, 2021b.

Akter, M.A.; Mehraj, H.; Miyaji N.; Takahashi, S.; Takasaki-Yasuda, T.; Seki, M.; Dennis, E.S.; Fujimoto, R.; Osabe, K. Transcriptional association between mRNAs and their paired natural antisense transcripts following *Fusarium oxysporum* inoculation in *Brassica rapa* L. *Horticulturae* **2022**, *8,* 17.

Annonymous. Fusarium yellows of cabbage and related crops. Report on *plant disease,* Department of Crop Sciences University of Illinois, USA, **1988**, Rpd no. *901*, pp. 1–3.

Ariel, F.; Romero-Barrios, N.; Jégu, T.; Benhamed, M.; Crespi, M. Battles and hijacks: Noncoding transcription in plants. *Trends Plant Sci.* **2015**, *20*, 362–371.

Arora, H.; Padmaja, K.L.; Kumer, P.; Mukhi, N.; Tewari, A.K.; Mukhopadhyay, A.; Gupta, V.; Pradhan, A.K.; Penta, D. *BjuWRR1*, a CC-NB-LRR gene identified in *Brassica juncea*, confers resistance to white rust caused by *Albugo candida*. *Theor. Appl. Genet*. **2019**, *132*, 2223–2236.

Ayub, A.L.; Soares, R.D.S. Jasiulionis, M.G.The Function of lncRNAs as Epigenetic Regulators. In Tutar, L.; Aras, S.; Tutar, E. (Eds.) *Non-Coding RNAs,* IntechOpen: London, UK, 2019.

Bari, R.; Jones, J.D.G. Role of plant hormones in plant defence responses. *Plant Mol. Biol.* **2009**, *69*, 473–488.

Bolger, A.M.; Lohse, M.; Usadel, B. Trimmomatic: a flexible trimmer for Illumina sequence data. *Bioinformatics* **2014**, *30*, 2114–2120.

Caarls, L.; Pieterse, C.M.; Van Wees, S.C.M. How salicylic acid takes transcriptional control over jasmonic acid signaling. *Front. Plant Sci.* **2015**, *6*, 170.

Campos, M.D.; Félix, M.D.R.; Patanita, M.; Materatski, P.; Varanda, C. High throughput sequencing unravels tomato-pathogen interactions towards a sustainable plant breeding. *Hortic. Res.* **2021**, *8*, 171.

Cech, T.R.; Steitz, J.A. The noncoding RNA revolution-trashing old rules to forge new ones. *Cell* **2014**, *157*, 77–94.

Chekanova, J.A. Long non-coding RNAs and their functions in plants. *Curr. Opin. Plant Biol*. **2015**, *27*, 207–216.

Chen, J.; Pang, W.; Chen, B.; Zhang, C.; Piao, Z. Transcriptome analysis of *Brassica rapa* near-isogenic lines carrying clubroot-resistant and -susceptible alleles in response to *Plasmodiophora brassicae* during early infection. *Front. Plant Sci.* **2016**, *6*, 1183.

Chen, J.; Zhang, J.; Kong, M.; Freeman, A.; Chen, H.; Liu, F. More stories to tell: *NONEXPRESSOR OF PATHOGENESIS-RELATED GENES1*, a salicylic acid receptor. *Plant Cell Environ.* **2021b**, *44*, 1716–1727.

Chen, L.; Zhu, Q.H.; Kaufmann, K. Long non-coding RNAs in plants: Emerging modulators of gene activity in development and stress responses. *Planta* **2020**, *252*, 92.

Chen, Q.; Liu, K.; Yu, R.; Zhou, B.; Huang, P.; Cao, Z.; Zhou, Y.; Wang, J. From "Dark Matter" to "Star": Insight into the regulation mechanisms of plant functional long non-coding RNAs. *Front. Plant Sci.* **2021a**, *12*, 650926.

Cheng, F.; Sun, R.; Hou, X.; Zheng, H.; Zhang, F.; Zhang, Y.; Liu, B.; Liang, J.; Zhuang, M.; Liu, Y.; et al. Subgenome parallel selection is associated with morphotype diversification and convergent crop domestication in *Brassica rapa* and *Brassica oleracea*. *Nat. Genet.* **2016**, *48*, 1218–1224.

Cheng, F.; Wu, J.; Wang, X. Genome triplication drove the diversification of *Brassica* plants. *Hort. Res.* **2014**, *1*, 14024.

Choi, Y.J.; Shin, H.D.; Hong, S.B.; Thines, M. Morphological and molecular discrimination among *Albugo candida* materials infecting *Capsella bursa-pastoris* world-wide. *Fungal Diversity* **2007**, *27*, 11–34.

Coleman, A.D.; Maroschek, J.; Raasch, L.; Takken, F.L.W.; Ranf, S.; Hückelhoven, R. The Arabidopsis leucine-rich repeat receptor-like kinase MIK2 is a crucial component of early immune responses to a fungal-derived elicitor. *New Phytol.* **2021**, *229*, 3453–3466.

Collins, L.J.; Penny, D. The RNA infrastructure: Dark matter of the eukaryotic cell? *Trends Genet.* **2009**, *25*, 120–128.

Cui, J.; Luan, Y.; Jiang, N.; Bao, H.; Meng, J. Comparative transcriptome analysis between resistant and susceptible tomato allows the identification of lncRNA16397 conferring resistance to *Phytophthora infestans* by co-expressing glutaredoxin. *Plant J.* **2017**, *89*, 577–589.

Daly, P.; Tomkins B. Production and postharvest handling of Chinese cabbage (*Brassica rapa* var. *pekinensis*). *RIRDC* **1995**, *97*, 41.

Deforges, J.; Reis, R.S.; Jacquet, P.; Sheppard, S.; Gadekar, V.P.; Hart-Smith, G.; Tanzer, A.; Hofacker, I.L.; Iseli, C.; Xenarios, I.; et al. Control of cognate sense mRNA translation by cis-Natural Antisense RNAs. *Plant Physiol.* **2019**, *180*, 305–322.

Ding, J.; Lu, Q.; Ouyang, Y.; Mao, H.; Zhang, P.; Yao, J.; Xu, C.; Li, X.; Xiao, J.; Zhang, Q. A long noncoding RNA regulates photoperiod-sensitive male sterility, an essential component of hybrid rice. *Proc. Natl. Acad. Sci. U. S. A*. **2012**, *109*, 2654–2659.

Ding, L.N.; Li, Y.T.; Wu, Y.Z., Li, T.; Geng, R.; Cao, J.; Zhang, W.; Tan, X.L. Plant disease resistance-related signaling pathways: Recent progress and future prospects. *Int. J. Mol. Sci.* **2022**, *23*, 16200.

Dixon, G.R. Vegetable Brassicas and Related Crucifers. CABI: Wallingford, UK, **2007**; pp.1–2.

Dodds, P.N.; Rathjen, J.P. Plant immunity: Towards an integrated view of plant-pathogen interactions. *Nat. Rev. Genet.* **2010**, *11*, 539–548.

Du, Z.; Zhou, X.; Ling, Y.; Zhang, Z.; Su, Z. agriGO: A GO analysis toolkit for the agricultural community. *Nucleic Acids Res.* **2010**, *38*, W64–W70.

Enya, J.; Togawa, M.; Takeuchi, T.; Yoshida, S.; Tsushima, S.; Arie, T.; Sakai, T. Biological and phylogenetic characterization of *Fusarium oxysporum* complex, which causes yellows on *Brassica* spp., and proposal of *F. oxysporum* f. sp *rapae*, a novel forma specialis pathogenic on *B. rapa* in Japan. *Phytopathology* **2008**, *98*, 475–483.

FAO. FAOSTAT Database, Top Exports of "Cabbages and Other Brassicas". 2018. (accessed on 13 September 2020) http://www.fao.org/faostat/en/#data/QC.

Fedak, H.; Palusinska, M.; Krzyczmonik, K.; Brzezniak, L.; Yatusevich, R.; Pietras, Z.; Kaczanowski, S.; Swiezewski, S. Control of seed dormancy in Arabidopsis by a cis-acting noncoding antisense transcript. *Proc. Natl. Acad. Sci. U. S. A.* **2016**, *113*, E7846–E7855.

Fujimoto, R.; Sasaki, T.; Nishio, T. Characterization of DNA methyltransferase genes in *Brassica rapa*. *Genes. Genet. Syst.* **2006**, *81*, 235–242.

Fujimoto, R.; Uezono, K.; Ishikura, S.; Osabe, K.; Peacock, W.J.; Dennis, E.S. Recent research on the mechanism of heterosis is important for crop and vegetable breeding systems. *Breed. Sci.* **2018**, *68*, 145–158.

Garber, M.; Grabherr, M.G.; Guttman, M.; Trapnell, C. Computational methods for transcriptome annotation and quantification using RNA-seq. *Nat. Methods* **2011**, *8*, 469–477.

Glazebrook, J. Contrasting mechanisms of defense against biotrophic and necrotrophic pathogens. *Annu. Rev. Phytopathol.* **2005**, *43*, 205–227.

Hatakeyama, K.; Suwabe, K.; Tomita, R.N.; Kato, T.; Nunome, T.; Fukuoka, H.; Matsumoto, S. Identification and characterization of *Crr1a*, a gene for resistance to clubroot disease (*Plasmodiophora brassicae* Woronin) in *Brassica rapa* L. *PLoS One* **2013**, *8*, e54745.

Heath, M.C. Hypersensitive response-related death. *In* Lam. E.; Fukuda, H.; Greenberg, J.; (Eds.) *Programmed Cell Death in Higher Plants*. Springer: Dordrecht, Netherlands, **2000**, pp. 77–90.

Heo, J.B.; Sung, S. Vernalization-mediated epigenetic silencing by a long intronic noncoding RNA. *Science* **2011**, *331*, 76–79.

Huang, L.; Dong, H.; Zhou, D.; Li, M.; Liu, Y.; Zhang, F.; Feng, Y.; Yu, D.; Lin, S.; Cao, J. Systematic identification of long non-coding RNAs during pollen development and fertilization in *Brassica rapa*. *Plant J.* **2018b**, *96*, 203–222.

Huang, X.X.; Zhu, G.Q.; Liu, Q.; Chen, L.; Li, Y.J.; Hou, B.K.; Modulation of plant salicylic acid-associated immune responses via glycosylation of dihydroxybenzoic acids. *Plant Physiol.* **2018a**, *176*, 3103–3119.

Huh, S.U.; Cevik, V.; Ding, P.; Duxbury, Z.; Ma, Y.; Tomlinson, L.; Sarris, P.F.; Jones, J.D.G. Protein-protein interactions in the RPS4/RRS1 immune receptor complex. *PLoS Pathog.* **2017**, *13*, e1006376.

Jones, J.D.G.; Dangl, J.L. The plant immune system. *Nature* **2006**, *444*, 323–329.

Karlik, E.; Ari, S.; Gozukirmizi, N. LncRNAs: genetic and epigenetic effects in plants. *Biotechnol. Biotechnol. Equip.* **2019**, *33*, 429–439.

Kaur, P.; Jost, R.; Sivasithamparam, K.; Barbetti, M.J. Proteome analysis of the *Albugo candida Brassica juncea* pathosystem reveals that the timing of the expression of defense-related genes is a crucial determinant of pathogenesis. *J. Exper. Bot.* **2011**, *62*, 1285–1298.

Kawamura, K.; Kawanabe, T.; Shimizu, M.; Okazaki, K.; Kaji, M.; Dennis, E.S.; Osabe, K.; Fujimoto, R. Genetic characterization of inbred lines of Chinese cabbage by DNA markers: Towards the application of DNA markers to breeding of F_1 hybrid cultivars. *Data Brief* **2016**, *6*, 229–237.

Kawamura, K.; Shimizu, M.; Kawanabe, T.; Pu, Z.; Kodama, T.; Kaji, M.; Osabe, K.; Fujimoto, R.; Okazaki, K. Assessment of DNA markers for seed contamination testing and selection of disease resistance in cabbage. *Euphytica* **2017**, *213*, 28.

Khan, M.S.S.; Islam, F.; Chen, H.; Chang, M.; Wang, D.; Liu, F.; Fu, Z.Q.; Chen, J. Transcriptional coactivators: Driving force of plant immunity. *Front. Plant Sci.* **2022,** *13*, 823937.

Kieu, N.P.; Lenman, M.; Wang, E.S.; Petersen, B.L.; Andreasson, E. Mutations introduced in susceptibility genes through CRISPR/Cas9 genome editing confer increased late blight resistance in potatoes. *Sci. Rep.* **2021**, *11*, 4487.

Kim, C.K.; Seol, Y.J.; Perumal, S.; Lee, J.; Waminal, N.E.; Jayakodi, M.; Lee, S.C.; Jin, S.; Choi, B.S.; Yu, Y.; Ko, H.C.; Choi, J.W.; Ryu, K.Y.; Sohn, S.H.; Parkin, I.; Yang, T.J. Re-exploration of U's Triangle *Brassica* species based on chloroplast genomes and 45S nrDNA sequences. *Sci. Rep.* **2018**, *8*, 7353.

Kim, D.; Paggi, J.M.; Park, C.; Bennett, C. Salzberg SL Graph-based genome alignment and genotyping with HISAT2 and HISAT-genotype. *Nat. Biotechnol.* **2019**, *37*, 907–915.

Kim, D.H.; Sung, S. Vernalization-triggered intragenic chromatin loop formation by long noncoding RNAs. *Dev. Cell*. **2017**, *40,* 302–312.

Kim, E.D.; Sung, S. Long noncoding RNA: unveiling hidden layer of gene regulatory networks. *Trends Plant Sci*. **2012**, *17*, 16–21.

Kim, T.J.; Lim, G.H. Salicylic acid and mobile regulators of systemic immunity in plants: Transport and Metabolism. *Plants* **2023**, *12*, 1013.

Klessig, D.F.; Choi, H.W.; Dempsey, D.A. Systemic acquired resistance and salicylic acid: Past, present, and future. *Mol. Plant Microbe Interact.* **2018**, *31*, 871–888.

Kole, C.; Teutonico, R.; Mengistu, A.; Williams, P.H.; Osborn, T.C. Molecular mapping of a locus controlling resistance to *Albugo candida* in *Brassica rapa. Phytopathol*. **1996**, *86*, 367–369.

Kumar, D. Salicylic acid signaling in disease resistance. *Plant Sci.* **2014**, *228*, 127–134.

Lee, J.; Park, I.; Lee, Z.W.; Kim, S.W.; Baek, N.; Park, H.S.; Park, S.U.; Kwon, S.; Kim, H. Regulation of the major vacuolar Ca^{2+} transporter genes, by intercellular Ca^{2+} concentration and abiotic stresses, in tip-burn resistant *Brassica oleracea*. *Mol. Biol. Rep.* **2013**, *40*,177–188.

Lin, X.; Lin, W.; Ku, Y.S.; Wong, F.L.; Li, M.W.; Lam, H.M.; Ngai, S.M.; Chan, T.F. Analysis of soybean long non-coding RNAs reveals a subset of small peptide-coding transcripts. *Plant Physiol*. **2020**,*182*, 1359–1374.

Liu, M.; Wu, F.; Wang, S.; Lu, Y.; Chen, X.; Wang, Y.; Gu, A.; Zhao, J.; Shen, S. Comparative transcriptome analysis reveals defense responses against soft rot in Chinese cabbage. *Hortic. Res.* **2019**, *6*, 68.

Liu, X.; Hao, L.; Li, D.; Zhu, L.; Hu, S. Long non-coding RNAs and their biological roles in plants. *Genom. Proteom. Bioinform.* **2015**, *13*, 137–147.

Lu, Y.; Tsuda, K. Intimate association of PRR- and NLR-mediated signaling in plant immunity. *Mol. Plant Microbe Interact.* **2021**, *34*, 3–14.

Lv, H.; Fang, Z.; Yang, L.; Zhang, Y.; Wang, Q.; Liu, Y.; Zhuang, M.; Yang, Y.; Xie, B.; Liu, B.; et al. Mapping and analysis of a novel candidate Fusarium wilt resistance gene *FOC1* in *Brassica oleracea*. *BMC Genom.* **2014**, *15*, 1094.

Lv, H.; Fang, Z.; Yang, L.; Zhang, Y.; Wang, Y. An update on the arsenal: Mining resistance genes for disease management of *Brassica* crops in the genomic era. *Hortic. Res*. **2020b**, *7*, 34.

Lv, H.; Miyaji, N.; Osabe, K.; Akter, A.; Mehraj, H.; Shea, D.J.; Fujimoto, R. The importance of genetic and epigenetic research in the *Brassica* vegetables in the face of climate change. In Kole, C. (Ed.) *Genomic Designing of Climate-Smart Vegetable Crops* Springer: Cham, Switzerland, **2020a**; pp. 161–255.

Lyons, R.; Stiller, J.; Powell, J.; Rusu, A.; Manners, J.M.; Kazan, K. *Fusarium oxysporum* triggers tissue-specific transcriptional reprogramming in *Arabidopsis thaliana*. *PLoS ONE*, **2015**, *10*, e0121902.

Ma, Y.; Guo, H.; Hu, L.; Martinez, P.P.; Moschou, P.N.; Cevik, V.; Ding, P.; Duxbury, Z.; Sarris, P.F.; Jones, J.D.G. Distinct modes of derepression of an *Arabidopsis* immune receptor complex by two different bacterial effectors. *Proc. Natl. Acad. Sci. U. S. A.* **2018**, *115*, 10218–10227.

Martel, A.; Ruiz-Bedoya, T.; Breit-Mcnally, C.; Laflamme, B.; Desveaux, D.; Guttman, D.S. The ETS-ETI cycle: evolutionary processes and metapopulation dynamics driving the diversification of pathogen effectors and host immune factors. *Curr. Opin. Plant Biol.* **2021**, *62*, 102011.

Meena, P.D.; Verma, P.R.; Saharan, G.S.; Borhan, M.H. Historical perspectives of white rust caused by *Albugo candida* in oilseed Brassica. *J. Oilseed Brassica* **2014**, *5*, 1–41.

Mehraj, H.; Akter, A.; Miyaji, N.; Miyazaki, J.; Shea, D.J.; Fujimoto, R.; Doullah, M.A.U. Genetics of clubroot and Fusarium wilt disease resistance in Brassica vegetables: The application of marker assisted breeding for disease resistance. *Plants* **2020**, *9*, 726.

Mehraj, H.; Shea, D.J.; Takahashi, S.; Miyaji, N.; Akter, A.; Seki, M.; Dennis, E.S.; Fujimoto, R.; Osabe, K. Genome-wide analysis of long noncoding RNAs, 24-nt siRNAs, DNA methylation and H3K27me3 marks in *Brassica rapa*. *PLoS One* **2021**, *16*, e0242530.

Miura, K.; Tada, Y. Regulation of water, salinity, and cold stress responses by salicylic acid. *Front. Plant Sci.* **2014**, *5*, 4.

Miyaji, N.; Akter, M.A.; Suzukamo, C.; Mehraj, H.; Shindo, T.; Itabashi, T.; Okazaki, K.; Shimizu, M.; Kaji, M.; Katsumata, M.; et al. Development of a new DNA marker for Fusarium yellows resistance in *Brassica rapa* vegetables. *Plants* **2021b**, *10*, 1082.

Miyaji, N.; Shimizu, M.; Miyazaki, J.; Osabe, K.; Sato, M.; Ebe, Y.; Takada, S.; Kaji, M.; Dennis, E.S.; Fujimoto, R.; et al. Comparison of transcriptome profiles by *Fusarium oxysporum* inoculation between Fusarium yellows resistant and susceptible lines in *Brassica rapa* L. *Plant Cell Rep.* **2017**, *36*, 1841–1854.

Miyaji, N.; Shimizu, M.; Takasaki-Yasuda, T.; Dennis, E.S.; Fujimoto, R. The transcriptional response to salicylic acid plays a role in Fusarium yellows resistance in *Brassica rapa* L. *Plant Cell Rep.* **2021a**, *40*, 605–619.

Murray, M.G.; Thompson, W.F. Rapid isolation of high molecular weight plant DNA. *Nucleic Acids Res.* **1980**, *8*, 4321–4325.

Nagaoka, T.; Doullah, M.A.U.; Matsumoto, S.; Kawasaki, S.; Ishikawa, T.; Hori, H.; Okazaki, K. Identification of QTLs that control clubroot resistance in *Brassica oleracea* and comparative analysis of clubroot resistance genes between *B. rapa* and *B. oleracea*. *Theor.Appl. Genet.* **2010**, *120*, 1335–1346.

Nalini, S.; Parthasarathi, R. Optimization of rhamnolipid biosurfactant production from Serratia rubidaea SNAU02 under solid-state fermentation and its biocontrol efficacy against Fusarium wilt of eggplant. *Ann. Agric. Sci*. **2018**, *16*,108–115.

Navarrete, F.; Gallei, M.; Kornienko, A.E.; Saado, I.; Khan, M.; Chia, K.S.; Darino, M.A.; Bindics, J.; Djamei, A. TOPLESS promotes plant immunity by repressing auxin signaling and is targeted by the fungal effector Naked1. *Plant Commun*. **2022**, *3*, 100269.

Neik, T.X.; Barbetti, M. J.; Batley, J. Current status and challenges in identifying disease resistance genes in *Brassica napus*. *Front. Plant Sci.* **2017**, *8*, 1788.

Neik, T.X.; Amas, J.; Barbetti, M.; Edwards, D.; Batley, J. Understanding host-pathogen interactions in *Brassica napus* in the omics era. *Plants* **2020**, *9*, 1336.

Nomura, K.; Minegishi, Y.; Kimizuka-Takagi, C.; Fujioka, T.; Moriguchi, K.; Shishido, R.; Ikehashi, H. Evaluation of F_2 and F_3 plants introgressed with QTLs for clubroot resistance in cabbage developed by using SCAR markers. *Plant Breed.* **2005**, *124*, 371–375.

Petkowski, J.E.; Minchinton, E.; Thomson, F.; Faggian, R.; Cahill, D. Races of *Albugo candida* causing white blister rust on *Brassica* vegetables in Australia. *Acta Hort.* **2008**, *867*, 133–142.

Pieterse, C.M.; Leon-Reyes, A.; Van der Ent, S.; Van Wees, S.C. Networking by small-molecule hormones in plant immunity. *Nat. Chem. Biol*. **2009**, *5*, 308–316.

Pieterse, C.M.; Van der Does, D.; Zamioudis, C.; Leon-Reyes, A.; Van Wees, S.C. Hormonal modulation of plant immunity. *Annu. Rev. Cell Dev. Biol*. **2012**, *28*, 489–521.

Ponting, C.P.; Oliver, P.L.; Reik, W. Evolution and functions of long noncoding RNAs. *Cell* **2009**, *136*, 629–641.

Poveda, J.; Francisco, M.; Cartea, M.E.; Velasco, P. Development of Transgenic *Brassica* Crops Against Biotic Stresses Caused by Pathogens and Arthropod Pests. *Plants* **2020**, *9*,1664.

Prakash, S.; Hinata, K. Taxonomy, cytogenetics and origin of crop Brassicas, a review. *Opera. Bot*. **1980**, *55*, 3–57.

Pruitt, R.N.; Locci, F.; Wanke, F.; Zhang, L.; Saile, S.C.; Joe, A.; Karelina, D.; Hua, C.; Fröhlich, K.; Wan, W.L.; et al. The EDS1-PAD4-ADR1 node mediates *Arabidopsis* pattern-triggered immunity. *Nature* **2021**, *598*, 495–499.

Pu, Z.; Shimizu, M.; Zhang, Y.; Nagaoka, T.; Hayashi, T.; Hori, H.; Matsumoto, S.; Fujimoto, R.; Okazaki, K. Genetic mapping of a fusarium wilt resistance gene in *Brassica oleracea*. *Mol. Breed.* **2012**, *30*, 809–818.

Rai, M.I.; Alam, M.; Lightfoot, D.A.; Gurha, P.; Afzal, A.J. Classification and experimental identification of plant long non-coding RNAs. *Genomics* **2019**, *111*, 997–1005.

Ramirez, D.; Abellán-Victorio, A.; Beretta, V.; Camargo, A.; Moreno, D.A. Functional ingredients from brassicaceae species: Overview and perspectives. *Int. J. Mol. Sci.* **2020**, *21*,1998.

Reis, R.S.; Poirier, Y. Making sense of the natural antisense transcript puzzle. *Trends Plant Sci.* **2021**, *26*, 1104–1115.

Rekhter, D.; Lüdke, D.; Ding, Y.; Feussner, K.; Zienkiewicz, K.; Lipka, V.; Wiermer, M.; Zhang, Y.; Feussner, I. Isochorismate-derived biosynthesis of the plant stress hormone salicylic acid. *Science* **2019**, *365*, 498–502.

Rhodes, J.; Yang, H.; Moussu, S.; Boutrot, F.; Santiago, J.; Zipfel, C. Perception of a divergent family of phytocytokines by the Arabidopsis receptor kinase MIK2. *Nat. Commun.* **2021**, *12*, 705.

Saeki, N.; Kawanabe, T.; Ying, H.; Shimizu, M.; Kojima, M.; Abe, H.; Okazaki, K.; Kaji, M.; Taylor, J. M.; Sakakibara, H.; Peacock, W.J.; Dennis, E.S.; Fujimoto, R. Molecular and cellular characteristics of hybrid vigour in a commercial hybrid of Chinese cabbage. *BMC Plant Biol.* **2016,** *16*, 45.

Saharan, G.; Verma, P.; Meena, P.; Kumar, A. The disease. In Saharan, G.; Verma, P.; Meena, P.; Kumar, A. (Eds.) *White rust of crucifers: biology, ecology and management,* Springer: New Delhi, India, **2014**; pp. 7–54

Salehi, B.; Quispe, C.; Butnariu, M.; Sarac, I.; Marmouzi, I.; Kamle, M.; Tripathi, V.; Kumar, P.; Bouyahya, A.; Capanoglu, E. Phytotherapy and food applications from brassica genus. *Phytother. Res.* **2021**, *35*, 3590–3609.

Sato, M.; Shimizu, M.; Shea, D.J.; Hoque, M.; Kawanabe, T.; Miyaji, N.; Fujimoto, R.; Fukai, E.; Okazaki, K. Allele specific DNA marker for fusarium resistance gene *FocBo1* in *Brassica oleracea*. *Breed. Sci.* **2019**, *69*, 308–315.

Savary, S.; Willocquet, L.; Pethybridge, S.J.; Esker, P.; Mcroberts, N.; Nelson, A.J. The global burden of pathogens and pests on major food crops. *Nat. Ecol. Evol.* **2019**, *3*, 430–439.

Seo, J.S.; Sun, H.X.; Park, B.S.; Huang, C.H.; Yeh, S.D.; Jung, C.; Chua, N.H. ELF18-INDUCED LONG-NONCODING RNA associates with mediator to enhance expression of innate immune response genes in Arabidopsis. *Plant Cell*. **2017**, *29*,1024–1038.

Shea, D.J.; Nishida, N.; Takada, S.; Itabashi, E.; Takahashi, S.; Akter, A.; Miyaji, N.; Osabe, K.; Mehraj, H.; Shimizu, M.; et al. Long noncoding RNAs in *Brassica rapa* L. following vernalization. *Sci. Rep.* **2019**, *9*, 9302.

Shigenaga, A.M.; Argueso, C.T. No hormone to rule them all: interactions of plant hormones during the responses of plants to pathogens. *Semin. Cell Dev. Biol.* **2016**, *56*, 174–189.

Shigenaga, A.M.; Berens, M.L.; Tsuda, K.; Argueso, C.T. Towards engineering of hormonal crosstalk in plant immunity. *Curr. Opin. Plant Biol.* **2017**, *38*, 164–172.

Shimizu, M.; Fujimoto, R.; Ying, H.; Pu, Z.J.; Ebe, Y.; Kawanabe, T.; Saeki, N.; Taylor, J.M.; Kaji, M.; Dennis, E.S.; et al. Identification of candidate genes for Fusarium yellows resistance in Chinese cabbage by differential expression analysis. *Plant Mol. Biol.* **2014**, *85*, 247–257.

Shimizu, M.; Pu, Z.; Kawanabe, T.; Kitashiba, H.; Matsumoto, S.; Ebe, Y.; Sano, M.; Funaki, T.; Fukai, E.; Fujimoto, R.; et al. Map-based cloning of a candidate gene conferring Fusarium yellows resistance in *Brassica oleracea*. *Theor. Appl. Genet.* **2015**, *128*, 119–130.

Shurtleff, M.C.; Pelczar, M.J.; Kelman, A.; Pelczar, R.M. *Plant disease. Encyclopedia Britannica* **2021**.

Singh, K.P.; Kumari, P.; Rai, P.K. Current status of the disease-resistant gene(s)/QTLs, and strategies for improvement in *Brassica juncea*. *Front. Plant Sci.* **2021**, *12*, 617405.

Song, X.; Hu, J.; Wu, T.; Yang, Q.; Feng, X.; Lin, H.; Feng, S.; Cui, C.; Yu, Y.; Zhou, R.; et al. Comparative analysis of long noncoding RNAs in angiosperms and characterization of long noncoding RNAs in response to heat stress in Chinese cabbage. *Hortic. Res.* **2021**, *8*, 48.

Spoel, S.H.; Dong, X. How do plants achieve immunity? Defence without specialized immune cells. *Nat. Rev. Immunol.* **2012**, *12*, 89–100.

Stark, R.; Grzelak, M.; Hadfield, J. RNA sequencing: the teenage years. *Nat. Rev. Genet.* **2019**, *20*, 631–656.

Suwabe, K.; Tsukazaki, H.; Iketani, H.; Hatakeyama, K.; Fujimura, M.; Nunome, T.; Fukuoka, H.; Matsumoto, S.; Hirai, M. Identification of two loci for resistance to clubroot (*Plasmodiophora brassicae* Woronin) in *Brassica rapa* L. *Theor. Appl. Genet.* **2003**, *107*, 997–1002.

Swiezewski, S.; Liu, F.; Magusin, A.; Dean, C. Cold-induced silencing by long antisense transcripts of an Arabidopsis polycomb target. *Nature* **2009**, *462*,799–802.

Takagi, H.; Abe, A.; Yoshida, K.; Kosugi, S.; Natsume, S.; Mitsuoka, C.; Uemura, A.; Utsushi, H.; Tamiru, M.; Takuno, S.; et al. QTL-seq: Rapid mapping of quantitative trait loci in rice by whole genome resequencing of DNA from two bulked populations. *Plant J.* **2013**, *74*, 174–183.

Tanhuanp, P. Identification and mapping of resistance gene analogs and a white rust resistance locus in *Brassica rapa* ssp. *oleifera. Theor. Appl. Genet.* **2004**, *108*, 1039–1046.

Tena G. PTI and ETI are one. *Nat. Plants*. **2021**, *7*, 1527.

Thomazella, D.P.T.; Seong, K.; Mackelprang, R.; Dahlbeck, D.; Geng, Y.; Gill, U.S.; Qi, T.; Pham, J.; Giuseppe, P.; Lee, C.Y.; Ortega, A.; Cho, M.J.; Hutton, S.F.; Staskawicz, B. Loss of function of a DMR6 ortholog in tomato confers broad-spectrum disease resistance. *Proc. Natl. Acad. Sci. U. S. A.* **2021**, *118*, e2026152118.

Trapnell, C.; Hendrickson, D.G.; Sauvageau, M.; Goff, L.; Rinn, J.L.; Pachter, L. Differential analysis of gene regulation at transcript resolution with RNA-seq. *Nat. Biotechnol*. **2013**, *31*, 46–53.

Trapnell, C.; Roberts, A.; Goff, L.; Pertea, G.; Kim, D.; Kelley, D.R.; Pimentel, H.; Salzberg, S.L.; Rinn, J.L.; Pachter, L. Differential gene and transcript expression analysis of RNA-seq experiments with TopHat and Cufflinks. *Nat. Protoc.* **2012**, *7*, 562–578.

U.N. Genome analysis in Brassica with special reference to the experimental formation of *B. napus* and peculiar mode of fertilization. *Jpn. J. Bot.* **1935**, *7*, 389–452.

Ueno, H.; Matsumoto, E.; Aruga, D.; Kitagawa, S.; Matsumura, H.; Hayashida, N. Molecular characterization of the *CRa* gene conferring clubroot resistance in *Brassica rapa*. *Plant Mol. Biol.* **2012**, *80*, 621–629.

Uszczynska-Ratajczak, B.; Lagarde, J.; Frankish, A.; Guigó, R.; Johnson, R. Towards a complete map of the human long noncoding RNA transcriptome. *Nat. Rev. Genet.* **2018**, *19*, 535–548.

Van Damme, M.; Andel, A.; Huibers, R.P.; Panstruga, R.; Weisbeek, P.J.; Van den Ackerveken, G. Identification of *Arabidopsis* loci required for susceptibility to the downy mildew pathogen *Hyaloperonospora parasitica*. *Mol. Plant Microbe Interact.* **2005**, *18*, 583–592.

Van Damme, M.; Huibers, R.P.; Elberse, J.; den Ackerveken, G.V. Arabidopsis *DMR6* encodes a putative 2OG-Fe (II) oxygenase that is defense-associated but required for susceptibility to downy mildew. *Plant J.* **2008**, *54*, 785–793.

Van der Does, D.; Boutrot, F.; Engelsdorf, T.; Rhodes, J.; McKenna, J.F.; Vernhettes, S.; Koevoets, I.; Tintor, N.; Veerabagu, M.; Miedes, E.; *et al*. The Arabidopsis leucine-rich repeat receptor kinase MIK2/LRR-KISS connects cell wall integrity sensing, root growth and response to abiotic and biotic stresses. *PLoS Genet.* **2017**, *13*, e1006832.

Van Doorn, W.G. Classes of programmed cell death in plants, compared to those in animals. *J. Exp. Bot*. **2011**, *62*, 4749–4761.

Varshney, A.; Mohapatra, T.; Sharma, R.P. Development and validation of CAPS and AFLP markers for white rust resistance gene in *Brassica juncea*. *Theor. Appl. Genet*. **2004**, *109*, 153–159.

Verma, P.R.; Petrie, G.A. Effect of seed infestation and flower inoculation on systemic infection of turnip rape by *Albugo candida*. *Can J Plant Sci*. **1980**, *60*, 267–271.

Vlot, A.C.; Dempsey, D.M.A.; Klessig, D.F. Salicylic acid, a multifaceted hormone to combat disease. *Annu. Rev. Phytopathol.* **2009**, *47*, 177–206.

Walker, J.C. Inheritance of fusarium resistance in cabbage. *J Agric Res*. **1930**, *40*, 721–745.

Wang, H.; Chung, P.J.; Liu, J.; Jang, I.C.; Kean, M.J.; Xu, J.; Chua, N.H. Genome-wide identification of long noncoding natural antisense transcripts and their responses to light in *Arabidopsis*. *Genome Res.* **2014**, *24*, 444– 453.

Wang, H.; Niu, Q.W.; Wu, H.W.; Liu, J.; Ye, J.; Yu, N.; Chua, N.H. Analysis of non-coding transcriptome in rice and maize uncovers roles of conserved lncRNAs associated with agriculture traits. *Plant J.* **2015**, *84*, 404–416.

Wang, H.L.; Chekanova, J.A. Long noncoding RNAs in plants. *Adv. Exp. Med. Biol.* **2017**, *1008*, 133–154.

Wang, N.N.; Li Y.; Chen, Y.H.; Lu, R.; Zhou, L.; Wang, Y.; Zheng, Y.; Li, X.B. Phosphorylation of WRKY16 by MPK3-1 is essential for its transcriptional activity during fiber initiation and elongation in cotton (*Gossypium hirsutum*). *Plant Cell.* **2021**, *33*, 2736–2752.

Wang, Y.; Fan, X.; Lin, F.; He, G.; Terzaghi, W.; Zhu, D.; Deng, X.W. Arabidopsis noncoding RNA mediates control of photomorphogenesis by red light. *Proc. Nat. Acad. Sci. U. S. A*. **2014**, *111*,10359–10364.

Wu, L.; Liu, S.; Qi, H.; Cai, H.; Xu, M. Research progress on plant long non-coding RNA. *Plants* **2020**, *9*, 408.

Wunderlich, M.; Gross-Hardt, R.; Schöffl, F. Heat shock factor HSFB2a involved in gametophyte development of *Arabidopsis thaliana* and its expression is controlled by a heat-inducible long non-coding antisense RNA. *Plant Mol. Biol.* **2014**, *85*, 541–550.

Xin, M.; Wang, Y.; Yao, Y.; Song, N.; Hu, Z.; Qin, D.; Xie, C.; Peng, H.; Ni, Z.; Sun, Q. Identification and characterization of wheat long non-protein coding RNAs responsive to powdery mildew infection and heat stress by using microarray analysis and SBS sequencing. *BMC Plant Biol*. **2011**, *11*, 61.

Xing, M.; Lv, H.; Ma, J.; Xu, D.; Li, H.; Yang, L.; Kang, J.; Wang, X.; Fang, Z. Transcriptome profiling of resistance to *Fusarium oxysporum* f. sp. *conglutinans* in cabbage (*Brassica oleracea*) roots. *PLoS ONE* **2016**, *11*, e0148048.

Yadav, S.K.; Srivastava, D. Biotic stress management in rice through RNA interference. In Shamim, M.; Singh, K.N. (Eds.) *Biotic Stress Management in Rice*. Apple Academic Press: Florida, USA, **2017**, pp. 363–394.

Yang, Y.; Fang, A.; Yu, Y.; Bi, C.; Zhou, C. Integrated transcriptomic and secretomic approaches reveal critical pathogenicity factors in *Pseudofabraea citricarpa* inciting citrus target spot. *Microb. Biotechnol*. **2019**, *12*, 1260–1273.

Yu, Y.; Zhang, Y.; Chen, X.; Chen, Y. Plant noncoding RNAs: Hidden players in development and stress responses. *Annu. Rev. Cell Dev. Biol.* **2019**, *35*, 407–431.

Yuan, M.; Jiang, Z.; Bi, G.; Nomura, K.; Liu, M.; Wang, Y.; Cai, B.; Zhou, J.M.; He, S.Y.; Xin, X.F. Pattern-recognition receptors are required for NLR-mediated plant immunity. *Nature* **2021a**, *592*, 105–109.

Yuan, M.; Ngou, B.P.M.; Ding, P.; Xin, X.F. PTI-ETI crosstalk: An integrative view of plant immunity. *Curr. Opin. Plant Biol.* **2021b**, *62*, 102030.

Yuan, Y.; Qin, L.; Su, H.; Yang, S.; Wei, X.; Wang, Z.; Zhao, Y.; Li, L.; Liu, H.; Tian, B.; Zhang, X. Transcriptome and coexpression network analyses reveal hub genes in Chinese cabbage (*Brassica rapa* L. ssp. *pekinensis*) during different stages of *Plasmodiophora brassicae* infection. *Front. Plant Sci.* **2021c**, *12*, 650252.

Zeilmaker, T.; Ludwig, N.R.; Elberse, J.; Seidl, M.F.; Berke, L.; Van Doorn, A.; Schuurink, R.C.; Snel, B.; Van den Ackerveken, G. DOWNY MILDEW RESISTANT 6 and DMR6-LIKE OXYGENASE 1 are partially redundant but distinct suppressors of immunity in Arabidopsis. *Plant J.* **2015**, *81*, 210–222.

Zhang, H.; Guo, H.; Hu, W.; Ji, W. The emerging role of long non-coding RNAs in plant defense against fungal stress. *Int. J. Mol. Sci.* **2020**, *21*, 2659.

Zhang, K., Mason, A.S., Farooq, M.A., Islam, F., Quezada-Martinez, D., Hu, D., Yang, S., Zou, J., Zhou, W. Challenges and prospects for a potential allohexaploid *Brassica* crop. *Theor. Appl. Genet.* **2021**, *134*, 2711–2726.

Zhang, W.; Zhao, F.; Jiang, L.; Chen, C.; Wu, L.; Liu, Z. Different pathogen defense strategies in *Arabidopsis*: more than pathogen recognition. *Cells* **2018**, *7*, 252.

Zhang, Y.; Li, X. Salicylic acid: Biosynthesis, perception, and contributions to plant immunity. *Curr. Opin. Plant Biol.* **2019**, *50*, 29–36.

Zhang, Y.; Zhao, L.; Zhao, J.; Li, Y.; Wang, J.; Guo, R.; Gan, S.; Liu, C.J.; Zhang, K. *S5H/DMR6* encodes a salicylic acid 5-hydroxylase that fine-tunes salicylic acid homeostasis. *Plant Physiol.* **2017**, *175*, 1082–1093.

Zhao, X.; Li, J.; Lian, B.; Gu, H.; Li, Y.; Qi, Y. Global identification of *Arabidopsis* lncRNAs reveals the regulation of *MAF4* by a natural antisense RNA. *Nat. Commun*. **2018**, *9*, 5056.

Zheng, H.; Zhang, Y.; Li, J.; He, L.; Wang, F.; Bi, Y.; Gao, J. Comparative transcriptome analysis between a resistant and a susceptible Chinese cabbage in response to *Hyaloperonospora brassicae*. *Plant Signal Behav.* **2020**, *15*, e1777373.

Zhong, Q.; Hu, H.; Fan, B.; Zhu, C.; Chen, Z. Biosynthesis and roles of salicylic acid in balancing stress response and growth in plants. *Int. J. Mol. Sci.* **2021**, *22*, 11672.

Zhu, Q.H.; Stephen, S.; Taylor, J.; Helliwell, C.A.; Wang, M.B. Long noncoding RNAs responsive to *Fusarium oxysporum* infection in *Arabidopsis thaliana*. *New Phytol.* **2014**, *201*, 574–584.